

# Dynamic organization of transcription-coupled DNA repair

Dynamische organisatie van transcriptie-gekoppeld DNA herstel

## Proefschrift

ter verkrijging van de graad van doctor  
aan de Erasmus Universiteit Rotterdam  
op gezag van  
Rector Magnificus  
Prof.dr. S.W.J. Lamberts  
en volgens besluit van het College voor Promoties

De openbare verdediging zal plaatsvinden op  
woensdag 17 december 2003 om 13:45 uur

door

**Vincent van den Boom**

geboren te Utrecht

## Promotiecommissie

Promotor: Prof.dr. J.H.J. Hoeijmakers

Overige leden: Prof.dr. F. Grosveld  
Prof.dr. B. Oostra  
Prof.dr. L.H.F. Mullenders

Copromotor: Dr. W. Vermeulen

Dit proefschrift kwam tot stand binnen de vakgroep Celbiologie en Genetica van de faculteit der Geneeskunde en Gezondheidswetenschappen van de Erasmus Universiteit Rotterdam. De vakgroep maakt deel uit van het Medisch Genetisch Centrum Zuid-West Nederland. Het onderzoek is financieel ondersteund door het Centre for Biomedical Genetics (CBG).

Voor mijn ouders

# Contents

Scope of the thesis	7
Chapter 1, General introduction	9
1.1 Background	10
1.2 Nucleotide excision repair	10
1.3 Molecular mechanism of NER	12
Chapter 2, Transcription-coupled repair	15
2.1 Introduction	16
2.2 TCR: a conserved mechanism	16
2.3 Mammalian transcription-coupled repair	16
2.4 Genetic heterogeneity of Cockayne Syndrome	18
2.4.1 CSA	18
2.4.2 CSB	19
2.4.3 XAB2	20
2.4.5 XPG	20
2.4.6 TFIIH	20
2.5 Mouse models of Cockayne Syndrome	21
2.6 Molecular basis for Cockayne features	21
2.7 Molecular mechanism of TCR	22
Chapter 3, Involvement of the CSB protein in transcription elongation	25
3.1 Introduction	26
3.2 Elongation factors	26
3.3 A function for CSB in transcription elongation?	28
3.4 Molecular mechanism of CSB in transcription	29
Chapter 4, Dynamic studies in living cells using GFP-tagged proteins	31
4.1 Introduction	32
4.2 Physical parameters of GFP	32
4.3 Mobility and interaction studies using GFP	33
4.4 FRAP-based mobility studies	35
4.4.1 FRAP	35
4.4.2 Simultaneous FLIP/FRAP	37
Chapter 5, Organization of nuclear processes in living cells	39
5.1 Introduction	40
5.2 Transcription in living cells	41
5.3 DNA repair in living cells	42
5.3.1 Homologous recombination	42
5.3.2 Nucleotide excision repair	43
5.3.3 Transcription-coupled repair	43

References	45
Chapter 6, ATP-dependent chromatin remodeling by the Cockayne Syndrome B DNA repair-transcription coupling factor	55
Chapter 7, Transient interactions of CSB with transcription elongation complexes are stabilized by DNA damage-induced stalling	77
Chapter 8, The Cockayne Syndrome B protein is connected to mRNA processing	99
Chapter 9, Differential cellular localization and dynamics of CSA and CSB in relation to transcription and TCR	111
Chapter 10, Concluding remarks and future directions	127
Summary	132
Samenvatting	135
List of abbreviations	138
List of publications	139
Curriculum vitae	140
Dankwoord	141



# Scope of the thesis

The aim of the work described in this thesis is to gain more insight in the role of the Cockayne Syndrome A (CSA) and B (CSB) proteins in the process of transcription-coupled DNA repair and transcription. Using biochemical analysis and live cell studies we investigated the molecular behavior of both proteins. First, we analyzed the chromatin remodeling activity of CSB. Secondly, using green fluorescent protein (GFP) technology (Chapter 4) and photobleaching we studied (i) the dynamic behavior of CSB in TCR and transcription in living cells, (ii) the kinetics of CSA in TCR and its molecular connection with the CSB protein and (iii) the cellular localization of CSB with respect to other nuclear processes like transcription and mRNA processing.

**Chapter 1** summarizes the origin of DNA damage and the consequences of lesions. In addition, mechanisms to remove DNA lesions are described focusing on nucleotide excision repair (NER), which is involved in removal of several types of DNA helix distorting lesions. In **Chapter 2** the specific NER subpathway of transcription-coupled repair (TCR) is described. Particular attention is given to factors involved in TCR, the current understanding of its molecular mechanism and the consequences of a defective TCR pathway in men and mice. In addition, the involvement of TCR in other, non-NER, pathways is discussed. In **Chapter 3** an overview is presented of the mechanism of RNA polymerase-dependent transcription. This chapter specifically focuses on transcription elongation and how CSB could be implicated as an elongation stimulatory factor. In **Chapter 4** the physical properties of the GFP, its implication in biological research by tagging of proteins and the possibility to study the localization of these proteins in living cells is discussed. In addition, different photobleaching techniques to study protein mobility are presented. Recent advances in the understanding of protein movement in the nucleus and how various nuclear processes like transcription and DNA repair are regulated *in vivo* are described in **Chapter 5**. In the subsequent chapters (6, 7, 8, 9) the experimental work, towards a better understanding of the CS factors in the more complex environment of chromatin and intact living cells is presented. **Chapter 6** focuses on the chromatin remodeling activity of purified recombinant CSB protein *in vitro*. The localization, protein mobility and differential interactions of CSB in transcription elongation and TCR in living cells are presented in **Chapter 7**. In **Chapter 8** an overview is given of the overlapping localization and *in vitro* interaction of CSB with various mRNA processing factors and describes the interaction of CSB with *in vitro* active RNA polymerase II. Within **Chapter 9**, the dynamic behavior and the functional implications of the CSA protein in TCR are presented. Finally, in **Chapter 10** the major conclusions of the experimental work described in this thesis are summarized, discussed and possible future directions are presented.





# Chapter 1

General introduction

# General introduction

## 1.1 Background

DNA, carrier of genetic information required for development, maintenance and characteristics of all organisms is continuously challenged by various damaging agents from exogenous and endogenous origin. Different types of environmental influences like the UV-component of sunlight and ionizing radiation disturb the chemical structure of DNA through induction of DNA breaks and helical distortions. In addition, carcinogenic compounds can directly modify the base moiety and sugar backbone of nucleotides. Similar injuries are induced by reactive oxygen species, which are a product of the metabolic activity of the cell [1]. Finally, spontaneous induction of DNA damage occurs due to intrinsic instability of chemical bonds in the DNA (e.g. depurination and deamination) [2]. All these DNA injuries directly interfere with vital cellular processes like DNA replication, transcription and cell cycle progression (Figure 1A). DNA damage-induced mis-insertions during DNA replication can induce permanent mutations, which may lead to inborn diseases or cancerous growth of cells (Figure 1B). Transcription blockage and cell cycle arrest are highly cytotoxic since both events give rise to apoptotic death of the cell. Increased levels of apoptosis will lead to typical features of ageing in several tissues, for example the aged appearance of heavily solar exposed skin.

For proper functioning of a cell preservation of the integrity of our DNA is therefore highly important. Fortunately, an intricate network of different DNA repair pathways has evolved that collectively remove virtually all DNA injuries (Figure 1C). Double- and single-strand DNA breaks of the DNA helix are repaired by the homologous recombination (HR) or non-homologous end-joining (NHEJ) pathway [3]. Mis-insertions, addition or deletions of single nucleotides during DNA replication are repaired by mismatch repair. Base excision repair (BER) pathway is responsible for the removal of lesions induced by oxidative and alkylating agents. Helix distorting lesions, such as lesions induced by UV-irradiation, are repaired by the nucleotide excision repair (NER) pathway [1,4].

## 1.2 Nucleotide excision repair

NER is a versatile DNA repair mechanism recognizing a wide variety of DNA lesions in the cell. More specifically, NER is responsible for recognition and elimination of helix-distorting lesions, bulky adducts and intra-strand cross-links. These lesions include: cyclo-butane pyrimidine dimers (CPDs), 6-4 photo-products (6-4PPs) and polycyclic aromatic hydrocarbons (e.g. N-acetoxy-2-acetylaminofluorene and benzo[a]pyrene). Efficiency of lesion recognition by NER is generally determined by the relative degree of helical distortion.

The biological relevance of NER is emphasized by the severe clinical features associated with syndromes that are caused by an inherited defect in the NER pathway: Xeroderma pigmentosum (XP), Cockayne Syndrome (CS) and Trichothiodystrophy (TTD). These three, sunlight hypersensitive disorders are partly overlapping diseases.

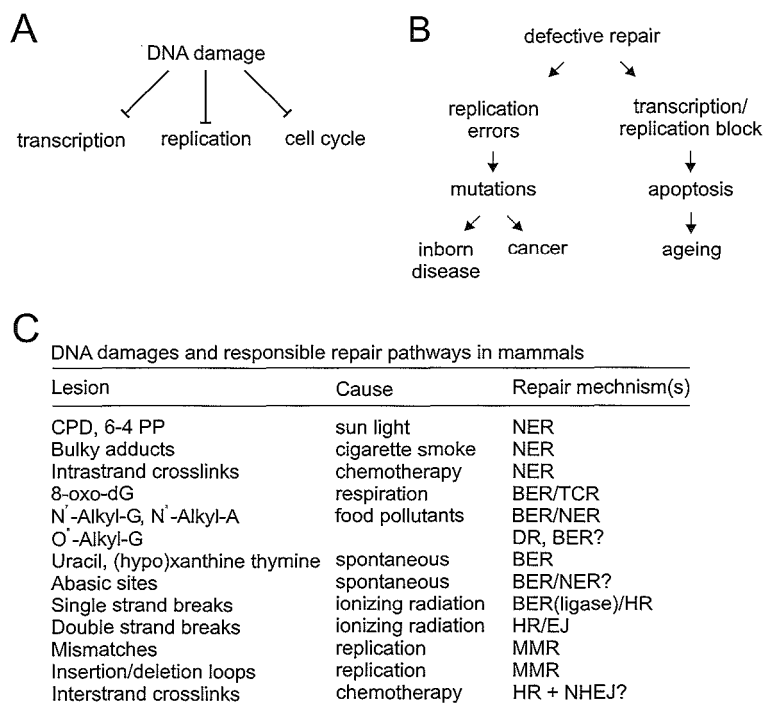


**Figure 1. Consequences of DNA damage and involved DNA repair pathways.** (A) Direct effects of DNA damage are inhibition of transcription, replication and cell cycle progression. (B) Defective repair will eventually lead to inborn diseases, cancer and ageing. (C) DNA lesions are introduced by various exogenous and endogenous factors. Several repair pathways are involved in removal of specific types of DNA damage.

Within XP, mutations in either one of seven different genes (*XPA-XPG*) gives rise to the phenotype, whereas CS is due to mutations in the *CSA* or *CSB* gene. Specific mutations in *XPB*, *XPD* or *XPG* give a rise to a combined form of XP and CS. TTD is found in patients with a mutation in the *TTDA* gene or a photosensitive form of TTD upon certain mutations in *XPB* or *XPD*. All three syndromes are characterized by extreme sensitivity to sunlight. XP patients are further characterized by a >1000x elevated risk for skin cancer and display pigmentation abnormalities in sun-exposed areas (for review: [5]). In addition, a subpopulation of XP patients (e.g. XP-A) also develops neuronal degeneration. In contrast to XP, CS patients are not predisposed to skin cancer. They show severe neurological and developmental problems, such as mental retardation, short stature, dysmorphic dwarfism and a bird-like face, and reach only an average age of 12.5 years. TTD patients are characterized by brittle hair and nails and ichthyosis, as caused by a reduced expression of cystein-rich matrix proteins.

### 1.3 Molecular mechanism of NER

NER is a complex multistep process involving the coordinated action of approximately 25-30 polypeptides. Three decades of cellular, genetic and biochemical studies has provided detailed insight into the molecular mechanism of this repair pathway (for review see [1]). The obvious first step to initiate NER is the detection of lesions amidst the background of non-damaged DNA. Two different modes of lesion recognition with NER have been identified: (1) global genome repair (GGR); (2) transcription-coupled repair (TCR; see chapter 2) (Figure 2). The process of GGR can be reconstituted *in vitro*, which provides a tool to dissect the individual steps.

Lesion recognition within GGR is performed by the XPC/hHR23B heterodimer, which binds DNA with high affinity and has increased affinity for damaged DNA (Figure 2) [6-9]. Upon binding of the complex to the damage bending of the DNA is induced, possibly providing an architectural condition, which is important for prolongation of the repair reaction [10]. The UV-DDB complex, consisting of (1) p125 or DDB1 (damaged DNA binding protein) and (2) p48 or DDB2 (mutated in XPE) probably plays a role in assisting XPC/hHR23b with recognition of low affinity lesions (e.g. CPDs) and/or facilitates binding of XPC/hHR23b to the damage through modification of the chromatin structure around the lesion [11,12].

Subsequent to stable association of the XPC-hHR23b complex, TFIIH, a transcription factor involved in initiation of RNA polymerase I and II transcription, is recruited to the lesion [13,14]. Similar to melting the DNA in the promoter region during transcription initiation, TFIIH unwinds of the DNA helix around the lesion in repair [15]. In an ATP-dependent reaction TFIIH is able to open up a region of ~25nt around the lesion [15]. Two ATP-dependent DNA helicases are found in TFIIH: XPB and XPD, a 3'-5' helicase and 5'-3' helicase respectively. The helicase activity of XPB is required for unwinding of the DNA around the promoter region during RNAPII initiation, whereas XPD is dispensable in transcription [16,17]. The role of XPD in transcription initiation seems to be a more structural one [18]. The TFIIH complex consists of nine subunits: XPB, p62, p52, p44 and p32 (for review see [19]). The XPD subunit forms a bridge between this core complex and the CAK (cdk-activating kinase) complex consisting of cyclin H, MAT1 and cdk7 [20-22].

After open complex formation by TFIIH, initial stability of the unwound region in the DNA is guaranteed by the physical presence of the XPG protein [15,23]. Final stabilization of the open complex is provided by XPA and RPA, which respectively demarcate the lesion and bind to the single-stranded DNA of the opposite strand [24,25]. In addition, RPA properly orientates the two structure-specific endonucleases: XPG and the ERCC1/XPF heterodimer, leading to excision of a DNA fragment of ~24-32 bp. XPG, making the 3' incision, performs its action first after which the ERCC1-XPF heterodimer nicks 5' of the lesion [15,26,27].

Finally, after release of the damaged DNA fragment, gap-filling DNA synthesis is performed by the DNA replication machinery consisting of RPA (replication protein A), PCNA (proliferating cell nuclear antigen), RFC (replication factor C) and DNA polymerase  $\delta$  and  $\epsilon$ , using the undamaged daughter strand as a template [28]. Subsequent to DNA synthesis the resulting nick is ligated by DNA ligase I.

## Global Genome Repair

## Transcription-coupled Repair

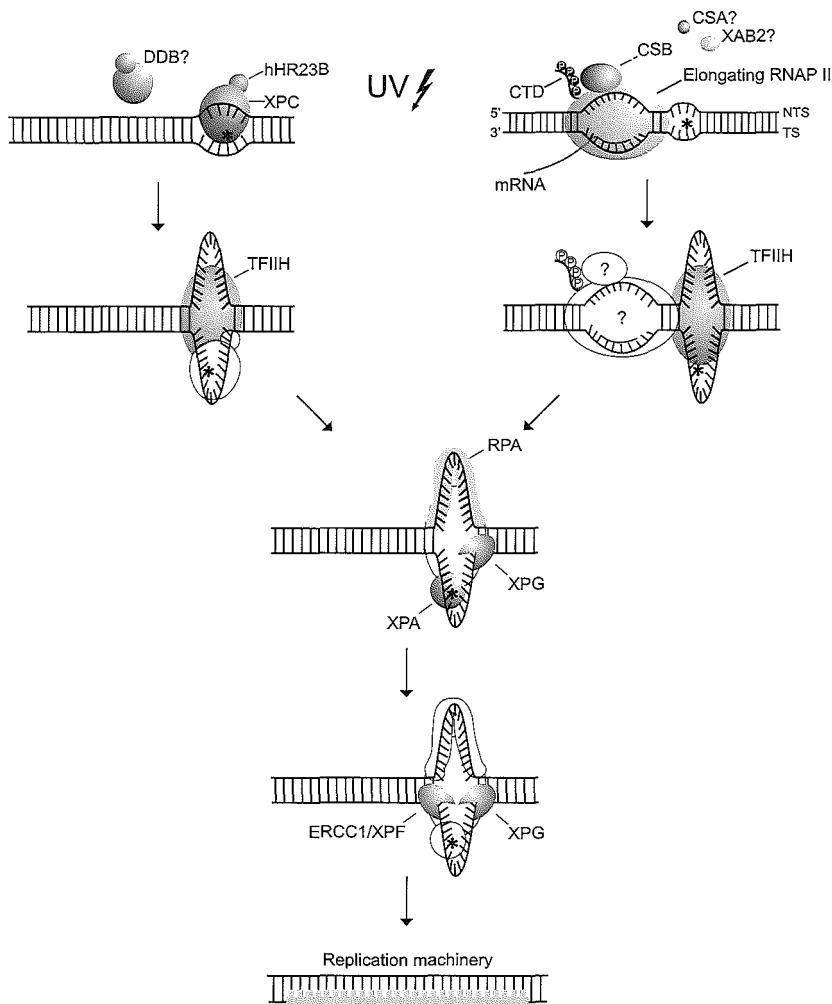


**Figure 2. Molecular model for global genome repair (GGR) and transcription-coupled repair (TCR).** Detection of helix distorting lesions in GGR is performed by the hHR23B/XPC heterodimer (for some less helix distorting injuries the DDB complex is required). Lesion detection via TCR is initiated by stalling of an RNA polymerase II elongation complex on a lesion. CSA, CSB and XAB2 are most likely implicated in the initial stages of TCR. After damage recognition, either via GGR or TCR, the mechanism of damage removal is probably identical. TFIIH is recruited to open up the DNA helix and XPG is sequestered to stabilize this initial open complex. Subsequently XPA demarcates the lesion and RPA binds to the strand opposite of the lesion. RPA further facilitates proper positioning of the two structure-specific endonucleases ERCC1/XPF and XPG, which cleave the damaged strand 5' and 3' of the lesion, respectively. Finally, the replication machinery performs gap-filling DNA synthesis and the nick is ligated.



# Chapter 2

Transcription-coupled repair

# Transcription-coupled repair

## 2.1 Introduction

Different DNA lesions (including CPDs) located in the transcribed strand of active genes induce the stalling of elongating RNA polymerase II (RNAPII) complexes. Permanent transcription blockage is a powerful inducer of apoptosis, rendering these lesions extremely cytotoxic [29]. It is of prime importance to quickly remove transcription-blocking lesions to allow resumption of transcription and to prevent triggering of the apoptotic pathway. First evidence for such a specific repair pathway was reported by the group of Hanawalt who demonstrated faster removal of cyclo-pyrimidine dimers (CPDs) from actively transcribed genes compared to surrounding non-transcribed chromosome regions [30,31]. In addition, this phenomenon, designated transcription-coupled repair (TCR), was found to be restricted to the transcribed strand and does not occur in the absence of transcription [32,33].

## 2.2 TCR: a conserved repair mechanism

TCR is a strongly conserved repair mechanism in a variety of organisms. A genetic screen for *mfd* (*mutation frequency decline*) mutants in *E. Coli* resulted in identification of a gene involved in strand-specific repair [34]. The 130 kDa protein product of this gene was named TRCF (transcription repair coupling factor) or Mfd. Functional analysis of the Mfd protein showed that it can release stalled *E. Coli* RNA polymerase from DNA in an ATP-dependent manner [35]. In addition, Mfd can also promote forward translocation of stalled elongation complexes in a backtracked position [36]. Furthermore, Mfd was found to interact with the damage recognition protein UvrA, which, together with UvrB and UvrC performs the excision repair reaction in *E. Coli*, indicating that subsequent to lesion recognition by Mfd actual repair of the lesion is analogous to global genome repair (GGR) [37].

In *S. cerevisiae*, the Rad26 gene product was found to be implicated in transcription-coupled repair [38]. Surprisingly, challenging a *rad26* deficient strain with UV does not result in an increased sensitivity compared to wild type cells, most likely caused by the high efficiency of GGR in yeast cells. Indeed, mutating *rad26* in a *rad7* or *rad16* (GGR deficient) background showed a synergistic effect on the UV-sensitivity of these strains [39]. Similar to Mfd, Rad26 is a DNA-dependent ATPase [35,40].

## 2.3 Mammalian transcription-coupled repair

In contrast to a mild phenotype in yeast, disruption of the TCR pathway in humans gives rise to the severe Cockayne Syndrome (CS), suggesting a more important role for TCR in cellular survival of multi-cellular organisms [41,42]. Unlike TCR-deficient yeast strains, cells derived from CS patients are highly sensitive to UV-irradiation and are unable to restore RNA and DNA synthesis after UV [43]. CS patients suffer from severe neurological problems, like neurodemyelination, mental retardation and hearing loss



## Common clinical features of Cockayne Syndrome patients

---

### **NER related**

Skin abnormalities  
  Photosensitivities  
  Thin, dry skin or hair

### **Non-NER related**

Developmental  
  Growth failure  
  Microcephaly  
  Impaired sexual development  
  Cachectic dwarfism  
  Skeletal deformations  
Neurologic dysfunctions  
  Accelerated neurological degeneration  
  Mental retardation  
  Delayed psychomotor development  
  Hearing loss  
  Wizened facial appearance  
  Calcification of basal ganglia of brain  
  Neurodysmyelination  
Ocular abnormalities  
  Cataracts  
  Progressive pigmentary retinopathy  
  Optic atrophy  
Dental abnormalities  
  Caries

---

Table adapted from Bootsma et al., 1997.

(Table 1). In addition, developmental pathologies arise, like growth failure, microcephaly and an impaired sexual development. The average life span of CS patients is ~12.5 years. Interestingly, CS patients do not show an increased incidence of skin cancer, like is seen in XP patients (>1000-fold elevated risk). In a detailed study of Nance and Berry, 140 cases of CS patients were reviewed and a careful definition of diagnostic criteria and pathological features was reported [44].

They describe three forms of CS: classical CS (CS I), severe CS (CS II) and mild CS. CS I patients are diagnosed by the presence of two of seven characteristic features: growth failure, neurodevelopmental problems, cutaneous photosensitivity, pigmentary retinopathy and cataracts, sensorineural hearing loss, dental caries and cachectic dwarfism. In addition, laboratory studies must show a sensitivity of patient cells to UV and an absence of RNA synthesis recovery after UV. CS II patients are characterized by a more severe and earlier onset of CS symptoms. They often have a low birth weight and show little postnatal growth. Symptoms like facial abnormalities, cataracts and eye abnormalities manifest already at two years of age. The mean age of death of this type of patients is usually 6-7 years old. In contrast, mild CS patients show a late onset of clinical features. Some patients in this group show normal intelligence and growth and have a normal reproductive capacity. In addition, patients exist that only

display mild UV-sensitivity and inability to recover RNA synthesis after UV, but do not show other particular CS features. These persons are diagnosed as UV-sensitive (UV-S) syndrome patients [45]. Also CS patients exist, which show normal UV-sensitivity and RNA synthesis recovery after UV but do exhibit other characteristic features of CS [46]. In addition, cerebro-oculo-facio-skeletal (COFS) syndrome patients with a mutation in CSB have been characterized [47]. COFS syndrome and CS II patients share progressive demyelination with brain calcification.

## **2.4 Genetic heterogeneity of Cockayne Syndrome**

Next to a heterogenic clinical manifestation of CS, also at the genetic level CS is a complex disease. Cell fusion studies showed the presence of two complementation groups in CS: CS-A and CS-B [48]. In addition, certain mutated alleles of *XPB*, *XPD* or *XPG* also give rise to a combined form of CS and XP, suggesting that these factors also play a central role in TCR. *XPB*, *XPD* (subunits of TFIIH) and *XPG* are also involved in global genome repair (GGR), explaining the presence of the combined XP and CS features. The characterization of the CS factors and other factors that play a crucial role in mammalian TCR are listed below.

### **2.4.1 CSA**

The Cockayne Syndrome A (CS-A) gene was cloned by Henning and coworkers and encoded for a five WD40 repeats containing polypeptide [49]. These particular protein domains do not exhibit any specialized enzymatic function but are thought to be involved in the formation of multiprotein complexes [50]. Biochemical gel filtration studies showed that indeed CSA resides in a high molecular weight complex of ~420 kDa [51].

Recently, using a cell line expressing epitope-tagged CSA, a CSA-containing complex was purified [52]. Careful analysis of the co-purifying peptides resulted in identification of DDB1, Cul4A (cullin 4A), Roc1 (also named Rbx1 or Hrt1) and CSN (COP9 signalosome) as complex partners of CSA. Unexpected is the presence of the GGR factor DDB1 in the complex (see Chapter 1). Interestingly, the authors also show purification of a DDB2 complex, which is identical to the CSA complex, except for either the presence of CSA or DDB2 in the complex. Although CSA and DDB2 are both WD40 proteins and show a high level of similarity (48%), both complexes do have separate activities in TCR and GGR [52]. Cul4A was previously found to co-immunoprecipitate with the UV-DDB complex [53]. Cul4A is a member of the cullin family of proteins, which are characterized by their ubiquitin ligase activity. These proteins, also referred to as E3s, accomplish the last step in transferring an ubiquitin moiety to a protein, which is a common modification to target proteins for degradation by the proteasome. Prior to ubiquitin ligation, ubiquitin activation and conjugation are performed by E1 and E2 enzymes, respectively. The ubiquitin ligase activity of Cul4A is suggested to be stimulated by conjugation of NEDD8 (Neural precursor cell-Expressed Developmentally Down-regulated) to the ubiquitin-like protein Cul4A, an activity which is also found for other cullin family members [54,55]. Roc1 is a RING finger protein and member of the F-box family of proteins, containing a characteristic 40 amino acid F-box motif. It is also a

component of the VCB (VHL/ElonginC/ElonginB) complex and the SCF (for Skp1, Cdc53, F-box protein) complex, which are both E3 ubiquitin ligases and interact with a variety of cullins (for review: [56]). Roc 1 enhances the ubiquitin ligating activity of these complexes by tethering the different components to each other, resulting in ubiquitin-dependent proteasomal degradation of proteins involved in cell cycle progression and signal transduction. The COP9 signalosome is build up of eight subunits (CSN1-8) and exists as a protein complex on its own. CSN has a NEDD8-deconjugating activity (also referred to as deneddylation) of the cullin component of SCF complexes. Groisman and coworkers show that upon UV, an increasing amount of the CSN complex binds to the core CSA complex, resulting in deneddylation of Cul4A and subsequent inhibition of the ubiquitin ligase activity of the CSA 'core' complex. Knocking down the CSN5 component of the CSN complex, using an RNA interference based strategy, resulted in a reduction of RNA synthesis recovery after UV, suggesting that the inhibition of ubiquitin ligating activity of the CSA complex is indispensable for TCR.

In addition, CSA was found to interact with the p44 subunit of TFIIH [49]. CSA was also reported to interact with CSB *in vitro* [49]. This latter finding however could not be confirmed by immunoprecipitation studies using whole cell extracts (WCEs) and classical chromatography of HeLa WCEs showed that CSB does not co-purify with CSA [51].

#### 2.4.2 CSB

The Cockayne Syndrome B (CS-B) gene encodes for a 168 kDa protein and is a member of the SWI/SNF family of putative helicases [57]. This family of proteins is characterized by the presence of seven typical regions, together forming the Snf2-like helicase domain. Other members of this protein family are involved in a variety of processes like transcriptional regulation, chromatin remodeling and other DNA repair pathways (post-replication repair and homologous recombination) [58]. Based on data from other SWI/SNF family members, like SWI2/SNF2 and Mot1, it has been proposed that these proteins typically translocate along the DNA and destabilize protein-DNA interactions upon hydrolysis of ATP [59]. Besides the Snf2-like helicase domains, the CSB protein also contains an acidic stretch (aa 356-394), a glycine-rich region (aa 442-446) and a nuclear localization signal (NLS; aa 466-481). In addition, two putative casein kinase II phosphorylation sites are found close to the NLS motif [57].

Biochemical analysis of the protein revealed that CSB is a dsDNA-dependent ATPase lacking classical helicase activity [60,61]. *In vitro*, dephosphorylation of CSB enhances the ATPase activity, indicate for a role for phosphorylation in regulating the activity of the CSB protein in repair [62]. Gel filtration experiments showed that CSB resides in a complex of >700 kDa [51]. Immunoprecipitation experiments showed a clear interaction with RNA polymerase II (RNAPII) in WCEs, whereas gel mobility shift assays provided evidence for an interaction of CSB with RNAPII ternary complexes containing DNA and RNA [51,63]. Other reports show an interaction of CSB with XPA, XPG, the p34 subunit of TFIIH and TFIIH by immunoprecipitation of *in vitro* translated proteins and GST-pull downs [60,64].

Experiments described in chapter 6 showed that CSB is able to induce negative supercoils in single nicked plasmid DNA. This activity is not dependent on active hydrolysis of ATP, since the CSB<sup>K538R</sup> mutant, which is still able to bind ATP, also displays topological activity. Furthermore, CSB can remodel chromatin at the expense of ATP and interacts with histones in a histone-tail dependent manner. The chromatin remodeling activity of CSB is dependent on the presence of the amino-terminal tails of the histones, which form a common target for chromatin modifying enzymes.

#### 2.4.3 XAB2

The XAB2 protein was identified on the basis of its capability to bind to the XPA protein, which is involved in the core NER reaction [65]. This protein contained 15 class I TPRs (tetratricopeptide repeats). Proteins with TPRs are implicated in various processes in the cell like splicing, mitosis and transcription [66]. The TPR repeats form helix-turn structures, which are thought to associate with helices in other proteins. Next to XPA binding, XAB2 also interacts with CSA, CSB and RNAPII [65]. It was suggested that XAB2 may function as a bridging factor between CSA and CSB in TCR. In addition, XAB2 may be implicated in recruitment of the repair machinery, thereby stimulating the repair rate of TCR.

#### 2.4.5 XPG

XPG is a 133 kDa endonuclease with sequence homology to members of the FEN1 family of endonucleases. These structure-specific endonucleases incise DNA at junctions of single- and double stranded DNA like bubble and loop structures [67,68]. Within NER, XPG is known to incise the DNA 3' of the lesion. Mutations in the XPG gene give rise to a broad range of phenotypes from mild XP symptoms to a much more severe phenotype with CS like features (combined XP and CS). It is believed that XP-G patients with solely XP pathology only have a defect in the function of XPG in NER. These patients have point mutations that leave the protein intact but only affect the 3' incision activity in the core NER reaction. Other mutations resulting in severe truncation of the protein are associated with the more severe XP-CS phenotype. In addition to a defect in NER, cells from these patients are also deficient in removal of 8-oxoG lesions and thymine glycols, suggesting that XPG has an additional role in TC-BER [69,70]. Klungland and coworkers additionally showed that in an *in vitro* reconstituted BER reaction, XPG can stimulate binding of the DNA glycosylase hNth1 to damaged DNA [71]. *In vivo*, XP-G/CS cells show reduced levels of repair of 8-oxoG lesions from non-transcribed sequences, indicating that XPG may have a role in both TC-BER and global BER [70].

#### 2.4.6 TFIIH

TFIIH is a nine-subunit basal transcription factor (see paragraph 1.3) and is involved in RNAPII-mediated transcription and NER. However, whether the CAK component of TFIIH is required for NER remains unclear. CAK is not required to accomplish a NER reaction *in vitro* [72]. However, a defect in Kin28, a component of yeast CAK, resulted in impaired TC-NER, whereas GG-NER was unaffected [73]. In

addition, immunofluorescence experiments using antibodies directed against CAK subunits show that the complex accumulates at sites of local damage but is absent from the site of damage in a TCR-defective background. This suggests that CAK is only required for repair events of TFIIH during TCR [74]. Cells from XPB/CS and XPD/CS patients were also found to be deficient in strand-specific removal of 8-oxoG lesions, suggesting that, next to its role in GG-NER, TFIIH is also implicated in TCR-dependent removal of BER type of lesions [69].

## 2.5 Mouse models for Cockayne Syndrome

A mouse model for CS was created by introducing a point mutation in the mouse *CSB* gene, resulting in a truncated form of the protein [75]. This modification of the *CSB* gene is analogous to the mutation found in CS1AN *CSB*-deficient human fibroblasts. *CSB*<sup>-/-</sup> mice show similar repair features as CS patients, like sensitivity to UV and absence of RNA synthesis recovery after UV. In addition, these mice display photosensitivity and mild forms of growth failure and neurological abnormalities. Interestingly, in contrast to human CS patients, *CSB*<sup>-/-</sup> mice are more susceptible to UV-induced cancer compared to wild type mice. A possible explanation for this difference between humans and mice is the fact that the activity of the GGR pathway is more prominent in humans compared to rodents. This makes mice more dependent on TCR and will result in higher mutation frequencies in *CSB*-deficient mice. Interestingly, crossing of *CSB*<sup>-/-</sup> mice into a NER deficient background results in a severely deteriorated phenotype. *CSB*<sup>-/-</sup>/*XPC*<sup>-/-</sup> and *CSB*<sup>-/-</sup>/*XPA*<sup>-/-</sup> mice show severe growth retardation, display neurological problems and die before weaning. This suggests that in the absence of GGR the *CSB* phenotype is more pronounced and most likely is caused by an accumulation of endogenous DNA lesions (lesions induced by cellular metabolites) in transcribed genes. In addition, the phenotype of these double knockout mice is more severe than that of *XPA* mice, which are totally NER deficient, indicative for an additional function of *CSB* next to its function in NER. Recently, a CSA-deficient mouse was made, which displays the same features as a *CSB*<sup>-/-</sup> mouse including the proneness to UV-induced formation of skin cancers [76].

## 2.6 Molecular basis for CS features

The basis for the clinical features of CS is a lack of TCR. However, it is difficult to contribute all characteristics of this syndrome to a DNA repair defect. Whereas cutaneous photosensitivity is clearly the result of a DNA repair defect, developmental problems cannot be directly explained by the absence of TCR or NER lesions.

Reactive oxygen species, inevitable side products of cellular metabolism, induce DNA lesions that are usually a target for BER. These lesions can be induced in all body parts, independent of environmental exposure. Accumulation of BER lesions in the nervous system may lead to the observed developmental defects in CS patients. Cells from CS-B patients are sensitive to ionizing radiation and strand-specific repair of ionizing radiation-induced DNA damage was reported, suggesting the existence of a transcription-

coupled BER pathway [77]. Cells from CS-A patients also show a reduced, although less prominent, survival after ionizing radiation. In addition, *CSB*<sup>-/-</sup> mouse embryonic fibroblasts (MEFs) are highly sensitive to ionizing radiation and paraquat (both giving rise to BER-type of lesions) [78]. In contrast, total NER-defective *XPA*<sup>-/-</sup> MEFs are not sensitive to oxidative damage. These results suggest that the absence of CSB in CS patients may lead to transcription blockage on oxidative damage as was reported for 8-oxoG lesions [69]. Interestingly, *CSB*<sup>-/-</sup> embryonic stem (ES) cells only show a marginal sensitivity to ionizing radiation compared to wild type ES cells, indicating that the relative contribution of TCR and GGR to repair of oxidative lesions may vary between different cell types [78].

Another explanation for the phenotype of CS patients is interference of other cellular processes. TTD patients, who display a phenotype similar to CS patients (except for brittle hair and nails), were reported to have an impaired transcription rate caused by low levels of TFIIH in the cell [79,80]. In addition, careful analysis of the transcriptional capacity of TFIIH complexes with different mutations in *XPD* showed that recombinant TFIIH containing TTD-type of mutated *XPD* display lowered levels of basal transcription *in vitro* as compared to TFIIH containing an XP-type of *XPD* mutation [81]. Similarly, disruption of the CS genes leads to a slightly affected transcription, suggesting an additional role for CSB in transcription (see next chapter). However, the viability of CS patients rules out an essential role for both proteins in this process. The resemblance in phenotype between TTD and CS patients let to the assumption that both are transcription syndromes [82].

## 2.7 Molecular mechanism of TCR

As described above, transcription blockage is a trigger for TCR. In addition, *in vitro* experiments clearly showed that the presence of CPD lesions in the transcribed strand form a strong block for RNAPII [83]. It is assumed that the helical distortion, as induced by NER-type of lesions, interferes with processive RNAPII elongation. DNA injuries in the non-transcribed strand do not interfere with efficient elongation of the RNAPII holo-enzyme. Footprint analysis of an RNAPII elongation complex stalled at a CPD lesion shows that the polymerase covers approximately 35nt around the lesion in an asymmetrical manner, forming a steric hindrance for the repair machinery [84]. This observation let to the question how DNA repair factors access the site of damage to repair the damaged strand. Various molecular models have been postulated for this accessibility problem in TCR (Figure 3).

(1) A backtracking mechanism by which RNAPII is displaced (pushed back) from the site of damage without releasing it from the DNA, allowing transcription resumption after repair. This is a similar mechanism as was found for the elongation factor TFIIIS, which induces endonucleic cleavage of the nascent mRNA, creating a new 3' end in the catalytic pocket of the polymerase [85]. Interestingly, Tornaletti and coworkers showed that TFIIIS is able to backtrack a RNAPII elongation complex stalled at a CPD lesion thereby promoting repair of the lesion by a photolyase [84].

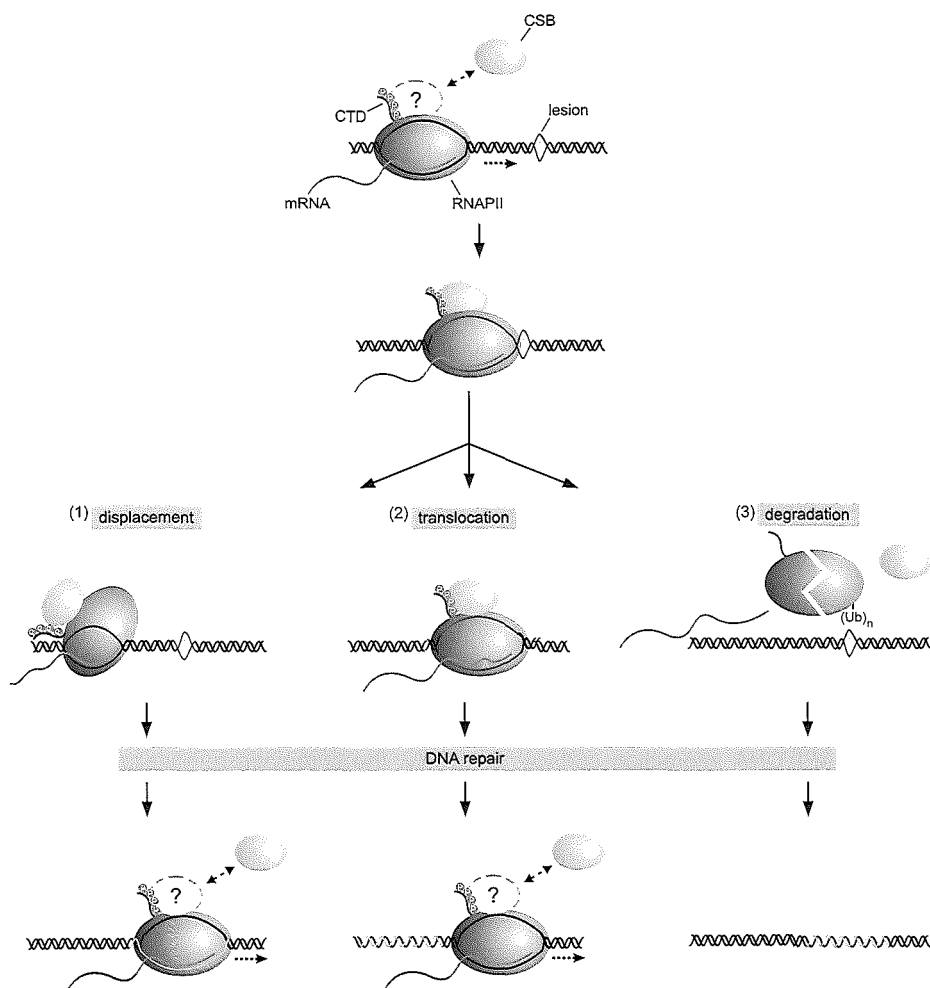


**Figure 3. Molecular models for functioning of CSB in TCR.** During transcription elongation of RNAP II it is unknown whether CSB stably associates or only transiently interacts with the polymerase. (1) Displacement of the stalled polymerases provides accessibility to the lesion for repair factors without actual removal of RNAPII and allowing transcription resumption after repair. (2) Translocation of the RNAP II past the lesion (trans-lesion RNA synthesis). (3) Polyubiquitination and subsequent degradation of the RNAP II molecules will result in loss of the nascent mRNA and requires reinitiation of transcription to synthesize a new mRNA.

(2) A completely opposite mechanism has also been postulated, in which blocked polymerases are pushed over the lesion (trans-lesion RNA synthesis). This latter activity was observed for the bacterial transcription-repair coupling factor Mfd acting on non-damage stalled RNA polymerase molecules [36]. Upon removal of the DNA injury elongation can be reactivated and transcription of the mRNA is finished.

(3) A third model suggests physical removal of the blocked polymerase from the template by ubiquitin-mediated proteolysis. [86,87]. Evidence for this model was obtained by the observed absence of polyubiquitination of RNAPII in both CS-A and CS-B cells [86]. During this process the unfinished mRNA is discarded and reinitiation of transcription is required to synthesize a new mRNA.

(4) Evidence for coexistence of both models (translocation versus degradation) in the cell came from a study on yeast TCR by Woudstra and colleagues [88]. They identified a polypeptide, designated Def1 (RNAPII degradation factor 1), which co-purifies with Rad26 (the yeast homologue of CSB). Def1 was found to stimulate polyubiquitination and proteosomal degradation of yeast RNA polymerase in a UV-dependent manner. In contrast, Rad26 was found to stimulate repair of the lesion without removing the RNA polymerase from its template. The authors suggest a model in which, upon transcription stalling on a DNA lesion, Rad26 first attempts to initiate TCR without removal of the polymerase. If Rad26 is unable to displace the RNA polymerase from the damaged site Def1 functions as a backup and stimulates degradation of the polymerase through induction of polyubiquitination of the enzyme [89].

In mammals, the molecular mechanism and function of CSA and CSB in TCR remain unclear. The recent finding that CSA resides in a complex with ubiquitin ligating activity suggests that CSA may play a role in polyubiquitination of the stalled RNAPII complex, although upon UV this activity is inhibited by association of the COP9 signalosome [52]. CSB is suggested to play a role in displacement of the polymerase. First, CSB can change the topology of the DNA helix by binding and wrapping the DNA around itself (Nancy Beerens, pers. communication). This activity may affect the stability of the RNAPII/DNA interaction surface. Secondly, the chromatin remodeling activity of CSB may be implicated in facilitating the accessibility of the repair machinery to the site of damage. Alternatively this activity of CSB may also extend to a function in partially dissociating RNAPII from its template, leading to displacement of the RNAPII complex. In addition, a strong UV-dependent reduction of RNAP II molecules with a hypophosphorylated C-terminal domain was observed in extracts of CSB cells [171]. This form of RNAPII is normally required for transcription initiation (see Chapter 3), suggesting that in the absence of CSB transcription initiation is severely reduced. The authors suggest a model in which transcription resumption after UV is also dependent on regeneration of the hypophosphorylated form of RNAPII.



# Chapter 3

Involvement of the CSB protein in  
transcription elongation

# Involvement of the CSB protein in transcription elongation

## 3.1 Introduction

Transcription in eukaryotes is performed by three distinct RNA polymerases. RNA polymerase I (RNAPI) is involved in transcription of the large ribosomal RNAs. RNA polymerase III (RNAPIII) is responsible for transcription of transfer RNAs and the 5S ribosomal RNA. Synthesis of mRNAs from all protein coding genes is performed by RNA polymerase II (RNAPII). Three stages have been recognized during a transcription cycle of a gene, i.e. initiation at the promoter, elongation and termination. For RNAPII-dependent transcription multiple basal transcription factors (BTFs) are required. Transcription initiation starts with the formation of the preinitiation complex (PIC). This complex consists of TFIID, TFIIB, TFIIF, TFIIIE and TFIIH and RNAPII. TFIID is the first BTF to bind the promoter. TFIID is composed of the TATA binding protein (TBP), which recognizes and binds the TATA box (position -25/-30), and multiple TBP-associated factors (TAFs). Subsequently, TFIIB binds TFIID and a specific sequence upstream of the TATA-box. Next, RNAPII and TFIIF enter the complex, followed by TFIIIE and TFIIH. TFIIH is specifically involved in unwinding of the promoter region.

Transcription initiation takes place in three separate steps [90]. First the promoter area (-9/+2) is unwound by TFIIH. Subsequently, moving of the PIC to position +4 stabilizes the open complex. Finally, when the PIC reaches position 9 to 11, the promoter is cleared and the activity of the RNAPII complex shifts to a productive elongating mode. During transcription initiation, kinase subunits of TFIIH are responsible for phosphorylation of the C-terminal domain (CTD) of the large subunit of RNAPII (Rpb1), which contains 52 heptapeptide repeats with the consensus sequence Tyr-Ser-Pro-Thr-Ser-Pro-Ser. CTD-hyperphosphorylation is thought to be the signal for promoter clearance and transition of the RNA polymerase into processive elongation, most likely by inducing dissociation of the SRB/Mediator complex and BTF's from RNAPII (for review: [91]). During promoter clearance TFIID, TFIIB and TFIIIE remain at the promoter. TFIIH is assumed to stay connected to the RNAPII holoenzyme during early elongation, whereas TFIIF remains stably associated to the elongating RNAPII complex.

## 3.2 Elongation factors

Transcription elongation is a discontinuous process. Processivity of RNAPII is affected by multiple factors like sequence context, DNA-bound proteins and DNA lesions, which can induce (transient) stalling of the RNAPII complex. However, multiple mechanisms guarantee the processivity of RNA polymerases during elongation. Recently, trailing RNA polymerases, purified from *E. Coli*, were found to display anti-arrest and anti-pausing activity by inducing forward translocation of leading polymerases *in vitro* [92]. However, the existence of such a mechanism in humans has as yet not been explored. One can envisage that such an elongation-stimulating mechanism can only be exploited on highly transcribed genes. However, most RNAPII-transcribed genes in humans are thought to contain only one or a few transcribing polymerases, suggesting that this

elongation stimulating system is not suitable for most transcribed genes in humans [93]. In addition, elongation factors can reactivate stalled polymerases, leading to an increased processivity of the RNAPII.

Mechanistically, elongation factors can be divided in different classes (for review: [85]). The first class of elongation factors stimulates the rate of elongation by suppressing transient pausing of the RNAPII complex (e.g. TFIIF, ELL and Elongin). These factors are suggested to reduce the time that RNAPII complexes are in an inactive mode on the template.

Another group of elongation factors can reactivate RNAPII molecules that are arrested on its template (TFIIS) [85]. Stalled RNAPII molecules slide back on the template, a phenomenon referred to as backtracking. This event displaces the 3'-end of the mRNA from the active site of the polymerase, which interferes with transcription reactivation. RNAPII has the intrinsic activity to cut the phosphodiester bond of the nascent backtracked mRNA in the active site, resulting in formation of a new 3' end of the mRNA, which allows transcription resumption. TFIIS is able to stimulate this intrinsic activity of the RNAPII complex. Recent analysis of TFIIS/yeast RNAPII crystals showed that domain III of TFIIS invades in the RNAPII pore and most likely participates in the ribonucleolytic cleavage by positioning two highly conserved acidic residues in the active site [94]. TFIIF, ELL and Elongin are thought to inhibit backtracking of the polymerase thereby preventing the transition of the polymerase from an active into an arrested state. This is illustrated by the fact that all these three elongation factors can counteract TFIIS-stimulated mRNA cleavage activity, most likely by preventing translocation of the 3' end of the mRNA from the catalytic site of the polymerase [95].

A third group of elongation promoting enzymes is capable of stimulating RNAPII-processivity through alteration of the chromatin context in the transcribed gene (HMG14, FACT, Elongator, SWI/SNF) [96]. When HMG-14 (high mobility group) is assembled in chromatin, this leads to an open chromatin structure, which results in higher levels of transcription. FACT (facilitates chromatin transcription) was found to enhance RNAPII elongation rate by overcoming nucleosome-dependent blockage [97]. In addition, the yeast FACT complex was found to interact with Sas3 (something about silencing), a histone acetyl transferase (HAT) [98]. HATs can acetylate lysine residues on histone tails of nucleosomes resulting in a more open chromatin structure, which is permissive to transcription elongation [99]. Probably, this FACT-associated HAT activity is responsible for the elongation stimulatory effect of FACT. Similarly, the Elp3 subunit of the yeast and human Elongator complex is able to acetylate histone H3 and H4, thereby opening up the chromatin structure, making it more permissive to transcription elongation [100-102]. Recently, SWI/SNF, initially isolated as an ATP-dependent chromatin-remodeling complex that repositions nucleosomes, was also found to enhance elongation of RNAPII [103]. It was shown that efficient mRNA production of the mouse *hsp70* gene is both dependent on the presence of functional HSF1 (heat shock factor 1) and recruitment of SWI/SNF to downstream positions in the gene, indicating that SWI/SNF-dependent chromatin remodeling activity is not only restricted to the promoter region of the gene.

Another form of regulation of transcription elongation takes place via phosphorylation of the CTD of Rpb1. Examples of elongation factors directly or indirectly

affecting the phosphorylation state of the CTD are the kinases P-TEFb (positive transcription elongation factor b), Hiv-Tat and the phosphatase Fcp1 [91]. P-TEFb is suggested to stimulate early elongation by interfering with the inhibitory effects of DSIF (DRB-sensitivity inducing factor) and NELF (negative elongation factor). This may explain the fact that P-TEFb is capable of stimulating early elongation in the presence of DRB, a transcription inhibitor acting via DSIF. Interestingly, also FACT was found to interact with DSIF and interfere with DSIF-mediated inhibition of transcription elongation on naked DNA templates, indicating that FACT may have multiple targets to control transcription elongation [104].

The question remains how the activities of these different elongation factors are organized in the living cell. Are they all stably associated to the transcribing RNAPII enzyme or rather sequestered when their specific actions are required? The large number of elongation factors gives rise to the question whether all these proteins can assemble on an RNAPII molecule at the same time?

### 3.3 A function for CSB in transcription elongation?

Next to a role in TCR, CSB is suggested to function in transcription elongation. Gel filtration and immunoprecipitation studies showed that CSB resides in a high molecular weight complex interacting with *in vitro* active RNAPII ([53], chapter 8). In addition, gel mobility shift assays demonstrated that CSB interacts with a ternary complex of DNA, RNAPII and nascent RNA [63,105]. More evidence for a role of CSB in transcription was provided by Selby and Sancar [106]. They showed that CSB is capable of enhancing transcription elongation in an *in vitro* reconstituted transcription system. In addition, it was reported that CS-B cells show reduced transcription levels *in vivo*. [107,108].

Similarly, Rad26-deficient (the yeast homologue of CSB) cells display reduced transcription levels of several genes [109]. Moreover, under conditions requiring high levels of transcription, *rad26Δ* cells show reduced growth. A synergistic increase of this phenotype is found in a *rad26Δ dst1Δ* (the yeast homologue of TFIIS) strain, suggesting that a general defect in transcription elongation causes the phenotype. Moreover, in a genetic screen *Spt4* was identified as a suppressor mutant of *Rad26* [110]. *Spt4* is a subunit of the DSIF complex, which associates with RNAPII and regulates its processivity [111,112]. The authors suggest a model in which Rad26 functions as an elongation factor causing transcription to be TCR competent in an *Spt4*-dependent manner.

Next to a role in RNAPII-dependent transcription, CSB is also linked to RNAPI and RNAPIII transcription. Immunofluorescent imaging showed that CSB locates to the nucleolus, the subnuclear compartment where RNAPI transcription takes place (chapter 7 and [113]). In addition, immunoprecipitation studies demonstrated that CSB interacts with the RPA116 and TAF-68 subunit of RNAPI, the transcription factor TIF-1B and the XPB and XPD subunits of TFIIH [113]. TFIIH was recently also found to be implicated in RNAPI-dependent transcription [114,115]. Furthermore, in an *in vitro* reconstituted RNAPI transcription system, CSB stimulated transcription on a ribosomal template up to 10-fold in a TFIIH-dependent manner [113]. The role of TFIIH-dependent stimulation of RNAPI

activity by CSB may be explained by the fact that CSB is required for the interaction between TFIIF and RNAPII. Finally, the authors show that CS-B cells are deficient in ribosomal RNA transcription, which can be rescued by introduction of wild type CSB. Evidence for implication of CSB in RNAPII-dependent transcription was reported by Yu and coworkers [116]. They showed that CSB-deficient cells display metaphase fragility of the *RNU1*, *RNU2* and *RNS5* loci, which are transcribed by RNAPII. Introduction of wild type CSB cDNA led to restoration of the normal metaphase packaging of the genes. The authors suggest a model in which CSB is required for transcription through highly structured RNAPII genes.

### 3.4 Molecular mechanism of CSB in transcription

Although multiple reports suggest a role for CSB in transcription, the mechanism for its role in elongation remains unclear. CSB induces lengthening of the transcript with one nucleotide of CPD-stalled RNAPII molecules [106]. In addition, CSB counteracts TFIIS-dependent shortening of the mRNA, suggesting that both proteins have an opposing mechanism for stimulating elongation *in vivo*. In this regard, CSB acts similar to TFIIF, ELL and Elongin, whom all inhibit backtracking of the polymerase and TFIIS-dependent cleavage of the 3' end of the mRNA [95]. A comparable activity was found for the Mfd protein, the *E.Coli* homologue of CSB [36,117]. Mfd promotes forward translocation of stalled RNA polymerases from a backtracked position and stimulated repositioning of the 3' end of the mRNA in the active site of the RNA polymerase, thereby reactivating transcription elongation. For this activity Mfd interacts with ~25 bp of DNA upstream of the RNA polymerase. In addition, Mfd was found to interact with a small part of the  $\beta$  subunit of the RNA polymerase. These findings suggest that Mfd has a distinct activity compared to other bacterial elongation factors like GreA and GreB (TFIIS-like proteins). In eukaryotes, CSB may function in a similar way, allowing transcription resumption of stalled RNAPII complexes on a pause site by translocating it along the DNA, in fact pushing it over the stalling-causing lesion (i.e. translesion synthesis), possibly through remodeling the interaction surface of the RNAPII on the DNA. A separate mechanism for a transcription stimulatory activity of TFIIS and CSB explains the synergistic effect of *rad26* and *dst1* deletions on the growth rate under conditions requiring high transcription levels in yeast [109].

The helical distortion, typical for NER-type of lesions, forms a physical block for RNAPII elongation, actually being a potent pause-site. In view of the postulated function of CSB in transcription elongation, a similar function of assisting translocation along the DNA can be envisaged. However, such a translocating activity of CSB was not observed *in vitro* on CPD lesion-blocked RNAPII molecules [106]. CSB may provoke a change in the interaction surface of RNAPII with the DNA when the elongation complex is stalled at lesions, thereby provoking access to repair factors to the site of damage. Alternatively, failure to displace the polymerase from the site of damage may lead to polyubiquitination and subsequent proteasome dependent degradation of the RNAPII enzyme [86].

It is evident that despite advanced studies of both transcription elongation and transcription-coupled repair a unifying model integrating both processes is still not

present. To identify the exact relationship between these nuclear processes, more sophisticated approaches than the current *in vitro* assays are required, since these do not allow to study these processes (transcription and repair) simultaneously. This failure to create reliable *in vitro* TCR assays is likely due to the absence of structural elements (such as chromatin and the nuclear matrix) for regulation of this complex process. Only recently new tools have become available to study complex cellular processes in their natural context. (1) The identification and cloning of the green fluorescent protein (GFP), which provided a tool to study localization of tagged proteins in time and space in living cells. (2) Advanced live cell microscopic and spectroscopic techniques to directly measure protein mobility, real-time complex assembly and reaction kinetics *in vivo*. In order to obtain further insight into the mechanism of CSB action in live cells, we have used these procedures (see chapters 7,8 and 9). Before describing the actual scientific and biological implications of these sophisticated procedures (chapter 5) first the details of this novel biological approach are described in chapter 4.

# Chapter 4

Dynamic studies in living cells  
using GFP-tagged proteins

# Dynamic studies in living cells using GFP-tagged proteins

## 4.1 Introduction

For a long time visualization of proteins in cells was performed using techniques like histochemical and immuno-histological detection. The antibodies used in these assays are raised against a specific epitope on the protein or recognize a specific tag, which is fused to the protein of interest. A drawback of these techniques is that they can only be carried out on fixed cells. Microinjection of fluorescently conjugated antibodies in living cells or other types of *in vivo* labeling do allow visualization of proteins in living cells. However, these techniques are limited by the fact that they affect the homeostasis of a cell and not a large population of cells can be studied. A new tool for protein visualization studies in living cells became available with the identification of the green fluorescent protein (GFP) [118]. This 27 kDa protein was initially isolated from the jellyfish *Aequorea victoria* [119]. The natural function of GFP appears to be converting blue bioluminescence of the  $\text{Ca}^{++}$ -sensitive phosphoprotein aequorin to green light. Characteristic for GFP is the autonomous fluorescent capacity, meaning that no exogenous cofactor or substrate is required for this activity.

## 4.2 Physical parameters of GFP

GFP absorbs blue light at 395 nm and has a smaller excitation peak at 475 nm but only one emission peak a wavelength of 508 nm [120]. The characteristics of this excitation- and emission spectrum are defined by the structure of the internal *p*-hydroxybenzylidene-imidazolidinone chromophore. The chromophore becomes functional upon cyclization and subsequent oxidation of the successive serine, tyrosine and glycine residues at position 65 to 67 [121]. These posttranslational modifications are established in an autocatalytic way, not depending on the presence of other *A. victoria* enzymes [122]. This feature allows formation a fluorescent molecule upon ectopic expression of this protein in other species, ranging from prokaryotes to eukaryotes.

GFP is predominantly in its neutral form, which absorbs light of 395 nm, whereas the ionized (anionic) form is excited at 475 nm. Mutation of the Serine at position 65 to a Tyrosine (S65T) causes permanent ionization of the chromophore, completely abolishing the 395 nm absorption peak, shifting the 475 nm peak to 489 nm and increasing the fluorescent intensity approximately 6-fold [123,124]. This mutant form of GFP is more attractive for live cell studies since excitation can be performed using standard 488 nm argon lasers. Further mutagenesis of the phenylalanine at position 64 to a leucine (F64L) led to the creation of the enhanced GFP (EGFP) variant, which displays a 35-fold increased brighter fluorescence [125,126]. To stimulate translation of EGFP mRNA in human cell systems this EGFP cDNA contains approximately 190 silent mutations stimulating usage of favored human codons [127].

Analysis of the crystal structure of the GFP revealed that it consists of  $\beta$ -sheets that form a barrel with a diagonal  $\alpha$ -helix in the inside of the barrel. In the middle of this inner helix the chromophore is positioned (Figure 4) [128,129]. In addition, distorted



helical segments cover both top and bottom of the barrel. The buried position of the chromophore probably ensures that radicals, generated during the process of excitation and emission, are quenched by the GFP molecule itself. This may be a reason that even at higher expression levels GFP is not toxic for the cell and can fluoresce without causing damage to the cell.

A screen for *A. victoria* mutants led to the identification of the blue fluorescent protein (BFP), cyan fluorescent protein (CFP) and the yellow fluorescent protein (YFP) [120,128]. The different excitation and emission spectra of these GFP-variants allow concomitant imaging of differentially tagged proteins in the same cell.

Studies of the excitation/emission behavior of the S65G/S72A/T203F GFP mutant showed that during excitation for longer times at 488 nm single GFP molecules are switching between an emissive anionic *on*-state or a non-emissive neutral *off*-state (both for a few seconds) [130]. This type of fluorescent behavior of GFP was designated 'blinking' (also referred to as reversible bleaching). After emission of approximately  $10^6$  photons a GFP moiety was found to transfer to a long lasting (>5 minutes) non-fluorescent or 'dark' state. In addition, studies performed on another GFP mutant showed that the *on*-time of a GFP molecule is strongly dependent on the excitation intensity, whereas the *off*-time is not affected by intensity changes [131]. Weber and coworkers also presented quantum chemical calculations, in which they suggest the existence of a, non-fluorescent, zwitterionic form of GFP [132]. Taken together, this shows that during excitation GFP molecules can reversibly transfer to a short photo-induced *off*-state and, with lower probability, to an irreversible dark state. Finally, similar to other organic dyes, GFP can transfer from its emissive 'singlet' state to a non-emissive 'triplet' state with a lifetime of 5-25  $\mu$ s [133,134]. This very short non-emissive state of GFP seems to coexist next to the *on*- and *off*-state described above.

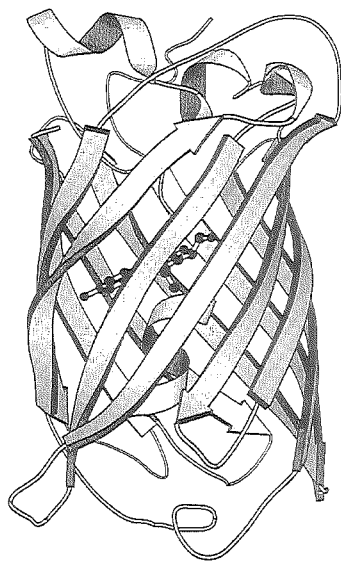


**Figure 4. Crystal structure of the green fluorescent protein (GFP).** The chromophore is encapsulated in a barrel-like structure consisting of  $\beta$ -sheets. Adapted from Ormo et al., 1996.

#### 4.3 Mobility and interaction studies using GFP

The fact that, upon high intensity excitation, the GFP chromophore transfers to a permanently bleached state made it possible to use photobleaching to study the dynamic behavior of a GFP-tagged protein (Figure 5). This technique is known as fluorescence redistribution after photobleaching (FRAP). In typical FRAP experiments a focussed high intensity laser pulse bleaches molecules in a small part of the cell. Subsequently, the redistribution of bleached and unbleached molecules can be monitored. This allows the

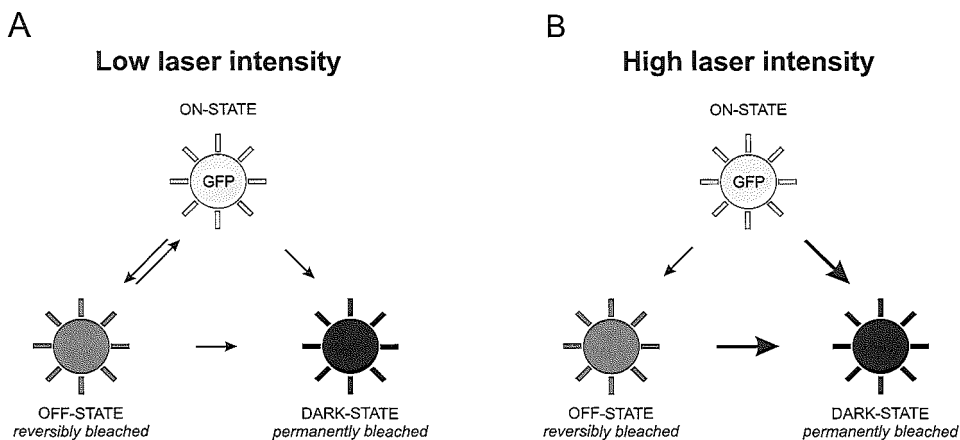


**Figure 5. Schematic diagram of photo-induced states of GFP molecules using different laser intensities.** (A) During excitation of GFP with low laser intensity a portion of GFP molecules temporarily transfers from a fluorescent *on*-state to a reversibly bleached *off*-state. A small amount of molecules will transfer to a permanently bleached dark state. (B) Excitation of GFP with high laser intensity will eventually induce permanent bleaching of the majority of the molecules.

determination of the mobility of a protein and to identify possible bound or (transient) immobile fractions. FRAP was initially developed to study the dynamics of plasma membrane-bound proteins in living cells [135,136]. Bleaching of organic fluorophores allowed measuring the dynamic redistribution of membrane-bound proteins. A drawback is the invasive character of these studies (e.g. microinjection of fluorophores). Photobleaching of GFP in living cells made it possible to perform FRAP measurements in a non-invasive manner.

Apart from analysis of the dynamic behavior of single proteins GFP can also be used to measure protein-protein interactions in living cells. Usually, interactions between different proteins are studied using *in vitro* co-immunoprecipitations or yeast-two-hybrid analysis. Fluorescence resonance energy transfer (FRET) experiments with CFP- and YFP-tagged proteins provide a tool to study protein-protein interactions in living cells (for review: [137]). When two differentially tagged proteins interact and the fluorophores are in close proximity ( $<100\text{\AA}$ ) excitation of CFP (donor) can result in 'sensitized' emission of YFP (acceptor), as caused by transmission of the energy from excited CFP. FRET can be visualized in different ways: (1) direct measurement of acceptor emission after donor excitation, (2) acceptor-bleaching resulting in increased fluorescent intensity of the donor fluorophore, (3) or fluorescence lifetime imaging (FLIM) [138]. Using FLIM, interactions are detected based on the lifetime of fluorescence of individual fluorophores, since the lifetime of the donor is reduced when FRET occurs. An advantage of this technique is that the two different GFP-variants do not have to be spectrally different, avoiding detection problems of short-wave emitting GFP-mutants like BFP or CFP.

Another fast developing technique to study protein mobility in living cells is fluorescence correlation spectroscopy (FCS) [139]. During FCS, the fluctuations of photons (emitted by the GFP-tagged proteins) in a very small, defined volume in the cell are measured. Upon determination of the autocorrelation function of these fluorescent fluctuations the average number of fluorescently tagged molecules in this volume (concentration) and their diffusion rate can be determined. Since FCS is highly sensitive, it is possible to measure different diffusing species of the protein of interest (i.e. freely mobile, transient interaction, complex formation) in the same volume. In addition, differentially tagging of two proteins of interest allows dual-color FCS, which, using cross-correlation analysis, can be used to identify an interacting fraction of proteins as a single diffusing species.

#### 4.4 FRAP-based mobility studies

The implementation of GFP fusion and expression to aid cellular studies has fully boosted the application of FRAP-based experimentation. Concomitant with the increased need FRAP-procedures have quickly developed. Below explanations of techniques that are used in this thesis are described.

##### 4.4.1 FRAP

During FRAP analysis a small part of the nucleus is bleached followed by measurement of the fluorescent recovery in the bleached area. Typically, a small 2  $\mu\text{m}$  strip is defined in the middle of the nucleus, in which the fluorescent intensity is monitored every tenth of a second (at low laser intensity) (Figure 6A and B). Approximately two seconds after start of the experiment, the marked area is bleached for 0.2 seconds using a high intensity laser pulse and the fluorescent recovery is measured. The rate of fluorescent recovery directly after bleaching is a measure for the effective diffusion coefficient ( $D_{\text{eff}}$ ) of the tagged protein. Calculation of  $D_{\text{eff}}$  is performed by fitting the initial recovery plot to a mathematically derived curve, describing one-dimensional diffusion in a plane. Note that the maximum fluorescent intensity after bleaching is slightly lower because of the bleached fraction of molecules.

In addition, an immobile fraction of the protein of interest can be deduced from a decreased influx of molecules in the strip. If the immobilized time of a protein is shorter than the duration of recovery monitoring, the recovery plot has a different character compared to a long-term immobilized protein. A transiently bound fraction of molecules will result in a biphasic recovery plot. First, the plot will show a relatively fast recovery of fluorescence caused by free diffusing proteins. Subsequently, more slowly, the bleached molecules that are released from their bound state will induce an additional increase of fluorescence in the strip. Taken together, this technique provides a tool to concomitantly study the diffusion behavior and the binding of a protein to less mobile cellular structures (e.g. binding to genomic DNA) in living cells.

Instead of measuring the recovery of fluorescent intensity in a bleached area (FRAP) also monitoring the loss of fluorescent intensity in a non-bleached area upon

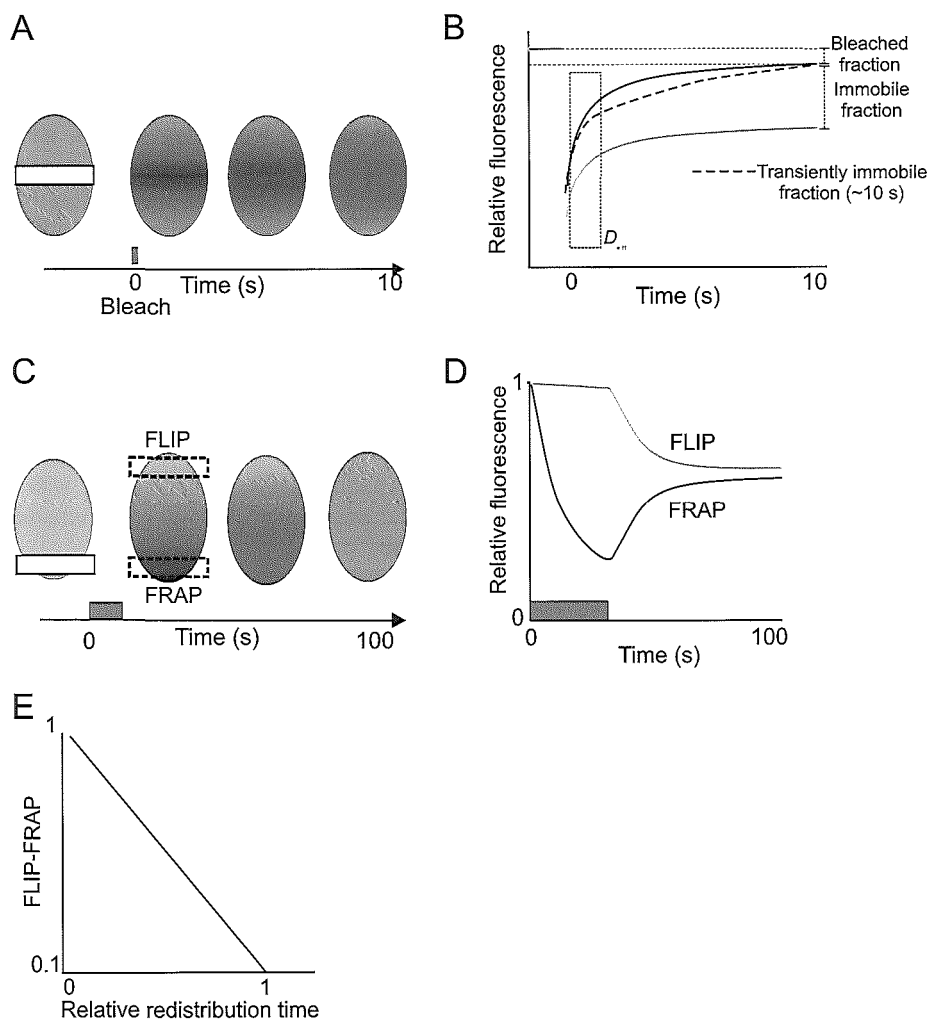


**Figure 6. Schematic representation of FRAP and combined FLIP-FRAP experiments.** (A) Using FRAP, the fluorescent molecules in a small defined volume in the strip spanning the nucleus are bleached and fluorescent recovery in time is measured. (B) The rate of influx of fluorescent molecules in the strip is a measure for the effective diffusion constant ( $D_{eff}$ ). In addition, a possible (transient) binding can be deduced from the complete recovery. (C) Using combined FLIP/FRAP, one pole of the cell is bleached and fluorescent recovery is measured (FRAP). Concomitantly the loss of fluorescence at the opposite pole of the cell is measured (FLIP). (D) The relative fluorescent intensities of the FRAP and FLIP areas plotted against time show that the difference between both regions disappears (both lines come together) because of total redistribution of the bleached and unbleached molecules. (E) When the FLIP and FRAP relative fluorescence intensities are subtracted and plotted on a logarithmic scale (y-axis), intersection with x-axis gives the relative redistribution time of a protein.

bleaching in another region of the cell is used to measure the mobility of a protein. This technique is designated FLIP (fluorescence loss in photobleaching).

#### *4.4.2 Simultaneous FLIP-FRAP*

Simultaneous FLIP-FRAP was developed to enlarge small differences measured using FRAP analysis. The simultaneous FLIP-FRAP protocol exploits the length of the whole nucleus during FRAP measurements. (Figure 6C-E) Briefly, a region at one pole of the nucleus is bleached and recovery of the fluorescent intensity is measured (FRAP). Concomitantly, on the opposite pole of the cell the decrease in fluorescence is monitored (FLIP). The time to reach the fluorescence equilibrium (i.e. the fluorescence at the bleached pole [FRAP] reached the same level as the non-bleached pole [FLIP]) is a measure for the overall nuclear mobility. The data are plotted as the difference in fluorescence intensity between both regions (FLIP-FRAP) on a logarithmic scale. The steepness of the curve is a measure for the speed of redistribution and the time point of crossing of the horizontal axis (set as a percentage of complete redistribution) indicates the total redistribution time.



# Chapter 5

Organization of nuclear processes  
in living cells

# Organization of nuclear processes in living cells

## 5.1 Introduction

Various nuclear processes are suggested to be a tightly regulated process based on energy-dependent transport of the protein complexes to their place of action. Chromosome positions were found to be restricted to particular subspaces in the nucleus, creating a defined nuclear architecture consisting of chromosome territories and interchromatin compartments (for review: [140]). Life cell imaging by Gerlich and coworkers even showed that chromosome positions are inherited to the next generation [141]. The compartmentalized distribution of chromosomes suggested that also chromatin-associated processes, like replication, transcription, splicing and repair, may be restricted to certain areas in the nucleus. It was proposed that proteins involved in these processes would form pre-assembled complexes in the interchromatin compartments, too big to diffuse through the chromosome territories and that chromatin-associated processes take place at the surface of these territories [142].

This compartmentalization model resulted in the idea that the transcriptional activity of a gene is defined by its relative positioning in the chromosome territory. Highly transcribed genes would be positioned close to the interchromatin compartment, whereas low expressed or silenced genes are found in the relative inaccessible center of a chromatin territory. Interestingly, activation of genes does lead to the formation of chromosomal loops protruding out of the chromatin territories, indicative for a spatial model for transcription regulation [143]. Actual transcription has been proposed to take place in so-called 'transcription factories', containing multiple transcribing RNA polymerases (for review: [93]). Quantification of the number of transcribing polymerases in HeLa cells showed approximately 15.000 RNAPI, 65.000 RNAPII and 10.000 RNAPIII molecules are transcribing in every cell [144,145].

Similarly, splicing factors are also localized in large molecular assemblies named 'speckles', which are localized to the interchromatin compartment [146]. Often transcription sites are found close to or even in speckles, suggesting that transcription and splicing are two processes, which are tightly regulated in a spatial manner [147]. However, other reports also show splicing activity in transcription sites, which are not associated with speckles, indicating that splicing may not be strictly compartmentalized [148]. Moreover, localization of splicing factors to transcription sites was found to be dependent on the C-terminal domain (CTD) of RNAPII, suggesting a direct co-transcriptional place of action for the splicing machinery [149]. These latter findings indicated that the structural organization of different nuclear processes is likely a dynamic organization that either changes at different stages through the cell cycle, differentiation status, species, specificity or environmental conditions or that all the different types of organization are just snapshots of metastable structures that are in equilibrium with each other.

The highly compartmentalized organization of nuclear processes further suggests that there is no free exchange of constituents and that the flow of material requires active transport. Moreover, movement of nuclear protein should be severely



restricted by exclusion of these compartments. However, evidence provided using an artificial system by Seksek and coworkers showed that protein mobility is not severely hampered by the various subnuclear structures and is not dependent on active transport through the nucleus [150]. Diffusion analysis of fluorescently labeled dextrans in living cells showed free diffusion through the nucleus up to a molecular weight of 500-750 kDa. The diffusion rate in the nucleus is only ~3-4 fold decreased compared to free diffusion in water, indicating that within the nucleus enough space is available to allow macromolecules to diffuse and that both the viscosity (high concentrations of protein) and obstacles (chromatin fibers) reduce the motility rate, resulting in an actual effective or constant diffusion. More recently, with the aid of GFP-tagging and photo bleaching (see chapter 4), FRAP experiments showed a highly dynamic behavior of proteins involved in transcription, splicing and repair [151,152]

## 5.2 Transcription in living cells

To directly visualize transcription in living cells and to study the dynamic behavior of factors involved various transcription factors like TBP, TFIIB, TFIIF and RNAPII have been fused to GFP. The localization and dynamic behavior of RNAPII was studied by tagging the large subunit of this holoenzyme (Rpb1) to GFP [153]. This chimeric protein was hyperphosphorylated on the CTD, located to active transcription sites and was able to correct the phenotype of a temperature-sensitive Rpb1 mutant CHO (chinese hamster ovary) cell line emphasizing the functionality of the protein. FRAP analysis showed that the majority of RNAPII-GFP (~75%) freely diffuses and that ~25% is immobilized. Assuming that this immobilization reflects actual engagement of RNAPII in transcription elongation this suggests that about one fourth of the total amount of polymerases is engaged in active transcription in a cell under normal circumstances [154]. Transcription inhibition using DRB resulted in a decrease of the immobilized fraction, probably because of release of inhibited RNAPII molecules, whereas the transcription inhibitor actinomycin D, enhanced the immobile fraction, most likely by an increased fraction of bound RNAPII molecules stalled on intercalated actinomycin D molecules. The measured half-life of immobile molecules was ~20 minutes, suggesting that average RNAPII molecules are immobilized for ~40 minutes. Radiolabeling of nascent RNA showed that accumulation of labeled transcripts has a  $t_{1/2}$  of ~14 minutes, which is in the same order as the  $t_{1/2}$  of the immobilized time of RNAPII molecules. Earlier experiments however, based on the typical length of a human gene (~14kb) and the average rate of RNAPII polymerization ( $1.1-2.5 \times 10^3$  nt/min), showed that a typical transcription unit is transcribed in 6-13 minutes [155,156]. This apparent discrepancy between binding time and mean elongation time can be explained by the idea that the observed immobilization time of RNAPII reflects the entire transcription cycle: binding, initiation (by proper binding of basal factors), elongation, termination and subsequent release rather the elongation alone. [154,157].

The basal transcription initiation factor TFIIB seems to have a diffusion rate corresponding to its own molecular size, suggesting that it is not preassembled in a transcription holocomplex [158]. TBP however, a component of TFIID, shows a very slow

recovery time after photobleaching ( $t_{1/2}$ ~20 minutes), suggesting that the TFIID complex may remain promoter-associated through different cycles of transcription [158]. Recently, TFIID was found to roam the nucleus according to its own molecular weight and is immobilized for ~6 seconds in RNAPII-dependent transcription initiation, emphasizing that initiation itself is a swift process, depending on shortly interacting BTFs [115].

A similar type short-term interaction was observed for the GFP-tagged glucocorticoid receptor (GR), a transcription activator belonging to the family of steroid nuclear receptors [159]. In addition, a similar type of such a 'hit and run' mode of interaction for binding GR molecules to their responsive element was observed for the glucocorticoid receptor interacting protein (GRIP-1), which also quickly exchanges between its bound and non-bound state ( $t_{1/2}$ ~5 seconds) [160].

The same dynamic principle of RNAPII interactions were observed with RNAPI [161]. A kinetic framework for RNAPI transcription was provided through GFP-tagging of multiple subunits of the RNAPI holoenzyme and RNAPI-specific transcription factors. All components localize to fibrillar centers in the nucleoli, which are typical places for RNAPI-dependent transcription. The initial influx in the nucleoli, directly after bleaching, is different for all components, indicating that they do not form a holocomplex outside the nucleolus, but rather assemble on the site of transcription initiation [157,161]. The exchange rates of RNAPI transcription preinitiation factors like Ubf1, Ubf2 and TAF<sub>48</sub> were found to be 30-35 seconds. TFIID, which also has a role in RNAPI transcription initiation is immobilized for ~25 seconds in the nucleolus [114,115]. The average time of RNAPI molecules to be actively engaged in elongation is 2-3 minutes.

## 5.3 DNA repair in living cells

### 5.3.1 Homologous recombination

Studying the nuclear organization of repair factors is an obvious approach to learn more about DNA repair. Immunofluorescence experiments in fixed cells showed that proteins involved in homologous recombination like Rad51, Rad52 and Rad54 are dispersed through the nucleus and are located to focal structures upon treatment with ionizing radiation (IR). These focal structures are most like formed at the site of a double-strand DNA break. FRAP experiments (described above) on cells expressing either GFP-tagged Rad51, Rad52 or Rad54 showed that all three proteins travel through the nucleus with different diffusion rates, arguing against the existence of a pre-assembled holocomplex in undamaged cells [162]. Like the untagged endogenous proteins, also the GFP-tagged proteins accumulated into foci after IR. FRAP experiments revealed a dramatic difference in residence time of these proteins in foci: Rad54 showed a fast recovery ( $t_{1/2}$ ~0.5 seconds), Rad52 a more delayed recovery ( $t_{1/2}$ ~26 seconds) and Rad51 hardly recovered over time suggesting that the latter is a more stably bound component of these structures.

### 5.3.2 Nucleotide excision repair

Immunofluorescence studies of the nuclear organization of NER in fixed cells showed that most NER factors, like XPA, TFIIH and XPC are homogeneously distributed throughout the nucleoplasm and do not have a specific nuclear distribution in the cell [14,163-166]. Only XPG was reported to localize to focal structures, which are dispersed through the nucleoplasm upon UV-irradiation [167]. The number of foci decreased within two hours after UV and was recovered eight hours after DNA damage induction. In addition, TFIIH was found in foci in a cell-cycle dependent manner, most likely dependent on the transcription levels in the cell [14].

GFP-tagging allowed localization of NER proteins in living cells without fixation, avoiding potential fixation artifacts. Functional ERCC1-GFP, expressed at physiological levels in ERCC1-deficient CHO cells, showed a homogeneous localization throughout the nucleus [151]. The measured effective diffusion rate demonstrated the fusion protein to travel through the nucleus according to its own molecular weight. Furthermore, the protein showed a UV-dose-dependent immobilization of maximally ~40%. This immobile fraction decreased in time after UV and the protein returned to a fully mobile state ~6 hours after irradiation, concomitant with removal of the bulk of induced 6-4PPs. Measurements of the immobilized state of ERCC1-GFP molecules revealed single polypeptides to bind for ~4 minutes, most likely reflecting the time of ERCC1 to be involved in repair. Similarly, XPA-GFP and XPB-GFP were also found to diffuse according to their molecular weight and were also immobilized upon UV-irradiation with a maximum of ~40% [115,168]. Both proteins were also found to accumulate at sites of local damage, and FRAP and FLIP measurements on these accumulations showed a residence time varying from 3-5 minutes, similar to ERCC1, indicating that a single NER repair event probably lasts for 4 minutes. Compared to ERCC1, XPA and TFIIH, XPC-GFP was found to have a different behavior [169]. First, XPC is not homogeneously distributed through the nucleus, more or less resembling the inhomogeneous distribution of DNA. Furthermore, FRAP experiments and subsequent computer simulations suggest a model in which the protein continuously associates and dissociates to an immobile nuclear structure, most likely DNA. Photobleaching experiments on XPC accumulated at a locally damaged area revealed that its residence time is only 1-2 minutes, which is shorter than found for the other repair proteins [115,151,168,169]. This indicates that XPC, as the first protein to recognize the lesion, may only be required for the initial moments of the NER reaction and leaves the complex prior to other NER proteins. Alternatively, the presence of abortive repair complexes may lead to a reduction of the residence time of XPC molecules at a locally damaged area.

### 5.3.3 Transcription-coupled repair

Since the bulk of DNA lesions are repaired by the GGR pathway, the measured dynamics of the ERCC1, XPA and TFIIH protein most likely reflect their activity in this subpathway of NER. However, the dynamic interaction and reaction kinetics of TCR are poorly understood. More specific experiments on the involvement of TFIIH in GGR and TCR showed that in transcription-inhibited cells, in which TCR is absent, the maximal immobilized fraction of TFIIH is decreased to from ~40% to ~25% and that this immobile

fraction is already absent two hours after UV [170]. This indicates that TCR-dependent immobilization accounts for ~15% of the immobilized fraction of TFIIH. Most surprisingly, it takes more time to recover from TCR-dependent immobilization compared to GGR-dependent immobilization, which is unexpected since TCR is generally thought to be a faster process than GGR. In addition, the residence time of TFIIH in both TCR and GGR appeared equal (~4 minutes). The dynamic properties of the TCR-specific proteins CSB and CSA are described in the chapters 7 and 9 respectively. GFP-CSB was found to immobilize up to ~15% in a UV-dose dependent manner, whereas GFP-CSA does not show any immobilization at all. The residence time for CSB at a locally damaged site was calculated to be ~2-2.5 minutes, indicating that similar to XPC, CSB probably leaves the assembled repair complex prior to other proteins. Interestingly, CSB transiently interacts with elongating RNAPII, probably monitoring the processivity of the enzyme and intervening upon transcriptional stalling of the polymerase on a DNA damage.

Taken together, GFP-based photobleaching studies in living cells revealed a highly dynamic behavior of various proteins involved in multiple nuclear processes. These observations lead to the proposition of a new probabilistic model for complex assembly in which pre-assembled holo-complexes do not exist as such and that separate components only assemble at the site of action, driven by stochastic exchange of freely mobile constituents. This suggests that final macromolecular machines are not stable, ready-to-use factories that are available multiple rounds of activity but are assembled and disassembled after each cycle of action. Although this process may seem inefficient and therefore energetically unfavorable, a potential advantage of stochastic behavior of proteins is the tremendous flexibility for cells to rapidly respond to changing environmental conditions. Multifunctional proteins can directly exchange between various cellular pathways in which they are involved. For example, TFIIH can exchange between separate kinetic pools, performing its function in transcription initiation of RNAPII-dependent transcription (~25 seconds), RNAPII-dependent transcription (~6 seconds) or repair of NER lesions (~4 minutes) [115]. Similarly, regulation of transcription elongation and TCR may be mediated through stochastic interactions, as illustrated by the differential binding kinetics of CSB to active and stalled RNAPII molecules.

Investigation of these DNA-transacting processes using quantitative fluorescence imaging in living cells hopefully will result in a better understanding of nuclear functioning. Integration of experimentally derived data and in silico computer modeling of kinetic processes may provide a tool to obtain a clear view on the integration of and interaction with various nuclear processes *in vivo*.

## References

1. **Hoeijmakers, J.H.** (2001) Genome maintenance mechanisms for preventing cancer. *Nature*, 411, 366-74.
2. **Lindahl, T.** (1993) Instability and decay of the primary structure of DNA. *Nature*, 362, 709-715.
3. **van Gent, D.C., Hoeijmakers, J.H. and Kanaar, R.** (2001) Chromosomal stability and the DNA double-stranded break connection. *Nat Rev Genet*, 2, 196-206.
4. **Lindahl, T. and Wood, R.D.** (1999) Quality control by DNA repair. *Science*, 286, 1897-905.
5. **de Boer, J. and Hoeijmakers, J.H.** (2000) Nucleotide excision repair and human syndromes. *Carcinogenesis*, 21, 453-60.
6. **Masutani, C., Sugawara, K., Yanagisawa, J., Sonoyama, T., Ui, M., Enomoto, T., Takio, K., Tanaka, K., van der Spek, P.J., Bootsma, D. and et al.** (1994) Purification and cloning of a nucleotide excision repair complex involving the xeroderma pigmentosum group C protein and a human homologue of yeast RAD23. *Embo J*, 13, 1831-43.
7. **Shivji, M.K., Eker, A.P. and Wood, R.D.** (1994) DNA repair defect in xeroderma pigmentosum group C and complementing factor from HeLa cells. *J Biol Chem*, 269, 22749-57.
8. **Reardon, J.T., Mu, D. and Sancar, A.** (1996) Overproduction, purification, and characterization of the XPC subunit of the human DNA repair excision nuclease. *J Biol Chem*, 271, 19451-6.
9. **Sugawara, K., Ng, J.M., Masutani, C., Iwai, S., van der Spek, P.J., Eker, A.P., Hanaoka, F., Bootsma, D. and Hoeijmakers, J.H.** (1998) Xeroderma pigmentosum group C protein complex is the initiator of global genome nucleotide excision repair. *Mol. Cell*, 2, 223-232.
10. **Janicijevic, A., Sugawara, K., Shimizu, Y., Hanaoka, F., Wijgers, N., Djurica, M., Hoeijmakers, J.H. and Wyman, C.** (2003) DNA bending by the human damage recognition complex XPC-HR23B. *DNA Repair (Amst)*, 2, 325-36.
11. **Tang, J.Y., Hwang, B.J., Ford, J.M., Hanawalt, P.C. and Chu, G.** (2000) Xeroderma pigmentosum p48 gene enhances global genomic repair and suppresses UV-induced mutagenesis. *Mol Cell*, 5, 737-44.
12. **Datta, A., Bagchi, S., Nag, A., Shiyonov, P., Adami, G.R., Yoon, T. and Raychaudhuri, P.** (2001) The p48 subunit of the damaged-DNA binding protein DDB associates with the CBP/p300 family of histone acetyltransferase. *Mutat Res*, 486, 89-97.
13. **Yokoi, M., Masutani, C., Maekawa, T., Sugawara, K., Ohkuma, Y. and Hanaoka, F.** (2000) The xeroderma pigmentosum group C protein complex XPC-HR23B plays an important role in the recruitment of transcription factor IIH to damaged DNA. *J Biol Chem*, 275, 9870-5.
14. **Volker, M., Mone, M.J., Karmakar, P., van Hoffen, A., Schul, W., Vermeulen, W., Hoeijmakers, J.H., van Driel, R., van Zeeland, A.A. and Mullenders, L.H.** (2001) Sequential assembly of the nucleotide excision repair factors in vivo. *Mol Cell*, 8, 213-24.
15. **Evans, E., Moggs, J.G., Hwang, J.R., Egly, J.M. and Wood, R.D.** (1997) Mechanism of open complex and dual incision formation by human nucleotide excision repair factors. *EMBO J*, 16, 6559-6573.
16. **Tirode, F., Busso, S., Coin, F. and Egly, J.M.** (1999) Reconstitution of the transcription factor TFIIH: assignment of functions for the three enzymatic subunits, XPB, XPD, and cdk7. *Mol. Cell*, 3, 87-95.
17. **Winkler, G.S., Araujo, S.J., Fiedler, U., Vermeulen, W., Coin, F., Egly, J.M., Hoeijmakers, J.H., Wood, R.D., Timmers, H.T. and Weeda, G.** (2000) TFIIH with inactive XPD helicase functions in transcription initiation but is defective in DNA repair. *J. Biol. Chem.*, 275, 4258-4266.
18. **Bradsher, J., Coin, F. and Egly, J.M.** (2000) Distinct Roles for the Helicases of TFIIH in Transcript Initiation and Promoter Escape. *J. Biol. Chem.*, 275, 2532-2538.
19. **Egly, J.M.** (2001) The 14th Datta Lecture. TFIIH: from transcription to clinic. *FEBS Lett*, 498, 124-8.

20. **Serizawa, H., Makela, T.P., Conaway, J.W., Conaway, R.C., Weinberg, R.A. and Young, R.A.** (1995) Association of Cdk-activating kinase subunits with transcription factor TFIIH. *Nature*, 374, 280-2.
21. **Shiekhatar, R., Mermelstein, F., Fisher, R.P., Drapkin, R., Dynlacht, B., Wessling, H.C., Morgan, D.O. and Reinberg, D.** (1995) Cdk-activating kinase complex is a component of human transcription factor TFIIH. *Nature*, 374, 283-7.
22. **Coin, F., Marinoni, J.C., Rodolfo, C., Fribourg, S., Pedrini, A.M. and Egly, J.M.** (1998) Mutations in the XPD helicase gene result in XP and TTD phenotypes, preventing interaction between XPD and the p44 subunit of TFIIH [see comments]. *Nat Genet*, 20, 184-8.
23. **Mu, D., Hsu, D.S. and Sancar, A.** (1996) Reaction mechanism of human DNA repair excision nuclease. *J. Biol. Chem.*, 271, 8285-8294.
24. **Evans, E., Fellows, J., Coffey, A. and Wood, R.D.** (1997) Open complex formation around a lesion during nucleotide excision repair provides a structure for cleavage by human XPG protein. *EMBO J.*, 16, 6625-6238.
25. **de Laat, W.L., Appeldoorn, E., Sugawara, K., Weterings, E., Jaspers, N.G. and Hoeijmakers, J.H.** (1998) DNA-binding polarity of human replication protein A positions nucleases in nucleotide excision repair. *Genes Dev.*, 12, 2598-2609.
26. **O'Donovan, A., Davies, A.A., Moggs, J.G., West, S.C. and Wood, R.D.** (1994) XPG endonuclease makes the 3' incision in human DNA nucleotide excision repair. *Nature*, 371, 432-435.
27. **Sijbers, A.M., De Laat, W.L., Ariza, R.R., Biggerstaff, M., Wei, Y.F., Moggs, J.G., Carter, K.C., Shell, B.K., Evans, E., De Jong, M.C., Rademakers, S., De Rooij, J., Jaspers, N.G.J., Hoeijmakers, J.H.J. and Wood, R.D.** (1996) Xeroderma pigmentosum group F caused by a defect in a structure-specific DNA repair endonuclease. *Cell*, 86, 811-822.
28. **Shivji, M.K., Podust, V.N., Hubscher, U. and Wood, R.D.** (1995) Nucleotide excision repair DNA synthesis by DNA polymerase epsilon in the presence of PCNA, RFC, and RPA. *Biochemistry*, 34, 5011-5017.
29. **Ljungman, M. and Zhang, F.** (1996) Blockage of RNA polymerase as a possible trigger for u.v. light-induced apoptosis. *Oncogene*, 13, 823-831.
30. **Bohr, V.A., Smith, C.A., Okumoto, D.S. and Hanawalt, P.C.** (1985) DNA repair in an active gene: removal of pyrimidine dimers from the *DHFR* gene of CHO cells is much more efficient than in the genome overall. *Cell*, 40, 359-369.
31. **Mellon, I., Bohr, V.A., Smith, C.A. and Hanawalt, P.C.** (1986) Preferential DNA repair of an active gene in human cells. *Proc Natl Acad Sci U S A*, 83, 8878-8882.
32. **Mellon, I., Spivak, G. and Hanawalt, P.C.** (1987) Selective removal of transcription-blocking DNA damage from the transcribed strand of the mammalian *DHFR* gene. *Cell*, 51, 241-249.
33. **Leadon, S.A. and Lawrence, D.A.** (1991) Preferential repair of DNA damage on the transcribed strand of the human metallothionein genes requires RNA polymerase II. *Mut. Research*, 255, 67-78.
34. **Selby, C.P., Witkin, E.M. and Sancar, A.** (1991) Escherichia-coli mfd mutant deficient in mutation frequency decline lacks strand-specific repair: in vitro complementation with purified coupling factor. *Proc. Natl. Acad. Sci. U.S.A.*, 88, 11574-11578.
35. **Selby, C.P. and Sancar, A.** (1995) Structure and function of transcription-repair coupling factor .1. structural domains and binding properties. *J. Biol. Chem.*, 270, 4882-4889.
36. **Park, J.S., Marr, M.T. and Roberts, J.W.** (2002) E. coli Transcription Repair Coupling Factor (Mfd Protein) Rescues Arrested Complexes by Promoting Forward Translocation. *Cell*, 109, 757-67.
37. **Sancar, A.** (1994) Mechanisms of DNA excision repair. *Science*, 266, 1954-1956.
38. **Van Gool, A.J., Verhage, R., Swagemakers, S.M.A., Van de Putte, P., Brouwer, J., Troelstra, C., Bootsma, D. and Hoeijmakers, J.H.J.** (1994) RAD26, the functional *Saccharomyces cerevisiae* homolog of the Cockayne syndrome-B gene ERCC6. *EMBO J.*, 13, 5361-5369.

39. **Verhage, R.A., Van Gool, A.J., De Groot, N., Hoeijmakers, J.H.J., Van de Putte, P. and Brouwer, J.** (1996) Double mutants of *Saccharomyces cerevisiae* with alterations in global genome and transcription-coupled repair. *Mol. Cell. Biol.*, 16, 496-502.
40. **Guzder, S.N., Habraken, Y., Sung, P., Prakash, L. and Prakash, S.** (1996) *Rad26*, the yeast homolog of human Cockayne's syndrome group B gene, encodes a DNA-dependent ATPase. *J. Biol. Chem.*, 271, 18314-18317.
41. **Venema, J., Mullenders, L.H.F., Natarajan, A.T., van Zeeland, A.A. and Mayne, L.V.** (1990) The genetic defect in Cockayne syndrome is associated with a defect in repair of UV-induced DNA damage in transcriptionally active DNA. *Proc. Natl. Acad. Sci. USA*, 87, 4707-4711.
42. **Van Hoffen, A., Natarajan, A.T., Mayne, L.V., Van Zeeland, A.A., Mullenders, L.H.F. and Venema, J.** (1993) Deficient repair of the transcribed strand of active genes in Cockayne's syndrome cells. *Nucl. Acids Res.*, 21, 5890-5895.
43. **Mayne, L.V. and Lehmann, A.R.** (1982) Failure of RNA synthesis to recover after UV irradiation: an early defect in cells from individuals with Cockayne's syndrome and xeroderma pigmentosum. *Cancer Res.*, 42, 1473-1478.
44. **Nance, M.A. and Berry, S.A.** (1992) Cockayne syndrome: Review of 140 cases. *Am. J. of Med. Genet.*, 42, 68-84.
45. **Itoh, T., Fujiwara, Y., Ono, T. and Yamaizumi, M.** (1995) UV<sup>s</sup> syndrome, a new general category of photosensitive disorder with defective DNA repair, is distinct from xeroderma pigmentosum variant and rodent complementation group 1. *Am. J. Hum. Gen.*, 56, 1267-1276.
46. **Colella, S., Nardo, T., Mallery, D., Borroni, C., Ricci, R., Ruffa, G., Lehmann, A.R. and Stefanini, M.** (1999) Alterations in the CSB gene in three Italian patients with the severe form of Cockayne syndrome (CS) but without clinical photosensitivity. *Hum. Mol. Genet.*, 8, 935-941.
47. **Meira, L.B., Graham, J.M., Jr., Greenberg, C.R., Busch, D.B., Doughty, A.T., Ziffer, D.W., Coleman, D.M., Savre-Train, I. and Friedberg, E.C.** (2000) Manitoba aboriginal kindred with original cerebro-oculo- facio-skeletal syndrome has a mutation in the Cockayne syndrome group B (CSB) gene. *Am J Hum Genet*, 66, 1221-8.
48. **Tanaka, K., Kawai, K., Kumahara, Y., Ikenaga, M. and Okada, Y.** (1981) Genetic complementation groups in cockayne syndrome. *Somatic Cell Genet*, 7, 445-55.
49. **Henning, K.A., Li, L., Iyer, N., McDaniel, L., Reagan, M.S., Legerski, R., Schultz, R.A., Stefanini, M., Lehmann, A.R., Mayne, L.V. and Friedberg, E.C.** (1995) The Cockayne syndrome group A gene encodes a WD repeat protein that interacts with CSB protein and a subunit of RNA polymerase II TFIIH. *Cell*, 82, 555-564.
50. **Neer, E.J., Schmidt, C.J., Nambudripad, R. and Smith, T.F.** (1994) The ancient regulatory-protein family of WD-repeat proteins. *Nature*, 371, 297-300.
51. **van Gool, A.J., Citterio, E., Rademakers, S., van Os, R., Vermeulen, W., Constantinou, A., Egly, J.M., Bootsma, D. and Hoeijmakers, J.H.J.** (1997) The Cockayne syndrome B protein, involved in transcription-coupled DNA repair, resides in a RNA polymerase II containing complex. *EMBO J.*, 16, 5955-5965.
52. **Groisman, R., Polanowska, J., Kuraoka, I., Sawada, J., Saijo, M., Drapkin, R., Kisselev, A.F., Tanaka, K. and Nakatani, Y.** (2003) The Ubiquitin Ligase Activity in the DDB2 and CSA Complexes Is Differentially Regulated by the COP9 Signalosome in Response to DNA Damage. *Cell*, 113, 357-67.
53. **Shiyanov, P., Nag, A. and Raychaudhuri, P.** (1999) Cullin 4A associates with the UV-damaged DNA-binding protein DDB. *J Biol Chem*, 274, 35309-12.
54. **Osaka, F., Kawasaki, H., Aida, N., Saeki, M., Chiba, T., Kawashima, S., Tanaka, K. and Kato, S.** (1998) A new NEDD8-ligating system for cullin-4A. *Genes Dev*, 12, 2263-8.
55. **Podust, V.N., Brownell, J.E., Gladysheva, T.B., Luo, R.S., Wang, C., Coggins, M.B., Pierce, J.W., Lightcap, E.S. and Chau, V.** (2000) A Nedd8 conjugation pathway is essential for proteolytic targeting of p27Kip1 by ubiquitination. *Proc Natl Acad Sci U S A*, 97, 4579-84.
56. **Craig, K.L. and Tyers, M.** (1999) The F-box: a new motif for ubiquitin dependent proteolysis in cell cycle regulation and signal transduction. *Prog Biophys Mol Biol*, 72, 299-328.

57. **Troelstra, C., Van Gool, A., De Wit, J., Vermeulen, W., Bootsma, D. and Hoeijmakers, J.H.J.** (1992) ERCC6, a member of a subfamily of putative helicases, is involved in Cockayne syndrome and preferential repair of active genes. *Cell*, 71, 939-953.
58. **Eisen, J.A., Sweder, K.S. and Hanawalt, P.C.** (1995) Evolution of the SNF2 family: subfamilies with distinct sequences and functions. *Nucleic Acids Res.*, 23, 2715-2723.
59. **Pazin, M.J. and Kadonaga, J.T.** (1997) SWI2/SNF2 and related proteins: ATP-driven motors that disrupt protein-DNA interactions? *Cell*, 88, 737-740.
60. **Selby, C.P. and Sancar, A.** (1997) Human transcription-repair coupling factor CSB/ERCC6 is a DNA- stimulated ATPase but is not a helicase and does not disrupt the ternary transcription complex of stalled RNA polymerase II. *J Biol Chem*, 272, 1885-90.
61. **Citterio, E., Rademakers, S., van der Horst, G.T., van Gool, A.J., Hoeijmakers, J.H. and Vermeulen, W.** (1998) Biochemical and biological characterization of wild-type and ATPase- deficient Cockayne syndrome B repair protein. *J. Biol. Chem.*, 273, 11844-11851.
62. **Christiansen, M., Stevnsner, T., Modin, C., Martensen, P.M., Brosh, R.M., Jr. and Bohr, V.A.** (2003) Functional consequences of mutations in the conserved SF2 motifs and post-translational phosphorylation of the CSB protein. *Nucleic Acids Res*, 31, 963-73.
63. **Tantin, D., Kansal, A. and Carey, M.** (1997) Recruitment of the putative transcription-repair coupling factor CSB/ERCC6 to RNA polymerase II elongation complexes. *Mol. Cell. Biol.*, 17, 6803-6814.
64. **Iyer, N., Reagan, M.S., Wu, K.-J., Canagarajah, B. and Friedberg, E.C.** (1996) Interactions involving the human RNA polymerase II transcription/nucleotide excision repair complex TFIIH, the nucleotide excision repair protein XPG, and Cockayne syndrome group B (CSB) protein. *Biochemistry*, 35, 2157-2167.
65. **Nakatsu, Y., Asahina, H., Citterio, E., Rademakers, S., Vermeulen, W., Kamiuchi, S., Yeo, J.P., Khaw, M.C., Saijo, M., Kodo, N., Matsuda, T., Hoeijmakers, J.H. and Tanaka, K.** (2000) XAB2, a novel tetratricopeptide repeat protein involved in transcription-coupled DNA repair and transcription. *J. Biol. Chem.*, 275, 34931-34937.
66. **Goebel, M. and Yanagida, M.** (1991) The TPR snap helix: a novel protein repeat motif from mitosis to transcription. *Trends Biochem Sci*, 16, 173-7.
67. **Scherly, D., Nospikel, T., Corlet, J., Ucla, C., Bairoch, A. and Clarkson, S.G.** (1993) Complementation of the DNA repair defect in xeroderma pigmentosum group G cells by a human cDNA related to yeast RAD2. *Nature*, 363, 182-5.
68. **O'Donovan, A., Scherly, D., Clarkson, S.G. and Wood, R.D.** (1994) Isolation of active recombinant XPG protein, a human DNA repair endonuclease. *The Journal of Biological Chemistry*, 269, 15965-15968.
69. **Le Page, F., Kwok, E.E., Avrutskaya, A., Gentil, A., Leadon, S.A., Sarasin, A. and Cooper, P.K.** (2000) Transcription-coupled repair of 8-oxoguanine: requirement for XPG, TFIIH, and CSB and implications for Cockayne syndrome. *Cell*, 101, 159-171.
70. **Cooper, P.K., Nospikel, T., Clarkson, S.G. and Leadon, S.A.** (1997) Defective transcription-coupled repair of oxidative base damage in Cockayne syndrome patients from XP group G. *Science*, 275, 990-993.
71. **Klungland, A., Hoss, M., Gunz, D., Constantinou, A., Clarkson, S.G., Doetsch, P.W., Bolton, P.H., Wood, R.D. and Lindahl, T.** (1999) Base excision repair of oxidative DNA damage activated by XPG protein. *Mol. Cell*, 3, 33-42.
72. **Wood, R.D., Biggerstaff, M. and Shivji, M.K.K.** (1995) Detection and measurement of nucleotide excision repair synthesis by mammalian cell extracts *in vitro*. *Methods, a companion to methods in enzymology.*, 7, 163-175.
73. **Tijsterman, M., Tasseron-de Jong, J.G., Verhage, R.A. and Brouwer, J.** (1998) Defective Kin28, a subunit of yeast TFIIH, impairs transcription-coupled but not global genome nucleotide excision repair. *Mutat Res*, 409, 181-8.
74. **Hoogstraten, D., Wijgers, N., Hoeijmakers, J.H. and Vermeulen, W.** A role for the cyclin-activating kinase complex in mammalian nucleotide excision repair. *manuscript in prep.*
75. **Van der Horst, G.T.J., Van Steeg, H., Berg, R.J.W., Van Gool, A.J., De Wit, J., Weeda, G., Morreau, H., Beens, R.B., Van Kreijl, C.F., De Gruijl, F.R., Bootsma, D. and Hoeijmakers, J.H.J.** (1997) Defective transcription-coupled repair in Cockayne syndrome B mice is associated with skin cancer predisposition. *Cell*, 89, 425-435.



76. van der Horst, G.T., Meira, L., Gorgels, T.G., de Wit, J., Velasco-Miguel, S., Richardson, J.A., Kamp, Y., Vreeswijk, M.P., Smit, B., Bootsma, D., Hoeijmakers, J.H. and Friedberg, E.C. (2002) UVB radiation-induced cancer predisposition in Cockayne syndrome group A (Csa) mutant mice. *DNA Repair (Amst)*, 1, 143-57.
77. Leadon, S.A. and Cooper, P.K. (1993) Preferential repair of ionizing-radiation induced damage in the transcribed strand of an active human gene is defective in Cockayne syndrome. *Proc.Natl.Acad.Sci.USA*, 90, 10499-10503.
78. de Waard, H., de Wit, J., Gorgels, T.G., van den Aardweg, G., Andressoo, J.O., Vermeij, M., van Steeg, H., Hoeijmakers, J.H. and van der Horst, G.T. (2003) Cell type-specific hypersensitivity to oxidative damage in CSB and XPA mice. *DNA Repair (Amst)*, 2, 13-25.
79. de Boer, J., de Wit, J., van Steeg, H., Berg, R.J., Morreau, H., Visser, P., Lehmann, A.R., Duran, M., Hoeijmakers, J.H. and Weeda, G. (1998) A mouse model for the basal transcription/DNA repair syndrome trichothiodystrophy. *Mol. Cell*, 1, 981-990.
80. Vermeulen, W., Bergmann, E., Auriol, J., Rademakers, S., Frit, P., Appeldoorn, E., Hoeijmakers, J.H. and Egly, J.M. (2000) Sublimiting concentration of TFIIH transcription/DNA repair factor causes TTD-A trichothiodystrophy disorder. *Nat Genet*, 26, 307-13.
81. Dubaele, S., De Santis, L.P., Bienstock, R.J., Keriell, A., Stefanini, M., Van Houten, B. and Egly, J.M. (2003) Basal transcription defect discriminates between xeroderma pigmentosum and trichothiodystrophy in XPD patients. *Mol Cell*, 11, 1635-46.
82. Bootsma, D. and Hoeijmakers, J.H.J. (1993) Engagement with transcription. *Nature*, 363, 114-115.
83. Donahue, B.A., Yin, S., Taylor, J.-S., Reines, D. and Hanawalt, P.C. (1994) Transcript cleavage by RNA polymerase II arrested by a cyclobutane pyrimidine dimer in the DNA template. *Proc. Natl. Acad. Sci. USA*, 91, 8502-8506.
84. Tornaletti, S., Reines, D. and Hanawalt, P.C. (1999) Structural characterization of RNA polymerase II complexes arrested by a cyclobutane pyrimidine dimer in the transcribed strand of template DNA. *J. Biol. Chem.*, 274, 24124-24130.
85. Fish, R.N. and Kane, C.M. (2002) Promoting elongation with transcript cleavage stimulatory factors. *Biochim Biophys Acta*, 1577, 287-307.
86. Bregman, D.B., Halaban, R., Van Gool, A.J., Henning, K.A., Freidberg, E.C. and Warren, S.L. (1996) UV-induced ubiquitination of RNA polymerase II: a novel modification deficient in Cockayne's syndrome cells. *Proc. Natl. Acad. Sci. USA*, 93, 11586-11590.
87. Ratner, J.N., Balasubramanian, B., Corden, J., Warren, S.L. and Bregman, D.B. (1998) Ultraviolet radiation-induced ubiquitination and proteasomal degradation of the large subunit of RNA polymerase II. Implications for transcription-coupled DNA repair. *J. Biol. Chem.*, 273, 5184-5189.
88. Woudstra, E.C., Gilbert, C., Fellows, J., Jansen, L., Brouwer, J., Erdjument-Bromage, H., Tempst, P. and Svejstrup, J.Q. (2002) A Rad26-Def1 complex coordinates repair and RNA pol II proteolysis in response to DNA damage. *Nature*, 415, 929-33.
89. van den Boom, V., Jaspers, N.G. and Vermeulen, W. (2002) When machines get stuck--obstructed RNA polymerase II: displacement, degradation or suicide. *Bioessays*, 24, 780-4.
90. Holstege, F.C., Fiedler, U. and Timmers, H.T. (1997) Three transitions in the RNA polymerase II transcription complex during initiation. *Embo J.*, 16, 7468-7480.
91. Kobor, M.S. and Greenblatt, J. (2002) Regulation of transcription elongation by phosphorylation. *Biochim Biophys Acta*, 1577, 261-275.
92. Epshtein, V. and Nudler, E. (2003) Cooperation between RNA polymerase molecules in transcription elongation. *Science*, 300, 801-5.
93. Cook, P.R. (1999) The organization of replication and transcription. *Science*, 284, 1790-5.
94. Kettenberger, H., Armache, K.J. and Cramer, P. (2003) Architecture of the RNA Polymerase II-TFIIS Complex and Implications for mRNA Cleavage. *Cell*, 114, 347-57.
95. Elmendorf, B.J., Shilatfard, A., Yan, Q., Conaway, J.W. and Conaway, R.C. (2001) Transcription factors TFIIF, ELL, and Elongin negatively regulate SII- induced nascent transcript cleavage by non-arrested RNA polymerase II elongation intermediates. *J Biol Chem*, 276, 23109-14.

96. **Svejstrup, J.Q.** (2002) Chromatin elongation factors. *Curr Opin Genet Dev*, 12, 156-61.
97. **Orphanides, G., LeRoy, G., Chang, C.H., Luse, D.S. and Reinberg, D.** (1998) FACT, a factor that facilitates transcript elongation through nucleosomes. *Cell*, 92, 105-116.
98. **John, S., Howe, L., Tafrov, S.T., Grant, P.A., Sternglanz, R. and Workman, J.L.** (2000) The something about silencing protein, Sas3, is the catalytic subunit of NuA3, a yTAF(II)30-containing HAT complex that interacts with the Spt16 subunit of the yeast CP (Cdc68/Pob3)-FACT complex. *Genes Dev*, 14, 1196-208.
99. **Protacio, R.U., Li, G., Lowary, P.T. and Widom, J.** (2000) Effects of histone tail domains on the rate of transcriptional elongation through a nucleosome. *Mol Cell Biol*, 20, 8866-78.
100. **Wittschieben, B.O., Otero, G., de Bizemont, T., Fellows, J., Erdjument-Bromage, H., Ohba, R., Li, Y., Allis, C.D., Tempst, P. and Svejstrup, J.Q.** (1999) A novel histone acetyltransferase is an integral subunit of elongating RNA polymerase II holoenzyme. *Mol. Cell*, 4, 123-128.
101. **Hawkes, N.A., Otero, G., Winkler, G.S., Marshall, N., Dahmus, M.E., Krappmann, D., Scheidereit, C., Thomas, C.L., Schiavo, G., Erdjument-Bromage, H., Tempst, P. and Svejstrup, J.Q.** (2002) Purification and characterization of the human elongator complex. *J Biol Chem*, 277, 3047-52.
102. **Kim, J.H., Lane, W.S. and Reinberg, D.** (2002) Human Elongator facilitates RNA polymerase II transcription through chromatin. *Proc Natl Acad Sci U S A*, 99, 1241-6.
103. **Corey, L.L., Weirich, C.S., Benjamin, I.J. and Kingston, R.E.** (2003) Localized recruitment of a chromatin-remodeling activity by an activator in vivo drives transcriptional elongation. *Genes Dev*, 17, 1392-401.
104. **Wada, T., Orphanides, G., Hasegawa, J., Kim, D.K., Shima, D., Yamaguchi, Y., Fukuda, A., Hisatake, K., Oh, S., Reinberg, D. and Handa, H.** (2000) FACT relieves DSIF/NELF-mediated inhibition of transcriptional elongation and reveals functional differences between P-TEFb and TFIIF. *Mol Cell*, 5, 1067-72.
105. **Tantin, D.** (1998) RNA polymerase II elongation complexes containing the Cockayne syndrome group B protein interact with a molecular complex containing the transcription factor IIH components xeroderma pigmentosum B and p62. *J. Biol. Chem.*, 273, 27794-27799.
106. **Selby, C.P. and Sancar, A.** (1997) Cockayne syndrome group B protein enhances elongation by RNA polymerase II. *Proc. Natl. Acad. Sci. USA*, 94, 11205-11209.
107. **Balajee, A.S., May, A., Dianov, G.L., Friedberg, E.C. and Bohr, V.A.** (1997) Reduced RNA polymerase II transcription in intact and permeabilized Cockayne syndrome group B cells. *Proc. Natl. Acad. Sci. USA*, 94, 4306-4311.
108. **Dianov, G.L., Houle, J.F., Iyer, N., Bohr, V.A. and Friedberg, E.C.** (1997) Reduced RNA polymerase II transcription in extracts of cockayne syndrome and xeroderma pigmentosum/Cockayne syndrome cells. *Nucleic Acids Res*, 25, 3636-42.
109. **Lee, S.K., Yu, S.L., Prakash, L. and Prakash, S.** (2001) Requirement for yeast RAD26, a homolog of the human CSB gene, in elongation by RNA polymerase II. *Mol Cell Biol*, 21, 8651-6.
110. **Jansen, L.E.T., den Dulk, H., Brouns, R.M., de Ruijter, M., Brandsma, J.A. and Brouwer, J.** (2000) Spt4 modulates Rad26 requirement in transcription-coupled nucleotide excision repair. *EMBO J.*, 19, 6498-6507.
111. **Hartzog, G.A., Wada, T., Handa, H. and Winston, F.** (1998) Evidence that Spt4, Spt5, and Spt6 control transcription elongation by RNA polymerase II in *Saccharomyces cerevisiae*. *Genes Dev*, 12, 357-69.
112. **Wada, T., Takagi, T., Yamaguchi, Y., Ferdous, A., Imai, T., Hirose, S., Sugimoto, S., Yano, K., Hartzog, G.A., Winston, F., Buratowski, S. and Handa, H.** (1998) DSIF, a novel transcription elongation factor that regulates RNA polymerase II processivity, is composed of human Spt4 and Spt5 homologs. *Genes Dev.*, 12, 343-356.
113. **Bradsher, J., Auriol, J., Proietti de Santis, L., Iben, S., Vonesch, J.L., Grummt, I. and Egly, J.M.** (2002) CSB is a component of RNA pol I transcription. *Mol Cell*, 10, 819-29.
114. **Iben, S., Tschochner, H., Bier, M., Hoogstraten, D., Hozak, P., Egly, J.M. and Grummt, I.** (2002) TFIIF plays an essential role in RNA polymerase I transcription. *Cell*, 109, 297-306.

115. **Hoogstraten, D., Nigg, A.L., Heath, H., Mullenders, L.H., van Driel, R., Hoeijmakers, J.H., Vermeulen, W. and Houtsmuller, A.B.** (2002) Rapid switching of TFIIH between RNA polymerase I and II transcription and DNA repair in vivo. *Mol Cell*, 10, 1163-74.
116. **Yu, A., Fan, H.-Y., Liao, D., Bailey, A.D. and Weiner, A.M.** (2000) Activation of p53 or Loss of the Cockayne Syndrome Group B Repair Protein Causes Metaphase Fragility of Human U1, U2, and 5S Genes. *Molecular Cell*, 5, 801-810.
117. **Svejstrup, J.Q.** (2002) Transcription repair coupling factor: a very pushy enzyme. *Mol Cell*, 9, 1151-2.
118. **Chalfie, M., Tu, Y., Euskirchen, G., Ward, W.W. and Prasher, D.C.** (1994) Green fluorescent protein as a marker for gene expression. *Science*, 263, 802-5.
119. **Prasher, D.C., Eckenrode, V.K., Ward, W.W., Prendergast, F.G. and Cormier, M.J.** (1992) Primary structure of the *Aequorea victoria* green-fluorescent protein. *Gene*, 111, 229-233.
120. **Heim, R., Prasher, D.C. and Tsien, R.Y.** (1994) Wavelength mutations and posttranslational autooxidation of green fluorescent protein. *Proc Natl Acad Sci U S A*, 91, 12501-4.
121. **Cody, C.W., Prasher, D.C., Westler, W.M., Prendergast, F.G. and Ward, W.W.** (1993) Chemical structure of the hexapeptide chromophore of the *Aequorea* green-fluorescent protein. *Biochemistry*, 32, 1212-8.
122. **Reid, B.G. and Flynn, G.C.** (1997) Chromophore formation in green fluorescent protein. *Biochemistry*, 36, 6786-91.
123. **Heim, R., Cubitt, A.B. and Tsien, R.Y.** (1995) Improved green fluorescence. *Nature*, 373, 663-4.
124. **Brejc, K., Sixma, T.K., Kitts, P.A., Kain, S.R., Tsien, R.Y., Ormo, M. and Remington, S.J.** (1997) Structural basis for dual excitation and photoisomerization of the *Aequorea victoria* green fluorescent protein. *Proc Natl Acad Sci U S A*, 94, 2306-11.
125. **Cormack, B.P., Valdivia, R.H. and Falkow, S.** (1996) FACS-optimized mutants of the green fluorescent protein (GFP). *Gene*, 173, 33-8.
126. **Yang, T.T., Cheng, L. and Kain, S.R.** (1996) Optimized codon usage and chromophore mutations provide enhanced sensitivity with the green fluorescent protein. *Nucleic Acids Res*, 24, 4592-3.
127. **Haas, J., Park, E.C. and Seed, B.** (1996) Codon usage limitation in the expression of HIV-1 envelope glycoprotein. *Curr Biol*, 6, 315-24.
128. **Ormo, M., Cubitt, A.B., Kallio, K., Gross, L.A., Tsien, R.Y. and Remington, S.J.** (1996) Crystal structure of the *Aequorea victoria* green fluorescent protein. *Science*, 273, 1392-5.
129. **Yang, F., Moss, L.G. and Phillips, G.N., Jr.** (1996) The molecular structure of green fluorescent protein. *Nat Biotechnol*, 14, 1246-51.
130. **Dickson, R.M., Cubitt, A.B., Tsien, R.Y. and Moerner, W.E.** (1997) On/off blinking and switching behaviour of single molecules of green fluorescent protein. *Nature*, 388, 355-8.
131. **Garcia-Parajo, M.F., Segers-Nolten, G.M., Veerman, J.A., Greve, J. and van Hulst, N.F.** (2000) Real-time light-driven dynamics of the fluorescence emission in single green fluorescent protein molecules. *Proc Natl Acad Sci U S A*, 97, 7237-42.
132. **Weber, W., Helms, V., McCammon, J.A. and Langhoff, P.W.** (1999) Shedding light on the dark and weakly fluorescent states of green fluorescent proteins. *Proc Natl Acad Sci U S A*, 96, 6177-82.
133. **Visser, A.J.W.G. and Hink, M.A.** (1999) New Perspectives of Fluorescence Correlation Spectroscopy. *J Fluoresc*, 9, 81-84.
134. **Widengren, J., Mets, U. and Rigler, R.** (1999) Photodynamic properties of green fluorescent proteins investigated by fluorescence correlation spectroscopy. *Chem. Phys*, 250, 171-186.
135. **Axelrod, D., Koppel, D.E., Schlessinger, J., Elson, E. and Webb, W.W.** (1976) Mobility measurement by analysis of fluorescence photobleaching recovery kinetics. *Biophys J*, 16, 1055-69.
136. **Edidin, M.** (1993) Patches and fences: probing for plasma membrane domains. *J Cell Sci Suppl*, 17, 165-9.
137. **Lippincott-Schwartz, J., Snapp, E. and Kenworthy, A.** (2001) Studying protein dynamics in living cells. *Nat Rev Mol Cell Biol*, 2, 444-56.

138. **Harpur, A.G., Wouters, F.S. and Bastiaens, P.I.** (2001) Imaging FRET between spectrally similar GFP molecules in single cells. *Nat Biotechnol*, 19, 167-9.
139. **Medina, M.A. and Schwille, P.** (2002) Fluorescence correlation spectroscopy for the detection and study of single molecules in biology. *Bioessays*, 24, 758-64.
140. **Cremer, T. and Cremer, C.** (2001) Chromosome territories, nuclear architecture and gene regulation in mammalian cells. *Nat Rev Genet*, 2, 292-301.
141. **Gerlich, D., Beaudouin, J., Kalbfuss, B., Daigle, N., Eils, R. and Ellenberg, J.** (2003) Global chromosome positions are transmitted through mitosis in mammalian cells. *Cell*, 112, 751-64.
142. **Houtsmuller, A.B. and Vermeulen, W.** (2001) Macromolecular dynamics in living cell nuclei revealed by fluorescence redistribution after photobleaching. *Histochem. Cell Biol.*, 115, 13-21.
143. **Volpi, E.V., Chevret, E., Jones, T., Vatcheva, R., Williamson, J., Beck, S., Campbell, R.D., Goldsworthy, M., Powis, S.H., Ragoussis, J., Trowsdale, J. and Sheer, D.** (2000) Large-scale chromatin organization of the major histocompatibility complex and other regions of human chromosome 6 and its response to interferon in interphase nuclei. *J Cell Sci*, 113 ( Pt 9), 1565-76.
144. **Jackson, D.A., Iborra, F.J., Manders, E.M. and Cook, P.R.** (1998) Numbers and organization of RNA polymerases, nascent transcripts, and transcription units in HeLa nuclei. *Mol. Biol. Cell*, 9, 1523-1536.
145. **Pombo, A., Jackson, D.A., Hollinshead, M., Wang, Z., Roeder, R.G. and Cook, P.R.** (1999) Regional specialization in human nuclei: visualization of discrete sites of transcription by RNA polymerase II. *Embo J*, 18, 2241-53.
146. **Spector, D.L.** (1993) Macromolecular domains within the cell nucleus. *Annu. Rev. Cell Biol.*, 9, 265-315.
147. **Wei, X., Somanathan, S., Samarabandu, J. and Berezney, R.** (1999) Three-dimensional visualization of transcription sites and their association with splicing factor-rich nuclear speckles. *J Cell Biol*, 146, 543-58.
148. **Zhang, G., Taneja, K.L., Singer, R.H. and Green, M.R.** (1994) Localization of pre-mRNA splicing in mammalian nuclei. *Nature*, 372, 809-12.
149. **Misteli, T. and Spector, D.L.** (1999) RNA polymerase II targets pre-mRNA splicing factors to transcription sites in vivo. *Mol. Cell*, 3, 697-705.
150. **Seksek, O., Biwersi, J. and Verkman, A.S.** (1997) Translational diffusion of macromolecule-sized solutes in cytoplasm and nucleus. *J. Cell. Biol.*, 138, 131-142.
151. **Houtsmuller, A.B., Rademakers, S., Nigg, A.L., Hoogstraten, D., Hoeijmakers, J.H.J. and Vermeulen, W.** (1999) Action of DNA repair endonuclease ERCC1/XPF in living cells. *Science*, 284, 958-961.
152. **Phair, R.D. and Misteli, T.** (2000) High mobility of proteins in the mammalian cell nucleus. *Nature*, 404, 604-609.
153. **Sugaya, K., Vigneron, M. and Cook, P.R.** (2000) Mammalian cell lines expressing functional RNA polymerase II tagged with the green fluorescent protein. *J Cell Sci*, 113 ( Pt 15), 2679-83.
154. **Kimura, H., Sugaya, K. and Cook, P.R.** (2002) The transcription cycle of RNA polymerase II in living cells. *J Cell Biol*, 159, 777-82.
155. **Lander, E.S. et al.** (2001) Initial sequencing and analysis of the human genome. *Nature*, 409, 860-921.
156. **Jackson, D.A., Pombo, A. and Iborra, F.** (2000) The balance sheet for transcription: an analysis of nuclear RNA metabolism in mammalian cells. *Faseb J*, 14, 242-54.
157. **Houtsmuller, A.B. and Vermeulen, W.** (2001) Macromolecular dynamics in living cell nuclei revealed by fluorescence redistribution after photobleaching. *Histochem Cell Biol*, 115, 13-21.
158. **Chen, D., Hinkley, C.S., Henry, R.W. and Huang, S.** (2002) TBP dynamics in living human cells: constitutive association of TBP with mitotic chromosomes. *Mol Biol Cell*, 13, 276-84.
159. **McNally, J.G., Müller, W.G., Walker, D., Wolford, R. and Hager, G.L.** (2000) The glucocorticoid receptor: rapid exchange with regulatory sites in living cells. *Science*, 287, 1262-1265.

160. **Becker, M., Baumann, C., John, S., Walker, D.A., Vigneron, M., McNally, J.G. and Hager, G.L.** (2002) Dynamic behavior of transcription factors on a natural promoter in living cells. *EMBO Rep*, 3, 1188-94.
161. **Dundr, M., Hoffmann-Rohrer, U., Hu, Q., Grummt, I., Rothblum, L.I., Phair, R.D. and Misteli, T.** (2002) A kinetic framework for a mammalian RNA polymerase in vivo. *Science*, 298, 1623-6.
162. **Essers, J., Houtsmuller, A.B., van Veelen, L., Paulusma, C., Nigg, A.L., Pastink, A., Vermeulen, W., Hoeijmakers, J.H. and Kanaar, R.** (2002) Nuclear dynamics of RAD52 group homologous recombination proteins in response to DNA damage. *Embo J*, 21, 2030-7.
163. **Miura, N., Miyamoto, I., Asahina, H., Satokata, I., Tanaka, K. and Okada, Y.** (1991) Identification and characterization of XPAC protein, the gene product of the human XPAC (xeroderma pigmentosum group A complementing) gene. *Journal of Biological Chemistry*, 266, 19786-19789.
164. **Grande, M.A., van der Kraan, I., de Jong, L. and van Driel, R.** (1997) Nuclear distribution of transcription factors in relation to sites of transcription and RNA polymerase II. *J. Cell. Sci.*, 110, 1781-1791.
165. **Ma, L., Westbroek, A., Jochemsen, A.G., Weeda, G., Bosch, A., Bootsma, D., Hoeijmakers, J.H. and van der Eb, A.J.** (1994) Mutational analysis of ERCC3, which is involved in DNA repair and transcription initiation: identification of domains essential for the DNA repair function. *Mol Cell Biol*, 14, 4126-34.
166. **Van der Spek, P.J., Eker, A., Rademakers, S., Visser, C., Sugawara, K., Masutani, C., Hanaoka, F., Bootsma, D. and Hoeijmakers, J.H.J.** (1996) XPC and human homologs of RAD23: intracellular localization and relationship to other nucleotide excision repair complexes. *Nucleic Acids Res.*, 24, 2551-2559.
167. **Park, M.S., Knauf, J.A., Pendergrass, S.H., Coulon, C.H., Strniste, G.F., Marrone, B.L. and MacInnes, M.A.** (1996) Ultraviolet-induced movement of the human DNA repair protein, Xeroderma pigmentosum type G, in the nucleus. *Proc Natl Acad Sci U S A*, 93, 8368-73.
168. **Rademakers, S., Volker, M., Hoogstraten, D., Nigg, A.L., Mone, M.J., Van Zeeland, A.A., Hoeijmakers, J.H., Houtsmuller, A.B. and Vermeulen, W.** (2003) Xeroderma Pigmentosum Group A Protein Loads as a Separate Factor onto DNA Lesions. *Mol Cell Biol*, 23, 5755-5767.
169. **Hoogstraten, D., Nigg, A.L., Van Cappellen, W.A., Hoeijmakers, J.H., Houtsmuller, A.B. and Vermeulen, W.** DNA-damage sensing in living cells by xeroderma pigmentosum group C. *manuscript in prep.*
170. **Hoogstraten, D., Auriol, J., Nigg, A.L., Hoeijmakers, J.H., Egly, J.M., Houtsmuller, A.B. and Vermeulen, W.** Kinetics of TFIIH in the TC-NER and GG-NER pathways. *manuscript in prep.*
171. **Rockx, D.A.P., Mason, R., Van Hoffen, A., Barton, M.C., Citterio, E., Bregman, D.B., Van Zeeland, A.A., Vrieling, H. and Mullenders, L.H.F.** (2000) UV-induced inhibition of transcription involves repression of transcription initiation and phosphorylation of RNA polymerase II. *Proc Natl Acad Sci U S A*, 97, 10503-08.



# Chapter 6

ATP-dependent chromatin remodeling by  
the Cockayne Syndrome B DNA repair-  
transcription coupling factor

*Adapted from Mol. Cell. Biol. 20:7643-7653 (2000)*

# ATP-dependent chromatin remodeling by the Cockayne Syndrome B DNA repair-transcription coupling factor

Elisabetta Citterio<sup>1</sup>, Vincent van den Boom<sup>1</sup>, Gavin Schnitzler<sup>2,3</sup>, Roland Kanaar<sup>1,4</sup>, Edgar Bonte<sup>1</sup>, Robert E. Kingston<sup>2</sup>, Jan H.J. Hoeijmakers<sup>1</sup>, and Wim Vermeulen<sup>1</sup>

<sup>1</sup>*Medical Genetic Center, Department of Cell Biology and Genetics, Center for Biomedical Genetics, Erasmus University Rotterdam, P.O. Box 1738, 3000 DR, Rotterdam, The Netherlands;* <sup>2</sup>*Department of Molecular Biology, Massachusetts General Hospital, Boston, Massachusetts 02114, USA;* <sup>3</sup>*Present address: Dept. of Biochemistry, Tufts University School of Medicine, Boston, MA 02111;* <sup>4</sup>*Department of Radiation Oncology, Daniël den Hoed Cancer Center, Rotterdam, The Netherlands.*

## Abstract

The Cockayne syndrome B protein (CSB) is required for coupling DNA excision repair to transcription in a process known as transcription-coupled repair (TCR). Cockayne syndrome patients show UV-sensitivity and severe neurodevelopmental abnormalities. CSB is a DNA-dependent ATPase of the SWI2/SNF2 family. SWI2/SNF2-like proteins are implicated in chromatin remodeling during transcription. Since chromatin structure affects also DNA repair efficiency, chromatin remodeling activities within repair are expected. Here we used purified recombinant CSB protein to investigate whether it can remodel chromatin *in vitro*. We show that binding of CSB to DNA results in an alteration of DNA double-helix conformation. In addition, We find that CSB is able to remodel chromatin structure at the expense of ATP hydrolysis. Specifically, CSB can alter DNase I accessibility to reconstituted mononucleosome cores and disarrange an array of nucleosomes regularly spaced on plasmid DNA. In addition, we show that CSB not only interacts with ds-DNA, but also directly with core histones. Finally, the presence of intact histone tails plays an important role for CSB remodeling function. CSB is the first repair protein found to play a direct role in modulating nucleosome structure. The relevance of this finding at the interplay between transcription and repair is discussed.

## Introduction

Nucleotide excision repair (NER) is a versatile DNA repair pathway that removes a wide range of DNA lesions, including the main ultraviolet (UV) light-induced lesions, i.e. cyclobutane pyrimidine dimers and 6/4 photoproducts. Approximately 30 proteins are involved in mammalian NER, that proceeds via a well-characterized, multistep reaction



(for a recent review see [1]). One of the immediate consequences of DNA damage is blockage of transcription. To allow a rapid resumption of this vital process, a specialized repair mode has evolved, that preferentially recognizes and repairs transcription-blocking lesions [2,3]. This process is known as transcription-coupled repair (TCR). Some aspects of TCR are highly conserved from *Escherichia coli*, to yeast and mammals [4]. Oxidative damage, mainly processed by the base excision repair pathway, is also removed in a transcription-coupled manner [5,6]. Thus, the importance of TCR is not limited to NER.

Inherited defects in TCR constitute the molecular basis of Cockayne syndrome (CS). CS patients are UV-sensitive and show severe developmental and neurological dysfunctions [7,8]. Two human genes are specifically required for TCR, *CSA* and *CSB*. These genes are defective in CS complementation groups A and B [9,10]. Several recent observations suggest that the CS proteins may have a subtle, additional role in transcription [11-15].

*CSA* specifies a five WD 40 repeat-containing protein [9]. The *CSB* gene encodes a nuclear protein of 168 kDa and its central part is highly homologous to the helicase domain present in the SWI2/SNF2 family of proteins [10,16]. The recombinant *CSB* protein is a double-stranded DNA-dependent ATPase (activated by both naked and nucleosomal DNA), but, like other members of the SWI2/SNF2 family, is not a classical helicase [17-20]. Changing the invariant lysine to an arginine residue within the Walker A motif, responsible for NTP-binding and hydrolysis, abolished *CSB* ATPase activity, but only partially affected its biological function in living cells [18]. Both *in vivo* and *in vitro* it was found that *CSB* interacts with RNA polymerase II [11,12,19]. However, the role of *CSB* both in TCR and in RNA polymerase II (RNAP II) transcription is unknown.

Several SWI2/SNF2-related proteins are part of large multiprotein complexes involved in transcription regulation [21]. *In vitro* studies have well documented the ability of these remodeling "machines" to alter chromatin structure in an ATP-dependent manner [22]. Recently, three ATPases, the human Brg1 and hBrm together with the *Drosophila* ISWI, have been reported to exhibit chromatin remodeling activities on their own [23,24]. Brg1 and hBrm are the ATPase components of two distinct human SWI/SNF complexes [25,26], while ISWI is part of three *Drosophila* remodeling complexes, ACF, CHRAC, and NURF [27]. These experiments have led to the view that the ATPase subunits are the catalytic core of the remodeling "machines", while the other associated proteins may have regulatory or auxiliary functions. Interestingly, the SWI2/SNF2 family includes also proteins involved in various DNA repair pathways, such as RAD 16 (global genome NER), RAD5 (post replication repair), RAD 54 (recombination repair) and *CSB* (transcription-coupled repair) [16]. The fact that chromatin structure hinders the repair process [28] suggests that these SWI2/SNF2-related DNA repair proteins may possess a similar remodeling activity in order to provide access to damaged DNA. However, very little is known about the proteins and the molecular mechanism involved in chromatin transitions in DNA repair. In this study, we examined the involvement of *CSB*, as an isolated recombinant protein, in chromatin remodeling by *in vitro* accessibility assays on nucleosomal DNA fragments. Our results show that *CSB* can alter DNA conformation and is able to induce changes in chromatin structure in an ATP-dependent fashion. In addition, we demonstrate that *CSB* directly interacts with the core histones. We provide evidence

that CSB exhibits chromatin remodeling activity, being the first activity linking repair to chromatin remodeling.

### Results

In this study, we utilized highly purified, recombinant CSB protein. Wild type and ATPase-deficient (CSB<sup>K538R</sup>) mutant CSB proteins, both epitope-tagged (HA-CSB-his<sub>6</sub>) were isolated from baculovirus infected Sf21 insect cells as described previously. The tags do not interfere with the biological function of CSB *in vivo* [18]. Both proteins were purified to near homogeneity, as determined by silver staining (Fig. 1A). As previously described, CSB ATPase activity was stimulated by double stranded but not by single stranded DNA. Both naked as well as nucleosomal DNA, with or without histone tails, gave a similar stimulation (data not shown and [18]). When HeLa core histones were tested as cofactors, no increase of ATP hydrolysis by CSB was detected (data not shown; see Materials and Methods). This emphasizes that CSB ATPase activity is strictly dependent on (ds) DNA. The hSWI/SNF complex was isolated from HeLa cells and functionally characterized as described [29].

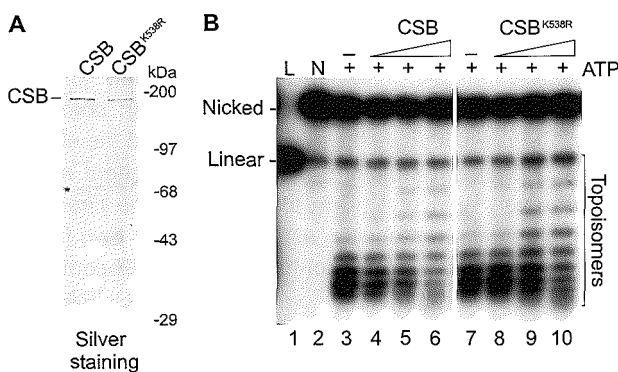


**Figure 1. CSB introduces negative supercoils in plasmid DNA upon binding.** A. Purified recombinant CSB and CSB<sup>K538R</sup> proteins. Aliquots of the Mono Q fractions of both proteins were separated by SDS-PAGE (8%) and visualized by silver staining. In addition to the major CSB band, two degradation products (as determined by Western blotting) were visible. \*represents keratins which were also present in empty lanes. Molecular weight markers are indicated in kiloDaltons. B. Shift in the topoisomers distribution upon CSB binding. Singly-nicked

plasmid DNA (100 ng) (lane 2) was incubated with increasing amounts of CSB or CSB<sup>K538R</sup> (20, 40, 80 ng, lanes 4-6 and 8-10, respectively) in the presence of ATP. The DNA molecules were closed by the addition of *E. coli* DNA ligase and the topoisomers were resolved by electrophoresis on a 1% agarose gel containing 0.5 µg/ml chloroquine.

#### *CSB influences DNA topology by inducing negative supercoiling*

CSB contains seven conserved motifs characteristic of the SNF2/SWI2 family of putative helicases [10,16]. Nevertheless, CSB, as well as most of the SWI2/SNF2-related proteins tested to date, fail to show classical helicase activity as assayed by oligonucleotide strand displacement [17-19,30]. However, the lack of overt helicase activity does not exclude the possibility that these proteins may work by altering the DNA

conformation thereby inducing a local separation of the DNA strands. To address this possibility, we tested CSB activity in a topological assay [31]. Singly-nicked DNA plasmid was incubated with increasing amounts of purified CSB or CSB<sup>K538R</sup> (Fig. 1B). Subsequently, *E. coli* DNA ligase was added to covalently close the nick in order to preserve any protein-induced change in linking number ( $\Delta Lk$ ) in the duplex DNA. To determine the extent and the direction of induced  $\Delta Lk$ , the topoisomer population was analyzed by agarose gel electrophoresis in the absence or presence of the intercalating agent chloroquine (Fig. 1B and data not shown). As visible in Figure 1B lane 5, addition of 40 ng of CSB shifted the topoisomers distribution. The amount of slowly migrating DNA topoisomers in the gel increased with increased CSB concentration (Fig. 1B, lane 6, and data not shown). We calculate that the presence of CSB at an approximate molar ratio of 10:1 per 2.96 kb plasmid DNA molecule, was sufficient to induce the topological effect seen in Figure 1B, lane 6.

To examine whether ATP hydrolysis was required for this reaction two experiments were performed. The ATPase-deficient CSB<sup>K538R</sup> mutant was used and - since the *E. coli* ligase does only require NAD<sup>+</sup> - we could perform the reaction in the absence of ATP. In both cases near wildtype  $\Delta Lk$  values were obtained (Fig. 1B, lanes 8-10, and results not shown). Furthermore, in control experiments we did not detect any significant contaminating topoisomerase activity in the CSB preparations (data not shown, see Materials and Methods). The chloroquine included in the gels shown in Figure 1B intercalates in the DNA double helix and introduces positive supercoiling in the covalently closed relaxed plasmid. CSB counteracted chloroquine action, causing an electrophoretic retardation of the DNA topoisomers (Fig. 1B, lanes 4-6). We conclude that binding of CSB causes a change in DNA conformation detected as negative supercoiling in our topological assay. The direction of CSB-induced  $\Delta Lk$  was confirmed by analysis of the topoisomers on two-dimensional gels (data not shown) [31].

#### *CSB remodels a nucleosome core in an ATP-dependent manner*

The high homology shared with the SWI2/SNF2-related proteins suggested that CSB might play a role in chromatin remodeling. However, such a property has not been established for any of the DNA repair members of this family. We first investigated this possibility at the basic level of chromatin organization, the nucleosome. For this purpose, we reconstituted rotationally phased mononucleosomes with purified histones on a radioactively labeled 155-bp DNA fragment using a salt dilution procedure. Alterations of the nucleosomal structure were assessed by DNase I footprinting [32], (see Materials and Methods). In the absence of remodeling activities, DNase I digestion of nucleosomes gave rise to the characteristic pattern of DNA fragments with a periodicity of 10 bp, which is clearly distinct from the pattern generated on naked DNA (Fig. 2A, compare lanes 1 and 11). Mononucleosomes were incubated with increasing amounts of purified CSB protein. In the presence of ATP, CSB visibly altered the DNase I accessibility to nucleosomal DNA. Remodeling is particularly evident from the change in intensity of some specific DNA bands (Fig. 2A, lanes 2-4, note bands marked by arrows). The changes in the digestion pattern were proportional to the amount of CSB added. When the naked 155bp DNA fragment was incubated with CSB, no specific DNA footprint by

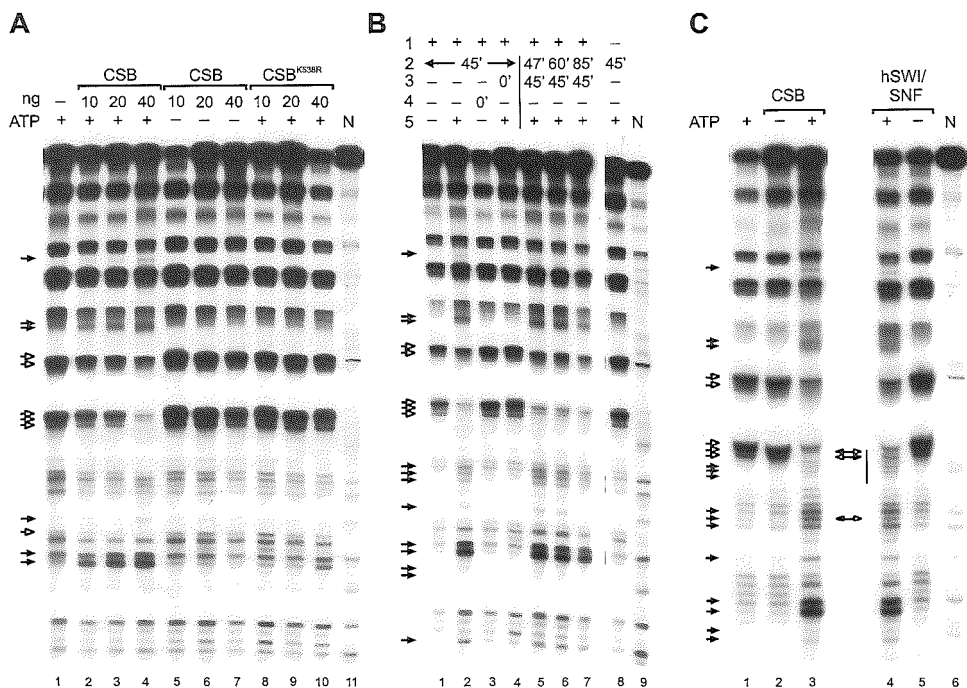


**Figure 2. Mononucleosome remodeling by CSB.** A. Mononucleosome remodeling by CSB is ATP-dependent. End-labeled nucleosome particles (approximately 3 ng of total nucleosomes) were incubated with increasing CSB amounts (10, 20 and 40 ng), in the presence (lanes 2-4) or absence of ATP (lanes 5-7). Similar reactions were performed with CSB<sup>K338R</sup> in the presence of ATP (lanes 8-10). Remodeling was assessed by DNase I digestion. Filled arrows represents sites of enhanced cutting due to the presence of CSB, while open arrows indicate sites of reduced cleavage. N represents naked control DNA. B. Nucleosome remodeling by CSB is stable upon removal of ATP by apyrase. Reactions contained 40 ng CSB (1) and were performed as in A, except that, where indicated, ATPγS (5; 2 mM), or apyrase (3; 1 U) were added. ATPγS (4) did not support remodeling (lane 3). Similarly, addition of apyrase (1 U) prior to CSB inhibited nucleosome remodeling (lane 4). However, addition of apyrase (1 U) after CSB had been present for 45 min did not inhibit nor reverse nucleosome disruption, as evidenced by DNase I digestion after 2 min (lane 5), 15 min (lane 6), and 40 min (lane 7). N represents naked DNA. C. CSB nucleosome remodeling pattern is very similar but not identical to the one generated by the hSWI/SNF complex. Reactions were performed as in A, and contained CSB (60 ng, lanes 2 and 3) or the isolated hSWI/SNF complex (300 ng, lanes 4 and 5). Sites of enhanced (filled arrows) and of decreased (open arrows) DNase I digestion are indicated. Double-headed arrows between lane 3 and 4 represent cleavage sites that distinguish the two nucleosome disruption activities. Bar: approximate position of the nucleosomal dyad axis. N is naked control DNA.

CSB was observed, as expected for a non sequence-specific DNA binding protein (data not shown). We estimate that an approximately 4:1 ratio of CSB versus core particles promoted alterations of the nucleosomal structure (Fig. 2A, lane 2). No alterations were observed in the absence of ATP (Fig. 2A, lanes 5-7), or with the addition of the non-hydrolyzable ATP analogue, ATPγS (Fig. 2B, lane 3), nor was the ATPase-deficient

CSB<sup>K538R</sup> able to promote significant remodeling (Fig. 2A, lanes 8-10). However, gel shift experiments have shown that binding of CSB to DNA and to nucleosomes is independent from the presence of ATP and is displayed with wildtype efficiency by the CSB<sup>K538R</sup> mutant (data not shown). This indicates that sole binding of CSB to DNA does not support changes in the DnaseI accessibility. In addition, the fact that CSB was not able to remodel mononucleosomes in the presence of the non-hydrolyzable ATP-analogue ATP $\gamma$ S (Fig. 2B, lane 3) indicates that ATP hydrolysis, rather than ATP binding, is required for remodeling by CSB.

Consistent with these findings, when apyrase, which hydrolyses ATP, was added to a reaction containing nucleosomes before addition of CSB, ATP-dependent nucleosome remodeling was inhibited (Fig. 2B, compare lanes 2 and 4). To analyze the stability of the altered nucleosome, we first incubated identical samples containing ATP, nucleosomes and CSB for 45 min, exposed them to apyrase, and subsequently digested with DNase I at time points ranging from 2 min to 40 min (Fig. 2B, lanes 5-7). The specific DNase I digestion pattern was conserved until 40 min past the addition of apyrase (Fig. 2B, lanes 5-7). These data suggests that the CSB-induced structural changes in the nucleosome are stable and that maintenance of the remodeled state does not require continuous ATP hydrolysis.

In order to qualitatively compare CSB activity with other chromatin remodeling factors, we assayed CSB and the purified hSWI/SNF multiprotein complex [29] in identical disruption reactions. The remodeling activity of the entire hSWI/SNF complex and of its two separate ATPase-subunits was recently shown to be qualitatively, although not quantitatively, similar [23]. The results presented in Figure 2C reveal that the DNase I digestion patterns mediated by CSB and by hSWI/SNF are very similar. However, subtle differences in DNase accessibility were visible in the central portion of the DNA fragment (Fig. 2C, compare lane 3 and 4), as consistently observed in independent experiments (data not shown).

#### *Plasmid chromatin remodeling by CSB*

To examine whether CSB could reorganize an array of nucleosomes, which more closely resembles the *in vivo* situation, we used *Drosophila* embryo extracts to reconstitute chromatin on a DNA plasmid *in vitro* [33]. The chromatin assembly and spacing complexes [34,35] active in these extracts catalyze deposition of nucleosomes with uniform spacing, as visualized by Micrococcal nuclease (MNase) digestion (see Fig. 3A and Materials and Methods). Before the chromatin templates were incubated with CSB, the endogenous *Drosophila* remodeling activities were disrupted by sarkosyl treatment [34]. Sarkosyl and ATP were subsequently removed by gel filtration (Fig. 3A, Materials and Methods). The regularity of the nucleosomal array, which was maintained after the sarkosyl treatment, was significantly perturbed by the addition of CSB in the presence of ATP (Fig. 3A, compare lanes 3 and 5). The loss of periodic spacing between the nucleosomes was visible when CSB was present in a ~20 fold molar excess compared to the 3.35 kb plasmid. Since this plasmid contains an average of 16 nucleosomes, we estimate that CSB is active at an approximate equimolar ratio with nucleosome particles.

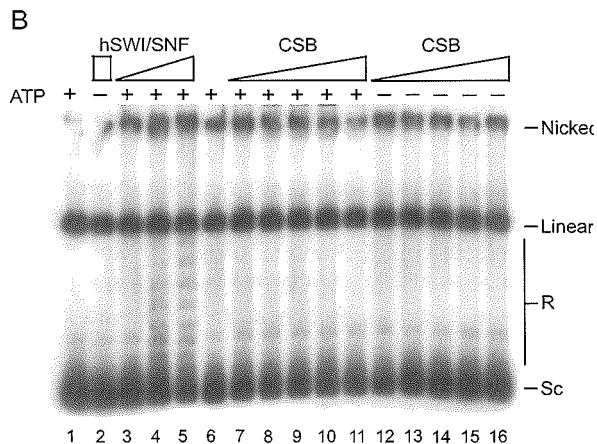
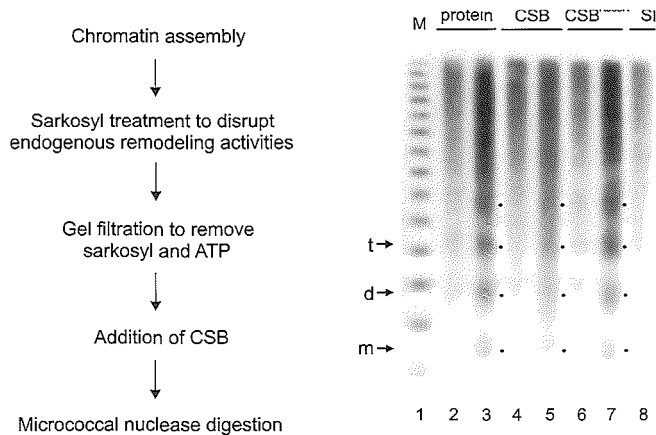


**Figure 3. Remodeling of plasmid chromatin by CSB** A. Remodeling of nucleosome arrays detected by Micrococcal nuclease (MNase) digestion. CSB induces loss of the regular nucleosome repeat characteristic of *Drosophila* reconstituted chromatin in an ATP dependent manner. Left panel: schematic outline of the assay. Right panel: Sarkosyl-stripped chromatin (40 ng) was incubated either in the absence of proteins (lanes 2, 3) or with CSB (lanes 4, 5), CSB<sup>K538R</sup> (lanes 6, 7), or hSWI/SNF (lanes 8, 9) in the presence of ATP (as described in Materials and Methods). Nucleosome organization was studied by MNase digestion (8 units), performed for 60 and 120 seconds, respectively. The position of mononucleosomes (m), dinucleosomes (d) and trinucleosomes (t) are indicated by arrows and by dots. The DNA size marker (M) represents a ladder of 123 bp repeats. B. Remodeling of nucleosome arrays visualized as ATP-dependent changes in supercoiling. CSB, unlike hSWI/SNF, does not induce visible changes in the topology of nucleosomal plasmid DNA. Nucleosomal template was incubated with topoisomerase I and either hSWI/SNF (200 ng in lane 2; 20, 60 and 200 ng, respectively in lanes 3, 4 and 5) or increasing amounts of CSB (3-fold increment starting from 2.9 ng in lanes 7 and 12), in the presence or absence of ATP. The molar ratio of CSB (in lane 11) to the ATPases subunits of hSWI/SNF (in lane 5) was approximately 20:1, as determined by silver staining (not shown). N, nicked DNA; L, linear; Sc, supercoiled; R, relaxed or partially supercoiled.

A similar irregular MNase pattern was induced by the hSWI/SNF complex in an ATP-dependent reaction (Fig. 3A, compare lanes 9 and 5, and data not shown). In contrast, in the presence of the CSB<sup>K538R</sup> ATPase-deficient mutant, the nucleosomes were found in the original regular array (Fig. 3A, compare lanes 7 and 3). Similar results were obtained in control reactions in which ATP was omitted (not shown). These data indicate that CSB uses the energy from ATP-hydrolysis to remodel nucleosomes on large DNA molecules. This change could result from repositioning of nucleosome octamers and/or generation of an altered nucleosome that is more accessible to nucleases.

One hallmark of the SWI2/SNF2 type complexes is the ability to change the topology of nucleosomal plasmid DNA in an ATP-dependent manner [25,32,36]. This particular property (to date only reported for SWI2/SNF2-related complexes) is also displayed by the isolated human SNF2 homologs Brg1 and hBrm [23]. To assay CSB for this activity, closed circular plasmid chromatin was reconstituted with *Xenopus* oocyte heat-treated extracts [32] (see Materials and Methods). Nucleosomes introduce negative supercoils in plasmid DNA, which can be visualized after deproteinization as a rapid migration (relative to relaxed DNA) in agarose gel electrophoresis (Fig. 3B, lane 1). As previously characterized, addition of hSWI/SNF, in the presence of ATP and Topoisomerase I, reduces the supercoiling of the reconstituted plasmid. This is detected as the appearance of topoisomers that have a reduced mobility (Fig. 3B, lanes 3-5; [32]). In contrast, CSB failed to show detectable activity in this assay (Figure 3B, lanes 7-11) even when present in an ~20-fold molar excess compared to the hSWI/SNF ATPase subunits, as determined by silver staining (Fig. 3B, compare lane 11 with lane 5; data not shown). Similar results were obtained on chromatin templates assembled with *Drosophila* embryo extracts [33] (data not shown; see Materials and Methods). These data indicate mechanistic differences in chromatin remodeling by CSB and hSWI/SNF.

*Nucleosome remodeling by CSB does not result in a complete disruption of the DNA-histones contacts, nor in octamer transfer to free DNA in trans*

The above results establish the ability of CSB to influence chromatin structure. To gain insight into the mechanism of remodeling by CSB, we used gel mobility shift experiments to determine whether CSB dissociates histones from DNA. As seen with other remodeling complexes, mixing CSB with labeled nucleosomes (or naked DNA) creates a mixture that does not enter the gel (Fig. 4, lanes 2-6 and 12-16 respectively) (see Materials and Methods). To determine whether histones have dissociated from DNA, we performed the remodeling reactions, and then we added an excess of unlabeled competitor DNA and analyzed the reaction products on native gels. Importantly, addition of naked DNA (see Materials and Methods) to the samples after remodeling but prior to electrophoresis, reverts the nucleosomes-CSB complexes and regenerates the two DNA species in the original ratio (Fig. 4, lanes 7-10). A comparison of lanes 7 and 8 with lane 1 indicates that the remodeling reaction did not release appreciable amounts of labeled non-nucleosomal DNA. Thus, under the conditions used, nucleosome remodeling by CSB does not involve a complete dissociation of the core histones from the DNA.

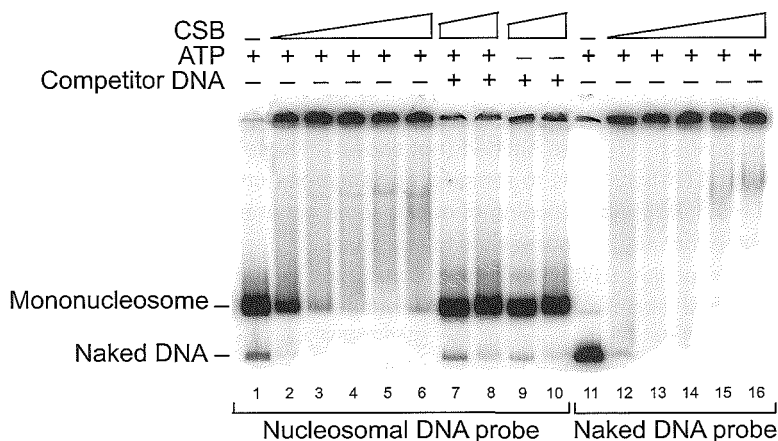


**Figure 4. Gel-shift analysis of CSB mononucleosome remodeling reactions.** CSB does not catalyze the complete dissociation of histone octamers from DNA upon nucleosome binding and remodeling. Mononucleosomes (lanes 1-10) or free DNA (lanes 11-16) were incubated with increasing amounts of CSB (10, 20, 30, 60, 100 ng for lanes 2-6 and 12-16; 60, 100 ng, respectively in lanes 7-8 and 9-10) and reactions were performed as those shown in Figure 2, with (+) or without (-) ATP. Reactions were analyzed directly on native polyacrylamide gels or, where indicated, were treated with excess of cold competitor plasmid DNA before loading (lanes 7-10) (see Materials and Methods). Multiple DNA-protein complexes are visible (bar).

Yeast SWI/SNF, yeast RSC and human SWI/SNF ([37,38]; G. Schnitzler *et al.*, unpublished observations) can transfer histone octamers from excess donor nucleosomes to labeled free DNA to form nucleosomes. In contrast, the ISWI ATPase and the ISWI-based complexes CHRAC and NURF cannot perform this activity [39,40]. We failed to detect octamer transfer activity by CSB under experimental conditions in which transfer was readily detected by SWI/SNF (data not shown; see Materials and Methods).

#### *CSB interacts with histone proteins*

The above findings indicate that CSB binds to nucleosomes and alters their structure upon ATP hydrolysis. To test how CSB is targeted to the core particles, we investigated whether CSB binds the histones by immunoprecipitation (IP) analysis. Isolated HeLa core histones (present as H2A-H2B dimers and a heterogeneous population of H3-H4 dimers and (H3-H4)<sub>2</sub> tetramers) [41-43] were incubated with purified CSB, and IP was carried out either with an anti-CSB antibody [11] or with an antibody that recognizes an epitope present on all histones (H11-4) (see Materials and Methods). After extensive washing of the protein-A beads, the bound fraction was analyzed by SDS-PAGE followed by silver staining. The results presented in Figure 5A show that the anti-CSB antibody was able to immunoprecipitate all four histones only when CSB was present (compare lanes 3 and 4, note that the weak bands visible in lane 4 do not correspond with histones and are derived from the serum used). Conversely, using anti-histone antibodies



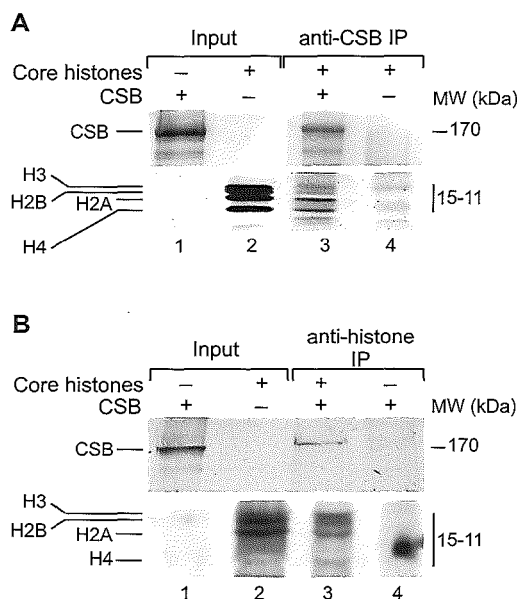


**Figure 5. CSB directly interacts with purified HeLa core histones.** Immunoprecipitation (IP) was performed on reaction mixtures containing purified CSB and core histones (lanes 1 and 2 respectively, in panels A and B) (see Materials and Methods). After extensive washing, the antibody-bound protein complexes were separated on 16.5% and 8% SDS-polyacrylamide gels to visualize the histones and CSB, respectively. Gels were stained with silver. A. IP was carried out with anti-CSB antibodies. Analysis of the beads by SDS PAGE, showed that all four core histones specifically co-immunoprecipitate with CSB (lane 3) and not in a mock IP (lane 4). B. IP with anti-histone, pan antibodies is shown. CSB is present in the bound fraction together with the histones (lane 3). No non-specific binding is detected in the mock IP (lane 4).

specific co-IP of CSB with histones was consistently observed (Fig. 5B, compare lanes 3 and 4). These data point to a specific direct interaction between CSB and the core histones.

The interaction of purified CSB with histones was further examined by far-Western analysis. Human H1-depleted polynucleosomes and several control proteins (see Materials and Methods) were separated by SDS-PAGE. The purity of the protein samples used is shown on the Coomassie stained gels (Fig. 6A). All four core histones were recognized by CSB as shown by far-Western analysis (Fig. 6B, lane 3). In addition, CSB was able to bind to each of the separate core histones (data not shown). Under identical conditions, no association with BSA nor with the highly basic cytochrome c protein was detected (Fig. 6B, lanes 1 and 2), suggesting that the net positive charge of the histones does not (solely) account for the binding. In the absence of the CSB protein, no background staining due to aspecific antibody binding was detected (Fig. 6C).

When DNA is wrapped around a histone octamer to form a nucleosome, only the 15-30 residues at the amino-termini of the histones, commonly named "tails", are protruding from the core structure [44]. Histone "tails" have been demonstrated to play a crucial role in the regulation of chromatin accessibility [45]. To analyze whether histone amino-termini are important for CSB targeting, we followed an established procedure to remove them from all four core histones ([46]; see Materials and Methods). HeLa polynucleosomes were digested with trypsin and analyzed by SDS-PAGE. After trypsin cleavage the histones ran with the characteristic size of "tailless" histones (Figure 6A, lane 4). In the far-Western analysis shown in Figure 6B, we could not detect binding of CSB to

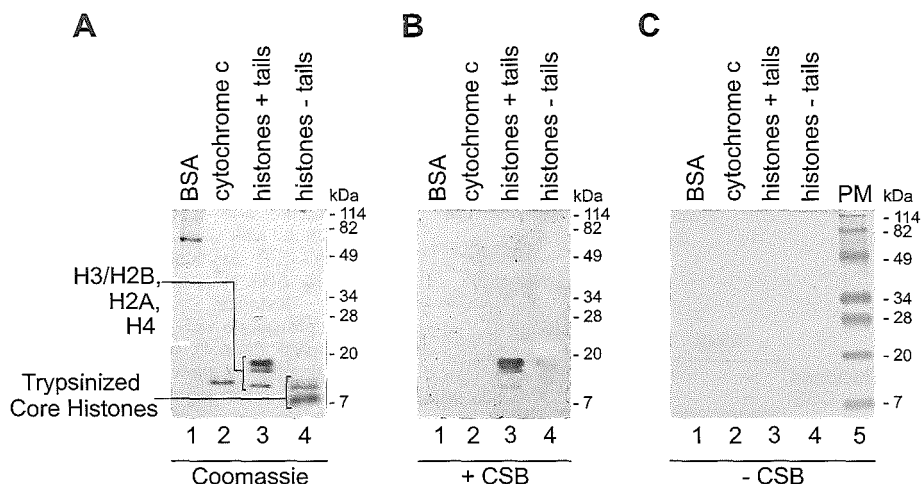


**Figure 6. CSB binds histone proteins in far-Western analysis.** Samples of H1-depleted HeLa polynucleosomes untreated (+tails) or trypsinized (- tails), BSA and cytochrome c, were separated by SDS-PAGE (16.5%) and stained with Coomassie (A) or immunoblotted (B and C) (see Materials and Methods). The membrane was probed with purified CSB (B) or mock-incubated (C). Anti-CSB antibodies detected binding of CSB to the immobilized histones (see Materials and Methods for details). No binding of CSB to the “tailless” histones was detected, suggesting that histones N-terminal “tails” are important for CSB-core histones interaction. The position of pre-stained molecular mass markers (PM) in kDa is shown.

the “tailless” histones (lane 4). This further confirms the specificity of the interaction and provides evidence that CSB associates with the exposed histone tails.

#### *CSB remodeling activity on trypsinized mononucleosomes*

To investigate the functional significance of the presence of histone tails on CSB remodeling activity, we used the DNase I accessibility assay to determine whether CSB was able to remodel a tailless mononucleosome substrate. Tailless mononucleosomes were prepared by digesting glycerol gradient-purified tailed mononucleosomes with trypsin ([46]; see Materials and Methods). The removal of the tails was confirmed by the faster electrophoretic mobility of tailless nucleosomes compared to their tailed counterparts (Fig. 7A). As expected the tailless nucleosomes have a slightly altered sensitivity to DNase I digestion when compared to the intact nucleosomes (Fig. 7B, lanes 2 and 7). We then incubated CSB with either tailed or tailless nucleosomes and compared the remodeling activity. CSB induced ATP-dependent changes in the DNase I cleavage pattern on tailed nucleosomes (Fig. 7 lanes 3-5) in a similar fashion as shown in Fig. 2. In contrast, at equivalent protein concentrations, CSB remodeling activity on the tailless substrates was strongly reduced (Fig. 7B, compare lanes 8-10 and 3-5). These results further support the significance of the histone tails for proper CSB functioning.

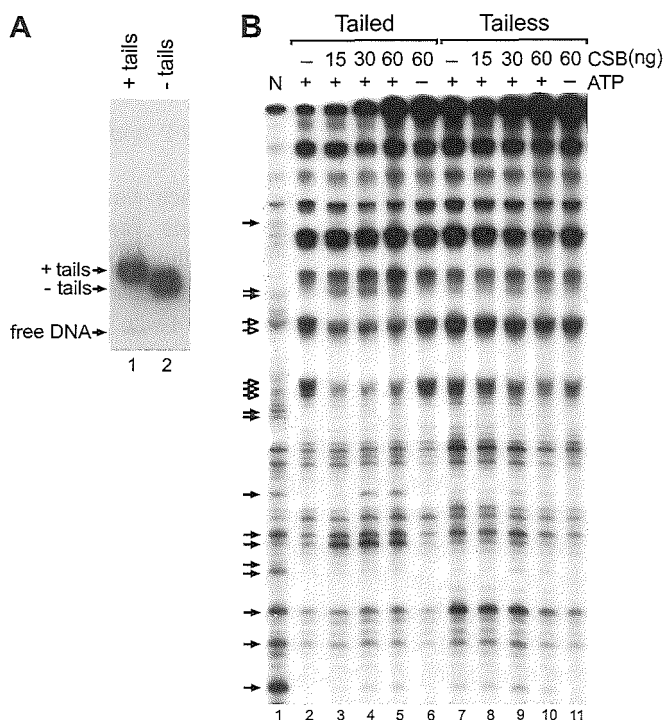


Figure 7. Remodeling of tailed (+ tails) and tailless (- tails) mononucleosomes by CSB. A. Reconstituted mononucleosomes were analyzed by electrophoretic mobility shift assay. Nucleosomes with tails are shown in lane 1. Nucleosomes without tails (lane 2) have been generated by trypsinization of labeled tailed nucleosomes after glycerol gradient purification (Materials and Methods). B. DNase I accessibility assay. Tailed (lanes 2-6) and trypsinized (lanes 7-11) mononucleosomes were incubated with increasing CSB amounts (15, 30 and 60 ng). DNase I accessibility assay. Tailed (lanes 2-6) and trypsinized (lanes 7-11) mononucleosomes were incubated with increasing CSB amounts (15, 30 and 60 ng) in the presence of ATP (lanes 3-5 and 8-10) or with 60 ng CSB in the absence of ATP (lanes 6 and 11). DNase I digestion and denaturing gel

## Discussion

In this study, we further characterize the biochemical activities of CSB by analyzing its interaction with DNA and chromatin.

### *CSB alters DNA double helix conformation upon binding*

Our results show that CSB binds to double-stranded DNA and that this binding causes a significant change in linking number as evidenced by the appearance of negatively supercoiled DNA in a topological assay (Fig. 1B). This activity is reminiscent of the hRad54 recombination-repair protein, another member of the SWI2/SNF2 family [31]. It also resembles the effect of binding of HMG-box-containing polypeptides, such as HMG-1, mtTF1 and LEF-1 to DNA [47-49]. In contrast, DNA binding of the yeast SWI/SNF complex induces positive supercoils. However, CSB and ySWI/SNF share the property that ATP hydrolysis is not required to alter DNA topology [50]. Relevant to this point is our observation that ATPase-deficient CSB (CSB<sup>K538R</sup>) still retains partial activity when microinjected into living CS-B cells [18]. In theory, CSB binding can induce negative supercoiling in two ways. One possibility is that CSB wraps the DNA around its surface in

a left-handed manner, which will cause a change in writhe. Alternatively, CSB DNA binding could induce a change in twist, which may result in local unwinding of the DNA double helix. At present, we can not discriminate between these two possibilities.

*CSB shares chromatin remodeling properties with both the SWI2/SNF2 and the ISWI containing complexes*

Purified, recombinant CSB has intrinsic chromatin remodeling activities *in vitro*. It catalyzes the remodeling of both reconstituted mononucleosomes, as well as nucleosomes uniformly spaced on plasmid DNA. Both activities require the energy of ATP hydrolysis. As demonstrated for hBRM and BRG1, additional proteins may be needed to increase the rate of remodeling by CSB [23]. Our findings are consistent with the current view that SWI2/SNF2-related ATPases form the functional core of chromatin remodeling “machines” [23,24].

Although ATP-dependent chromatin remodeling complexes perform similar activities, mechanistic differences distinguish the SWI2/SNF2 family from the ISWI-based complexes [22]. Additionally, the three ISWI-family remodeling complexes display different activities *in vitro* [27]. An interesting question is whether the CSB remodeling activity resembles more that of the SWI2/SNF2 type proteins or that of ISWI.

CSB activity on mononucleosomes is similar to that of the SWI2/SNF2 containing complexes [17,25]. In fact, CSB induces significant changes in the DNase I cleavage pattern on reconstituted mononucleosomes (Fig. 2). In contrast, the ISWI-based CHRAC complex does not support nucleosome remodeling in similar experiments [39]. The DNase I digestion patterns induced by CSB and by the hSWI/SNF complex are very similar (Fig. 2 C). Only subtle differences are observed near the nucleosomal dyad axis, the suggested location of SWI/SNF binding [29,50], possibly because CSB and hSWI/SNF bind slightly different sites on the nucleosome. During the mononucleosome remodeling reaction, both CSB and hSWI/SNF generate an altered nucleosome structure that is stable after removal of ATP (Fig. 2B and [32]). This activity has not been tested for ISWI-based complexes. CSB activity on reconstituted plasmid chromatin presents two aspects. On one hand, CSB shows the same behavior of hSWI/SNF and the *Drosophila* NURF as they all disorganize the regular repeat of nucleosome arrays (Fig. 3; G. Schnitzler, unpublished observations; [51]). This activity distinguishes CSB from ISWI [24] and from the ISWI-based remodeling complexes CHRAC and ACF [34,35]. On the other hand, CSB does not induce detectable loss of superhelical density of nucleosomal plasmid, a characteristic activity displayed by SWI2/SNF2 complexes (Fig. 3B; [32]). This might reflect differences in the details of the remodeling reactions. Generally, it is argued that chromatin remodeling complexes work without removal of histone octamers from the DNA. CSB results are consistent with this idea (Fig. 4). However, SWI2/SNF2 containing complexes (RSC, hSWI/SNF, ySWI/SNF) can transfer histone octamers to an acceptor DNA molecule *in trans* [37,38](Schnitzler *et al.*, unpublished results). We were not able to detect this type of activity for CSB (data not shown). In this respect, CSB is more like the ISWI-based complexes NURF and CHRAC [39,40]. In conclusion, the data presented here indicate that CSB remodeling activity has some properties in common with both the SWI2/SNF2-based and the ISWI-based family. This may be due to the fact that CSB was tested as isolated polypeptide and not as a

complex as in the case of the others. An additional interesting possibility is that CSB may be distinct in its capabilities from both classes of remodeling complexes.

#### *Intact histone tails are important for efficient nucleosome remodeling by CSB*

To get insight into the mechanism how CSB destabilizes the nucleosomal structure, it is important to identify its target sites. Does CSB recognize the DNA surface or can CSB also contact the histone proteins directly, or can it do both? Our *in vitro* data indicate that CSB can do both. Figure 1B reveals its interaction with double-stranded DNA. The results presented in Figure 5 and 6 show that CSB interacts with the core histones, suggesting multiple contacts between CSB and the histone proteins. Interestingly, trypsinized core histones completely failed to be recognized by CSB (Fig. 6B). Histone “tails” have been shown to differentially influence the activity of ATP-driven chromatin remodeling complexes. They are essential for the *Drosophila* NURF action [52], while hSWI/SNF and yeast SWI/SNF complexes can remodel tailless nucleosomes [46,53]. Here, we present evidence that CSB remodeling activity is severely reduced on tailless mononucleosomes (Fig 7B), providing a first indication that interaction with the histone tails is important for CSB function.

#### *Implications for transcription-coupled repair*

A dual functionality has been proposed for CSB. First, CSB is specifically required for the transcription-repair coupling reaction. Second, several observations support an additional, non-essential role of CSB in transcription itself [4,14]. Very recently, specific fragile sites in metaphase chromosomes have been detected at abundantly transcribed chromosomal loci in CSB deficient cells, suggesting an involvement of CSB in transcription elongation of highly transcribed (structured) genes [54]. The capacity of CSB to remodel nucleosome structure may be relevant for both the repair and the transcription function, as discussed below.

In relation to the role of CSB in repair, CSB may be involved in chromatin rearrangements at repair sites. These rearrangements may include both opening of chromatin, to facilitate displacement of the stalled polymerase complex and/or favor accessibility of NER enzymes to the damage, and the rapid refolding of nucleosomes following repair synthesis [55,56]. In addition, the capability of CSB to modulate DNA double helix conformation may directly facilitate TCR. In a mechanism similar to nucleosome disruption, CSB could use ATP hydrolysis to weaken the RNAP II-DNA contacts at the site of a DNA lesion, thereby accomplishing displacement or removal of the blocked polymerase which is an obligatory step to allow repair [6]. The observed interaction of CSB with RNAP II, both *in vivo* and *in vitro* [11-13], might specifically target CSB to sites of blocked transcription.

With respect to the role of CSB in transcription, it is well documented that nucleosomes constitute a strong barrier to transcription elongation [57,58]. A mild stimulation of transcription elongation by CSB on naked DNA templates has recently been reported *in vitro* ([13]; our unpublished observations). The data presented here open the possibility that CSB may play a role in facilitating transcription by RNAP II through pause sites on natural chromatin templates *in vivo*.

The experiments presented here extend CSB function to chromatin remodeling, and place the protein at the crossroad between DNA repair, transcription and chromatin structure. It is possible that defective chromatin rearrangements during DNA repair or transcription may contribute to the severe clinical symptoms of Cockayne syndrome patients, which cannot be explained solely by a DNA repair defect. Other examples of severe biological consequences of alterations of chromatin modifying activities have been recently reported, e.g. the hSNF5 component of the hSWI/SNF complex [59] and proteins that regulate histone acetylation [60,61]. Finally, CSB is the first of the class of repair proteins of the SWI/SNF family for which a chromatin remodeling activity is documented. This suggests that also the other repair members of this family mediate the crosstalk between repair and chromatin structure.

## Materials and methods

### *Proteins*

Recombinant, epitope tagged (N-terminal hemagglutinin antigen epitope, HA, and C-terminal histidine stretch, His<sub>6</sub>) CSB and CSB<sup>K538R</sup> mutant proteins were overexpressed using the Baculovirus system and purified as described [18], except that the final purification step was substituted by a Mono Q column. The eluate from the Ni<sup>2+</sup>-nitrilotriacetic acid-agarose column was loaded on a Mono Q column equilibrated with buffer A (25mM HEPES-KOH, pH7.9, 0.05% Nonidet P-40, 10% glycerol, 1mM EDTA, 1mM DTT, 0.1mM PMSF) in 0.1 M KCl and the adsorbed proteins were eluted by a 0.1M-1M KCl gradient. The elution profile and purity of the CSB fractions was monitored by SDS-PAGE followed by silver staining. Protein concentration was ~20 ng/μl. The hSWI/SNF complex was purified from HeLa cells by affinity chromatography to a FLAG epitope tag on the Ini1 subunit and its functional characterization was performed as described [29]. HeLa core histone octamers were purified as described by [62]. H1- depleted HeLa polynucleosomes were isolated and quantified as described previously [29].

### *ATPase assay*

Standard reactions (10 μl) were performed as described [18]. Plasmid DNA (300 ng), HeLa polynucleosomes (300 ng) untreated or trypsinized, and HeLa core histones (40 ng - 400 ng) were tested as cofactors. No ATPase activity intrinsic to HeLa polynucleosomes or core histones was detected. Incubation was for 30 min at 30°C, followed by separation on thin layer chromatography. ATP hydrolysis was determined by image analysis on a Phosphorimager (Molecular Dynamics).

### *Topological assay on plasmid DNA*

pBlueScript II KS was singly nicked by treatment with bovine pancreatic DNase I (Boehringer Mannheim) [63] and purified by phenol/chloroform extraction and ethanol precipitation. Reactions (60 μl) containing 100 ng of nicked plasmid and the indicated amounts of CSB or CSB<sup>K538R</sup> were performed as described [31] except for the KCl concentration, which was adjusted to 60 mM. After 10 min, one unit *E.coli* DNA ligase was added and the incubation was continued for 50 min. Where not specified, reactions did not contain ATP but NAD as cofactor of *E.Coli* DNA ligase. Topoisomers were resolved by electrophoresis on 1 % agarose gels containing 0.5 μg/ml

chloroquine. Gels were run in 1X TBE for 20 hrs at 70 V, followed by Southern blotting, hybridization with a pBluescript probe and autoradiography. Two-dimensional gel electrophoresis was performed as described [31,64]. In a control experiment, purified CSB was incubated with closed, supercoiled plasmid DNA under the above experimental conditions. Reactions were analyzed on a 0.8% agarose gel. No formation of relaxed DNA was observed.

#### *Mononucleosome assembly and DNase I accessibility assay*

Mononucleosome cores were assembled by step-wise salt dilution [32] on MluI-EcoRI DNA fragments obtained by digestion of the TPT plasmid [29]. The DNA sequence includes two GT-phasing sequences [65] and was 155 bp after labeling with Klenow and  $^{32}\text{P}$ -dCTP. After assembly, mononucleosomes were purified on a 5 to 30% glycerol gradient as described [32]. 10 ng of these tailed mononucleosomes were diluted in 100  $\mu\text{l}$  of buffer V (25 mM NaCl, 10 mM Tris-HCl [pH 8.0], 1 mM EDTA) and trypsinized for 10 minutes at RT with trypsin (5 ng/ $\mu\text{l}$ ) as described by Guyon *et al.*, 1999 [46]. Reactions were stopped with 15-fold excess (wt/wt) soybean trypsin inhibitor. Trypsinization was monitored by electrophoresis on a 5% nondenaturing acrylamide gel.

DNase I footprinting reactions (25  $\mu\text{l}$ ) were performed as described [29,32] except that 0.5 mg/ml BSA was added. Where indicated, the reactions contained the non-hydrolysable ATP analog ATP $\gamma$ S (Sigma) or 1U of apyrase (Sigma) (dissolved in 20 mM HEPES, pH 7.9, 1mM MgCl<sub>2</sub>, 1mM DTT, 1mM EDTA, 1 mg/ml BSA at a concentration of 1U/ $\mu\text{l}$ ). KCl concentration was adjusted at 60 mM in all reactions. After incubation at 30°C for 45 minutes, followed by 5 min at room temperature, the reactions were subjected to digestion with DNase I. Tailed mononucleosomes were digested with 0.1 U DNase I, tailless mononucleosomes were digested with 0.025 U DNase I. Processing and denaturing PAGE were performed as described [32].

#### *Gel-shift and histone octamer transfer reactions*

For gel shift analysis, remodeling reactions (containing either 0.3 ng labeled nucleosome particles or labeled naked DNA, and the indicated amount of CSB) were directly loaded onto 4% polyacrylamide gels (80:1 acrylamide/bisacrylamide ratio) containing 12.5 mM Tris, 100 mM glycine, 0.5 mM EDTA. Gels were run at ~150 V for ~2.5 hours at 4 °C. Where indicated, reactions were stopped by the addition of KCl (160 mM final), and competitor DNA (2  $\mu\text{g}$  plasmid DNA, 0.5  $\mu\text{g}$  polynucleosomes) prior to loading on the gel. Octamer transfer reactions contained unlabeled HeLa polynucleosomes in excess (10 ng), naked labeled TPT MluI-EcoRI fragment (1 ng) as possible acceptor of core particles, CSB (40 ng) or hSWI/SNF (200 ng) and were performed under the same conditions as for the DNase I footprinting. After 60 min at 30 °C, KCl and 2  $\mu\text{g}$  of plasmid DNA (as described above) were added to stop the reactions. Samples were further incubated at 30 °C for 10 min and analyzed by EMSA using 5% polyacrylamide gels [66]. Product analysis was performed using a PhosphorImager. Both in the presence or absence of ATP, no *de novo* formation of core particles on the naked DNA could be detected in the CSB reactions, whereas octamer transfer was catalyzed by hSWI/SNF in an ATP dependent manner (data not shown).

#### *Plasmid chromatin remodeling assays*

Chromatin was assembled on the 3.35-Kb pG<sub>5</sub>HC<sub>2</sub>AT plasmid [67] in *Drosophila* embryo extracts and subsequently treated with sarkosyl to disrupt endogenous remodeling activities according to published protocols [33,34]. Sarkosyl and ATP were removed by gel filtration on Micro

Bio-spin columns (Bio-Gel polyacrylamide P-6, Biorad). Sarkosyl-treated chromatin (~40 ng DNA) was incubated with CSB or CSB<sup>K538R</sup> (estimated amount 160 ng) or with hSWI/SNF complex (300 ng) for 90 min at 30 °C in 70 µl of EX buffer [33] containing 60 mM KCl. Micrococcal nuclease (MNase) digestion and agarose-gel electrophoresis were performed as described [33]. Southern blotting, hybridization with <sup>32</sup>P-labelled total plasmid DNA and autoradiography were used to visualize the DNA fragments.

The supercoiling assay on reconstituted plasmid chromatin was performed as described [32]. The pG<sub>5</sub>HC<sub>2</sub>AT plasmid was internally labeled and assembled into nucleosomes using purified HeLa core histones and a heat-treated *Xenopus* egg extract [32]. Glycerol gradient purified template (1 ng DNA) was incubated with the given amounts of CSB and hSWI/SNF and remodeling reactions were carried out in 12.5 or 25 µl for 90 min at 30 °C as described [32]. Reactions contained 60 mM KCl. Similar results were obtained when the pG<sub>5</sub>HC<sub>2</sub>AT plasmid was assembled with *Drosophila* embryo extracts [33], sarkosyl treated and reaction were carried out under the same experimental conditions described above for the MNase analysis.

#### *Antibodies and immunoprecipitations*

Purified CSB (500 ng) and HeLa core histones (2 µg) were incubated *in vitro* in buffer A containing 0.01% Nonidet-P 40 and 0.1 M KCl for 2 hours at 4 °C with rotation. Immunoprecipitation was performed overnight at 4 °C either with rabbit polyclonal antibodies raised against CSB (3 µl crude serum) [11] or with 2 µg mouse monoclonal antibodies that recognize an epitope present on all four histones (anti-histone, pan H11-4, Boehringer Mannheim). Mock immunoprecipitations were carried out either in the absence of CSB or in the absence of histones. Binding of the antibody-protein complexes to Protein-A sepharose beads, equilibrated in buffer A, was for 2 hours at 4 °C. The beads were washed three times with 20 volumes buffer A containing 0.1% Nonidet P-40 and 0.35 mM KCl and three times with buffer A containing 0.01% Nonidet P-40 and 0.1M KCl. After boiling of the beads, the bound proteins were analyzed by SDS-PAGE either using 8 % gels (to visualize CSB) or 16.5 % gels (to visualize the histones) followed by silver staining.

#### *Far-Western analysis*

Samples of H1-depleted HeLa polynucleosomes untreated (+tails) and trypsinized (-tails) (3.6 µg) and two controls proteins, cytochrome c (0.9 µg) (Sigma) and Bovine serum albumine, DNase-free (0.9 µg) (Pharmacia Biotech), were used. HeLa polynucleosomes were trypsinized following a previously described protocol [46]. The trypsinization reaction was for 30 min at room temperature, was stopped by the addition of 20-fold excess (wt/wt) of soybean trypsin inhibitor (Sigma) and monitored by SDS-PAGE and Coomassie staining. All protein samples were separated on 16.5 % SDS-polyacrylamide gels and stained with Coomassie or transferred to nitrocellulose membrane for far-Western analysis. The membrane was blocked with skimmed milk containing 0.05 % Tween-50 and incubated with purified CSB (100 ng/ml) overnight at 4°C. Bound protein complexes were visualized by incubation with affinity-purified anti-CSB antibodies [11], goat anti-rabbit secondary antibodies (BIOSOURCE), and the alkaline phosphatase detection method.



## Acknowledgements

We are very grateful to the entire Kingston lab for indispensable help, especially to J. Guyon and L. Corey for sharing reagents and protocols, and M. Phelan and G. Narlikar for fruitful suggestions. We are also indebted to P. Becker for *Drosophila* facilities. We thank the members of our lab for constant support and helpful discussion and Prof. D. Bootsma for his continued interest. S. van Baal is acknowledged for his assistance in computer work and M. Kuit for photography. This work was supported by EC grant n.7010-212; the Dutch Science Foundation (NWO 901-501-151); R.K. is a fellow of the Royal Netherlands Academy of Arts and Sciences; J.H.J.H. is recipient of a SPINOZA award from NWO.

## References

1. **de Laat, W.L., Jaspers, N.G. and Hoeijmakers, J.H.** (1999) Molecular mechanism of nucleotide excision repair. *Genes Dev.*, 13, 768-785.
2. **Bohr, V.A., Smith, C.A., Okumoto, D.S. and Hanawalt, P.C.** (1985) DNA repair in an active gene: removal of pyrimidine dimers from the *DHFR* gene of CHO cells is much more efficient than in the genome overall. *Cell*, 40, 359-369.
3. **Mellon, I., Spivak, G. and Hanawalt, P.C.** (1987) Selective removal of transcription-blocking DNA damage from the transcribed strand of the mammalian *DHFR* gene. *Cell*, 51, 241-249.
4. **Van Gool, A.J., Van der Horst, G.T.J., Citterio, E. and Hoeijmakers, J.H.J.** (1997) Cockayne syndrome: defective repair of transcription? *EMBO J.*, 16, 4155-4162.
5. **Cooper, P.K., Nusspikel, T., Clarkson, S.G. and Leadon, S.A.** (1997) Defective transcription-coupled repair of oxidative base damage in Cockayne syndrome patients from XP group G. *Science*, 275, 990-993.
6. **Le Page, F., Kwok, E.E., Avrutskaya, A., Gentil, A., Leadon, S.A., Sarasin, A. and Cooper, P.K.** (2000) Transcription-coupled repair of 8-oxoguanine: requirement for XPG, TFIIH, and CSB and implications for Cockayne syndrome. *Cell*, 101, 159-171.
7. **Bootsma, D., Kraemer, K.H., Cleaver, J.E. and Hoeijmakers, J.H.J.** (1997) Nucleotide excision repair syndromes: xeroderma pigmentosum, Cockayne syndrome and trichothiodystrophy. In Scriver, C.R., Beaudet, A.L., Sly, W.S. and Valle, D. (eds.), *The metabolic basis of inherited disease. Eight edition*. McGraw-Hill Book Co., New York.
8. **Nance, M.A. and Berry, S.A.** (1992) Cockayne syndrome: Review of 140 cases. *Am. J. of Med. Genet.*, 42, 68-84.
9. **Henning, K.A., Li, L., Iyer, N., McDaniel, L., Reagan, M.S., Legerski, R., Schultz, R.A., Stefanini, M., Lehmann, A.R., Mayne, L.V. and Friedberg, E.C.** (1995) The Cockayne syndrome group A gene encodes a WD repeat protein that interacts with CSB protein and a subunit of RNA polymerase II TFIIH. *Cell*, 82, 555-564.
10. **Troelstra, C., Van Gool, A., De Wit, J., Vermeulen, W., Bootsma, D. and Hoeijmakers, J.H.J.** (1992) ERCC6, a member of a subfamily of putative helicases, is involved in Cockayne syndrome and preferential repair of active genes. *Cell*, 71, 939-953.
11. **van Gool, A.J., Citterio, E., Rademakers, S., van Os, R., Vermeulen, W., Constantinou, A., Egly, J.M., Bootsma, D. and Hoeijmakers, J.H.J.** (1997) The Cockayne syndrome B protein, involved in transcription-coupled DNA repair, resides in a RNA polymerase II containing complex. *EMBO J.*, 16, 5955-5965.
12. **Tantini, D., Kansal, A. and Carey, M.** (1997) Recruitment of the putative transcription-repair coupling factor CSB/ERCC6 to RNA polymerase II elongation complexes. *Mol. Cell. Biol.*, 17, 6803-6814.
13. **Selby, C.P. and Sancar, A.** (1997) Cockayne syndrome group B protein enhances elongation by RNA polymerase II. *Proc. Natl. Acad. Sci. USA*, 94, 11205-11209.

14. **Balajee, A.S., May, A., Dianov, G.L., Friedberg, E.C. and Bohr, V.A.** (1997) Reduced RNA polymerase II transcription in intact and permeabilized Cockayne syndrome group B cells. *Proc. Natl. Acad. Sci. USA*, 94, 4306-4311.
15. **Citterio, E., Vermeulen, W. and Hoeijmakers, J.H.J.** (2000) Transcriptional healing. *Cell*, 101, 447-450.
16. **Eisen, J.A., Sweder, K.S. and Hanawalt, P.C.** (1995) Evolution of the SNF2 family: subfamilies with distinct sequences and functions. *Nucleic Acids Res.*, 23, 2715-2723.
17. **Cote, J., Quinn, J., Workman, J.L. and Peterson, C.I.** (1994) Stimulation of GAL derivative binding to nucleosomal DNA by the yeast SWI/SNF complex. *Science*, 265, 53-60.
18. **Citterio, E., Rademakers, S., van der Horst, G.T., van Gool, A.J., Hoeijmakers, J.H. and Vermeulen, W.** (1998) Biochemical and biological characterization of wild-type and ATPase-deficient Cockayne syndrome B repair protein. *J. Biol. Chem.*, 273, 11844-11851.
19. **Selby, C.P. and Sancar, A.** (1997) Human transcription-repair coupling factor CSB/ERCC6 is a DNA-stimulated ATPase but is not a helicase and does not disrupt the ternary transcription complex of stalled RNA polymerase II. *J. Biol. Chem.*, 272, 1885-1890.
20. **Pazin, M.J. and Kadonaga, J.T.** (1997) SWI2/SNF2 and related proteins: ATP-driven motors that disrupt protein-DNA interactions? *Cell*, 88, 737-740.
21. **Workman, J.L. and Kingston, R.E.** (1998) Alteration of nucleosome structure as a mechanism of transcriptional regulation. *Annu. Rev. Biochem.*, 67, 545-579.
22. **Kingston, R.E. and Narlikar, G.J.** (1999) ATP-dependent remodeling and acetylation as regulators of chromatin fluidity. *Genes Dev.*, 13, 2339-2352.
23. **Phelan, M.L., Sif, S., Narlikar, G.J. and Kingston, R.E.** (1999) Reconstitution of a core chromatin remodeling complex from SWI/SNF subunits. *Mol. Cell*, 3, 247-253.
24. **Corona, D.F., Langst, G., Clapier, C.R., Bonte, E.J., Ferrari, S., Tamkun, J.W. and Becker, P.B.** (1999) ISWI is an ATP-dependent nucleosome remodeling factor. *Mol. Cell*, 3, 239-245.
25. **Kwon, H., Imbalzano, A.N., Khavari, P.A., Kingston, R.E. and Green, M.R.** (1994) Nucleosome disruption and enhancement of activator binding by a human SWI/SNF complex. *Nature*, 370, 477-481.
26. **Wang, W., Cote, J., Xue, Y., Zhou, S., Khavari, P.A., Biggar, S.R., Muchardt, C., Kalpana, G.V., Goff, S.P., Yaniv, M., Workman, J.L. and Crabtree, G.R.** (1996) Purification and biochemical heterogeneity of the mammalian SWI-SNF complex. *EMBO J.*, 15, 5370-5382.
27. **Cairns, B.R.** (1998) Chromatin remodeling machines: similar motors, ulterior motives. *Trends Biochem. Sci.*, 23, 20-25.
28. **Smerdon, M.J. and Conconi, A.** (1999) Modulation of DNA damage and DNA repair in chromatin. *Prog. Nucleic Acid Res. Mol. Biol.*, 62, 227-255.
29. **Schnitzler, G., Sif, S. and Kingston, R.E.** (1998) Human SWI/SNF interconverts a nucleosome between its base state and a stable remodeled state. *Cell*, 94, 17-27.
30. **Swagemakers, S.M., Essers, J., de Wit, J., Hoeijmakers, J.H. and Kanaar, R.** (1998) The human RAD54 recombinational DNA repair protein is a double-stranded DNA-dependent ATPase. *J. Biol. Chem.*, 273, 28292-28297.
31. **Tan, T.L., Essers, J., Citterio, E., Swagemakers, S.M., de Wit, J., Benson, F.E., Hoeijmakers, J.H. and Kanaar, R.** (1999) Mouse Rad54 affects DNA conformation and DNA-damage-induced Rad51 foci formation. *Curr. Biol.*, 9, 325-328.
32. **Imbalzano, A.N., Schnitzler, G.R. and Kingston, R.E.** (1996) Nucleosome disruption by human SWI/SNF is maintained in the absence of continued ATP hydrolysis. *J. Biol. Chem.*, 271, 20726-20733.
33. **Varga-Weisz, P.D., Bonte, E.J. and Becker, P.B.** (1999) Analysis of modulators of chromatin structure in *Drosophila*. *Methods Enzymol.*, 304, 742-757.
34. **Varga-Weisz, P.D., Wilm, M., Bonte, E., Dumas, K., Mann, M. and Becker, P.B.** (1997) Chromatin-remodelling factor CHRAC contains the ATPases ISWI and topoisomerase II. *Nature*, 388, 598-602.
35. **Ito, T., Bulger, M., Pazin, M.J., Kobayashi, R. and Kadonaga, J.T.** (1997) ACF, an ISWI-containing and ATP-utilizing chromatin assembly and remodeling factor. *Cell*, 90, 145-155.

36. **Wilson, C.J., Chao, D.M., Imbalzano, A.N., Schnitzler, G.R., Kingston, R.E. and Young, R.A.** (1996) RNA polymerase II holoenzyme contains SWI/SNF regulators involved in chromatin remodeling. *Cell*, 84, 235-44.
37. **Whitehouse, I., Flaus, A., Cairns, B.R., White, M.F., Workman, J.L. and Owen-Hughes, T.** (1999) Nucleosome mobilization catalysed by the yeast SWI/SNF complex. *Nature*, 400, 784-787.
38. **Lorch, Y., Zhang, M. and Kornberg, R.D.** (1999) Histone octamer transfer by a chromatin-remodeling complex. *Cell*, 96, 389-392.
39. **Langst, G., Bonte, E.J., Corona, B.F. and Becker, P.B.** (1999) Nucleosome movement by CHRAC and ISWI without disruption or trans- displacement of the histone octamer. *Cell*, 97, 843-852.
40. **Hamiche, A., Sandaltzopoulos, R., Gdula, D.A. and Wu, C.** (1999) ATP-dependent histone octamer sliding mediated by the chromatin remodeling complex NURF. *Cell*, 97, 833-842.
41. **Eickbush, T.H. and Moudrianakis, E.N.** (1978) The histone core complex: an octamer assembled by two sets of protein- protein interactions. *Biochemistry*, 17, 4955-4964.
42. **Karantza, V., Baxevanis, A.D., Freire, E. and Moudrianakis, E.N.** (1995) Thermodynamic studies of the core histones: ionic strength and pH dependence of H2A-H2B dimer stability. *Biochemistry*, 34, 5988-5996.
43. **Baxevanis, A.D., Godfrey, J.E. and Moudrianakis, E.N.** (1991) Associative behavior of the histone (H3-H4)<sub>2</sub> tetramer: dependence on ionic environment. *Biochemistry*, 30, 8817-8823.
44. **Luger, K., Mader, A.W., Richmond, R.K., Sargent, D.F. and Richmond, T.J.** (1997) Crystal structure of the nucleosome core particle at 2.8 Å resolution. *Nature*, 389, 251-260.
45. **Luger, K. and Richmond, T.J.** (1998) The histone tails of the nucleosome. *Curr. Opin. Genet. Dev.*, 8, 140-146.
46. **Guyon, J.R., Narlikar, G.J., Sif, S. and Kingston, R.E.** (1999) Stable remodeling of tailless nucleosomes by the human SWI-SNF complex. *Mol. Cell. Biol.*, 19, 2088-2097.
47. **Stros, M., Stokrova, J. and Thomas, J.O.** (1994) DNA looping by the HMG-box domains of HMG1 and modulation of DNA binding by the acidic C-terminal domain. *Nucleic Acids Res.*, 22, 1044-1051.
48. **Fisher, R.P., Lisowsky, T., Parisi, M.A. and Clayton, D.A.** (1992) DNA wrapping and bending by a mitochondrial high mobility group-like transcriptional activator protein. *J. Biol. Chem.*, 267, 3358-3367.
49. **Giese, K., Pagel, J. and Grosschedl, R.** (1997) Functional analysis of DNA bending and unwinding by the high mobility group domain of LEF-1. *Proc. Natl. Acad. Sci. USA*, 94, 12845-12850.
50. **Quinn, J., Fyrberg, A.M., Ganster, R.W., Schmidt, M.C. and Peterson, C.L.** (1996) DNA-binding properties of the yeast SWI/SNF complex. *Nature*, 379, 844-847.
51. **Tsukiyama, T. and Wu, C.** (1995) Purification and properties of an ATP-dependent nucleosome remodeling factor. *Cell*, 83, 1011-1020.
52. **Georgel, P.T., Tsukiyama, T. and Wu, C.** (1997) Role of histone tails in nucleosome remodeling by Drosophila NURF. *EMBO J.*, 16, 4717-4726.
53. **Logie, C., Tse, C., Hansen, J.C. and Peterson, C.L.** (1999) The core histone N-terminal domains are required for multiple rounds of catalytic chromatin remodeling by the SWI/SNF and RSC complexes. *Biochemistry*, 38, 2514-2522.
54. **Yu, A., Fan, H.-Y., Liao, D., Bailey, A.D. and Weiner, A.M.** (2000) Activation of p53 or Loss of the Cockayne Syndrome Group B Repair Protein Causes Metaphase Fragility of Human U1, U2, and 5S Genes. *Molecular Cell*, 5, 801-810.
55. **Meijer, M. and Smerdon, M.J.** (1999) Accessing DNA damage in chromatin: insights from transcription. *BioEssays*, 21, 596-603.
56. **Moggs, J.G. and Almouzni, G.** (1999) Chromatin rearrangements during nucleotide excision repair. *Biochimie*, 81, 45-52.
57. **Izban, M.G. and Luse, D.S.** (1991) Transcription on nucleosomal templates by RNA polymerase II in vitro: inhibition of elongation with enhancement of sequence-specific pausing. *Genes Dev.*, 5, 683-696.

58. **Brown, S.A., Imbalzano, A.N. and Kingston, R.E.** (1996) Activator-dependent regulation of transcriptional pausing on nucleosomal templates. *Genes Dev.*, 10, 1479-1490.
59. **Versteeg, I., Sevenet, N., Lange, J., Rousseau-Merck, M.F., Ambros, P., Handgretinger, R., Aurias, A. and Delattre, O.** (1998) Truncating mutations of hSNF5/INI1 in aggressive paediatric cancer. *Nature*, 394, 203-206.
60. **Lin, R.J., Nagy, L., Inoue, S., Shao, W., Miller, W.H., Jr. and Evans, R.M.** (1998) Role of the histone deacetylase complex in acute promyelocytic leukaemia. *Nature*, 391, 811-814.
61. **Sobulo, O.M., Borrow, J., Tomek, R., Reshmi, S., Harden, A., Schlegelberger, B., Housman, D., Doggett, N.A., Rowley, J.D. and Zeleznik-Le, N.J.** (1997) MLL is fused to CBP, a histone acetyltransferase, in therapy-related acute myeloid leukemia with a t(11;16)(q23;p13.3). *Proc. Natl. Acad. Sci. USA*, 94, 8732-8737.
62. **Workman, J.L., Taylor, I.C., Kingston, R.E. and Roeder, R.G.** (1991) Control of class II gene transcription during in vitro nucleosome assembly. *Methods Cell Biol.*, 35, 419-447.
63. **Crisona, N.J., Kanaar, R., Gonzalez, T.N., Zechiedrich, E.L., Klippel, A. and Cozzarelli, N.R.** (1994) Processive recombination by wild-type gin and an enhancer-independent mutant. Insight into the mechanisms of recombination selectivity and strand exchange. *J. Mol. Biol.*, 243, 437-457.
64. **Stark, W.M., Sherratt, D.J. and Boocock, M.R.** (1989) Site-specific recombination by Tn3 resolvase: topological changes in the forward and reverse reactions. *Cell*, 58, 779-790.
65. **Shrader, T.E. and Crothers, D.M.** (1989) Artificial nucleosome positioning sequences. *Proc. Natl. Acad. Sci. U S A*, 86, 7418-7422.
66. **Huang, S.Y. and Garrard, W.T.** (1989) Electrophoretic analyses of nucleosomes and other protein-DNA complexes. *Methods Enzymol.*, 170, 116-142.
67. **Workman, J.L., Taylor, I.C. and Kingston, R.E.** (1991) Activation domains of stably bound GAL4 derivatives alleviate repression of promoters by nucleosomes. *Cell*, 64, 533-544.

# Chapter 7

Transient interactions of CSB with  
transcription elongation complexes are  
stabilized by DNA damage-induced  
stalling

*Submitted*

# Transient interactions of CSB with transcription elongation complexes are stabilized by DNA damage-induced stalling

Vincent van den Boom<sup>1\*</sup>, Elisabetta Citterio<sup>2\*</sup>, Deborah Hoogstraten<sup>1</sup>, Wiggert. A. van Cappellen<sup>3</sup>, Jan H.J. Hoeijmakers<sup>1</sup>, Adriaan B. Houtsmuller<sup>4</sup> and Wim Vermeulen<sup>1</sup>

1) *Department of Cell Biology and Genetics, Medical Genetic Center*, 3) *Department of Endocrinology and Reproduction, Medical Genetic Center*, 4) *Department of Pathology, Josephine Nefkens Institute, Erasmus MC Rotterdam, P.O. Box 1738, 3000 DR Rotterdam, The Netherlands*; 2) *current address: Present address: IFOM-FIRC Institute of Molecular Oncology, via Adamello 16, 20139 Milano, Italy.*

*\*these authors contributed equally to this work*

## Abstract

The Cockayne syndrome B (CSB) protein is essential for transcription-coupled DNA repair (TCR), which is dependent on RNA polymerase II elongation. TCR is required to quickly remove the cytotoxic transcription-blocking DNA lesions. GFP-CSB was homogeneously dispersed throughout the nucleoplasm in addition to bright nuclear foci and nucleolar accumulation. High-resolution imaging and fluorescence recovery after photobleaching (FRAP) showed that these nuclear assemblies are highly dynamic and respond to changes in transcriptional activity and DNA damage. GFP-CSB, as part of a high molecular weight complex, interacts with the transcription machinery in a quick 'on-off' mode, which is converted to a more stable binding upon (damage-dependent) transcription arrest, most likely reflecting actual engagement of CSB in TCR. These findings support a model in which CSB monitors progression of transcription by regularly probing elongation complexes and becomes more tightly associated to these complexes upon stalling to exert its function in TCR.

## Introduction

Metabolic by-products such as reactive oxygen species (ROS), environmental compounds and short-wave electromagnetic radiation ( $\gamma$  and UV) continuously jeopardize the DNA structure. DNA injuries directly disturb vital DNA-transacting processes such as replication, transcription and cell cycle progression. DNA damage-induced transcriptional interference triggers apoptosis [1,2], ultimately, leading to segmental ageing in mammals [3]. Moreover, DNA lesions may result in permanent mutations in the DNA sequence, eventually causing cancer. In order to prevent the severe consequences of genetic

erosion a variety of distinct and partially overlapping DNA repair pathways has evolved, each specialized in the removal of specific types of damage [4,5]. Priority is given to remove the highly cytotoxic transcription-blocking injuries, allowing quick resumption of transcription. This process, referred to as transcription-coupled repair (TCR) [6], is directly triggered by lesion-induced obstruction of elongating RNA polymerase II (RNAP II). Dependent on the type of the encountered lesion blocked RNAP II complexes are first addressed by TCR-specific factors and further processed by the core nucleotide and perhaps base excision repair (NER and BER, respectively) factors [7]. Removal of lesions in non-transcribed areas of the genome is dependent on global genome repair (GGR).

Inherited defects within genes involved in the TCR-pathway give rise to the rare autosomal recessive disorder Cockayne syndrome (CS). CS patients display mainly progeroid symptoms, growth failure and severe neurological abnormalities and are not cancer-prone [8]. Most of the salient clinical symptoms expressed among CS individuals, except sun-sensitive skin, are difficult to be explained by a DNA repair defect only. Within classical Cockayne syndrome two genes are involved, CSA and CSB [9,10]. The proteins encoded by these genes are essential for TCR, however their exact function in this process remains elusive. The 44 kDa CSA protein contains 5 WD repeats; polypeptides with these repeats are usually involved in formation of macromolecular complexes via the WD-repeat regions [11]. The 168 kDa CSB protein is a member of the SWI2/SNF2 protein family of putative helicases, which includes a variety of proteins involved in transcriptional regulation, chromatin remodelling and DNA repair [12]. Biochemical studies showed that recombinant CSB is a DNA-dependent ATPase and is able to remodel chromatin at the expense of ATP [13,14].

Since TCR only occurs in the presence of active transcription, it was suggested that the CS proteins probably interact with elongating RNA polymerase complexes. Moreover, besides a pivotal role in TCR, several lines of evidence suggest an additional function of CS proteins, particularly CSB, in the elongation phase of RNAP II transcription. Gel filtration and immunoprecipitation studies showed that CSB resides in a high molecular weight complex and that a part of these higher order assemblies contain RNAP II [15]. Gel mobility shift assays further reveal that CSB interacts with a ternary complex of DNA, RNAP II and nascent RNA [16]. In addition, *in vitro* transcription experiments showed that CSB stimulates RNAP II elongation [17]. Recently, in a genetic screen for suppressor mutants of Rad26 (the yeast counterpart of CSB), Spt4 was identified [18]. Spt4 is part of a protein complex known to associate with and regulate the processivity of RNAP II, further supporting a function of CSB in transcription elongation [19,20]. However, direct proof for a role of CSB in transcription elongation and whether CSB is an intrinsic component of elongating RNAP II *in vivo* is lacking.

A potential problem for the repair machinery is that lesion stalled polymerases impede the accessibility of repair factors to these lesions by steric hindrance [21]. Several models have been suggested that describe the function of the CS proteins and the fate of stalled RNAP II complexes at lesions: (i) backtracking of the RNAP II complex, providing access to lesions, (ii) pushing the elongating polymerase past the lesion, trans-lesion transcription (iii) physical removal of the complex, (iv) proteolytic degradation of the stalled polymerase or (v) recruiting NER proteins that compete with RNAP II. Efforts to

set up an *in vitro* system for TCR have met with little success. A possible explanation is that *in vitro* systems lack the structural elements that are required for proper TCR function (such as nuclear matrix attachment or chromatinated DNA). Particularly, the topological and ATP-dependent chromatin remodelling activity of CSB suggests a role for this protein in remodelling the chromatin structure or the interaction surface of the stalled RNAP II with DNA, to permit admission of the NER machinery to the lesion. However, an adequate model at which stage the TCR factors CSA and CSB are operational is lacking.

To directly address some of these issues, we investigated the involvement of CSB in TCR and RNAP II transcription elongation in the most relevant context, the living cell. We generated a cell line that stably expresses physiologically relevant levels of a biologically active fusion protein of the green fluorescent protein (GFP) and CSB. Spatial and temporal distribution of GFP-CSB was monitored with state-of-the-art live cell microscopy. In addition, advanced FRAP (for fluorescence recovery after photobleaching) analysis was used to specifically measure the mobility of the CSB protein under different conditions, such as upon DNA damage induction and after transcriptional interference. Moreover, we determined the *in vivo* reaction parameters of this protein when engaged in repair and transcription.

## Results

### *Expression of GFP-CSB in human fibroblasts*

To study the nuclear organization and dynamic properties of the CSB protein in living cells, we tagged the protein with GFP. Enhanced green fluorescent protein (eGFP) was fused to the amino-terminus of CSB (Fig. 1A), resulting in a GFP-CSB fusion protein, which was stably expressed in CSB-deficient human fibroblasts (CS1AN-Sv). Immunoblot analysis, using anti-CSB (Fig. 1B) and anti-GFP (data not shown) antibodies, showed that GFP-CSB migrates at the expected height of full-length fusion protein (~195 kDa) in two independent clones, and was expressed at physiological levels (Fig. 1B). In addition, the GFP-CSB cDNA was able to fully correct the UV-sensitivity of CS-B cells (Fig. 1C), indicating that GFP-CSB is functional *in vivo*.

### *Localization of GFP-CSB in living cells*

Confocal microscopy demonstrated that the tagged protein predominantly resides in the nucleus (Fig. 1D and 1E). In addition to a uniform fluorescent signal in the nucleoplasm, small bright accumulations of GFP-CSB were observed (Fig. 1D). These foci vary in size and number per nucleus and are present in a large fraction of the cells ( $73 \pm 9\%$ , Fig. 2). In addition, the fusion protein appeared more concentrated in the nucleolus (Fig. 2A). Immunofluorescence (IF) studies using affinity-purified polyclonal anti-CSB antibodies revealed a similar pattern in wild type human fibroblasts (MRC5-Sv) (Fig. 1F) and HeLa cells (Fig. 1G) as observed with GFP-CSB in living cells. Together these data suggest that the observed distribution is not due to a GFP-tagging artefact or to over-expression of the protein and likely reflects the endogenous nuclear organization of CSB.



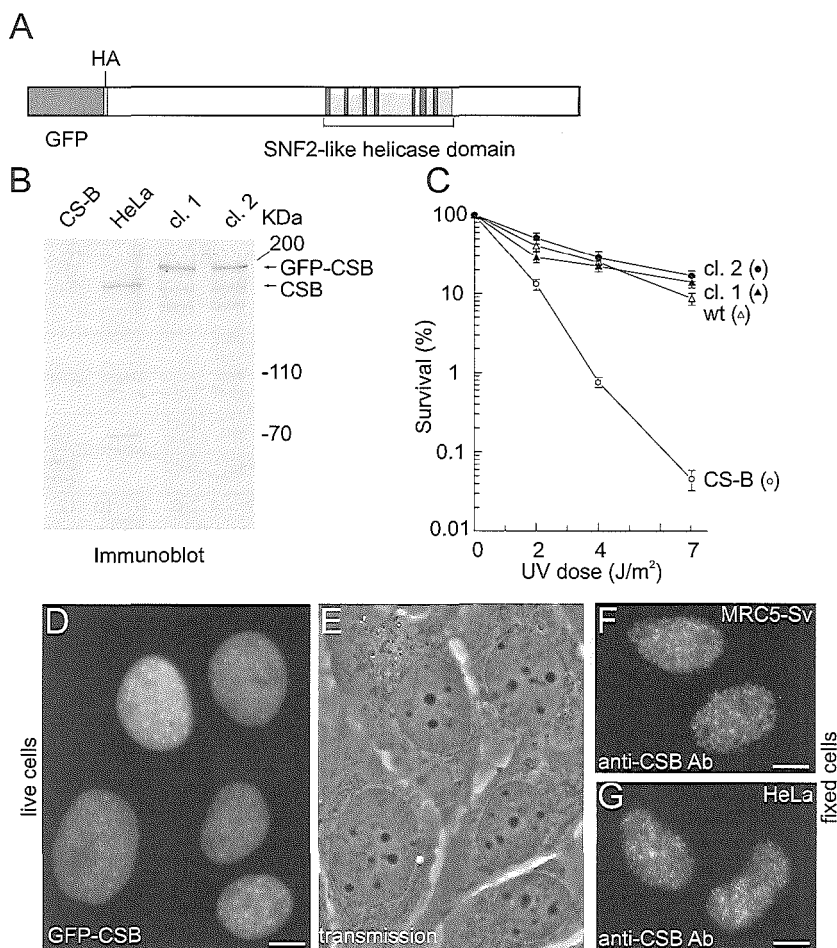
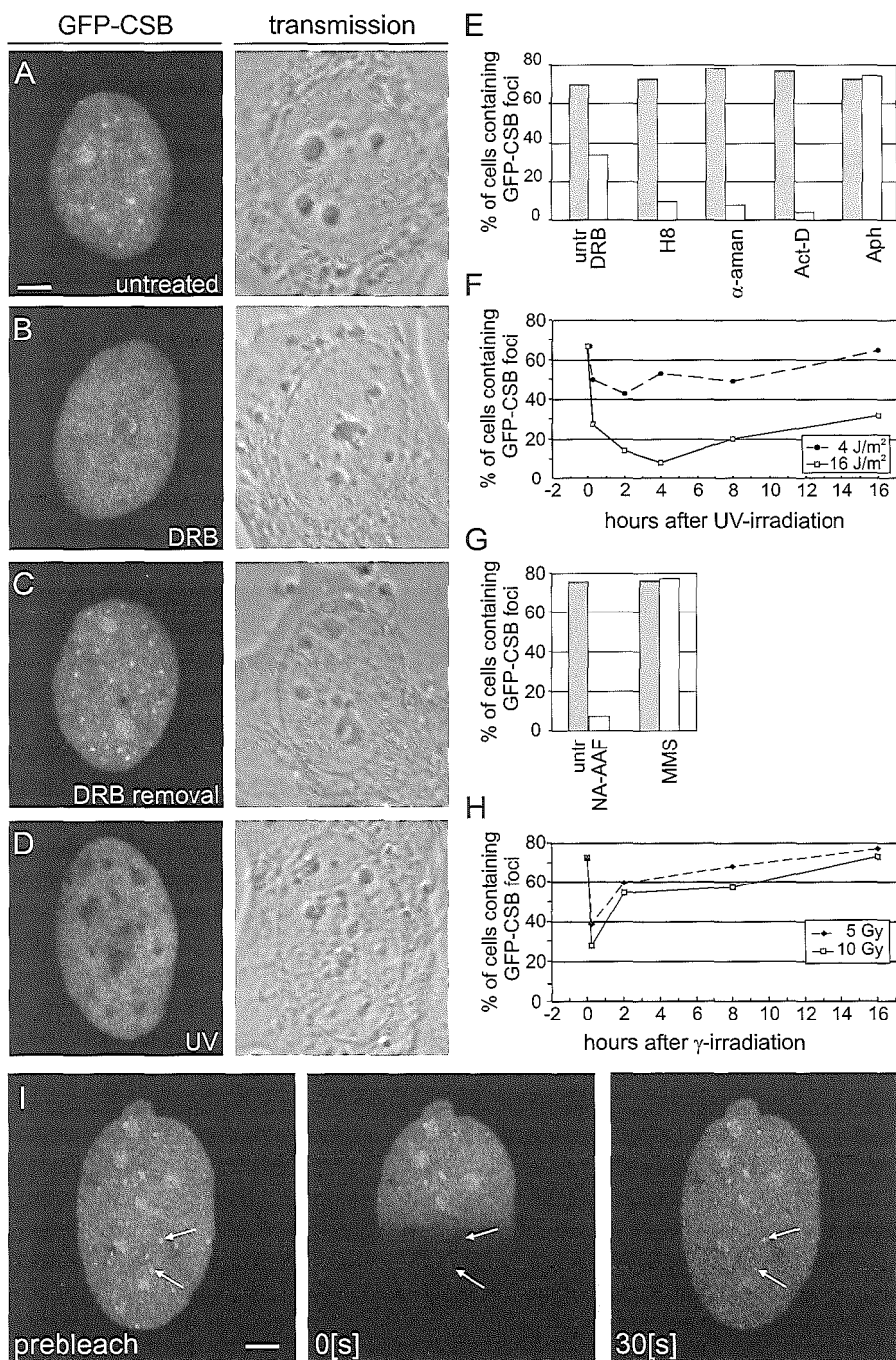


**Figure 1. Characterisation of stably expressed GFP-CSB in CS1AN-Sv human fibroblasts.** A. Schematic representation of GFP-CSB fusion protein. The SNF2-like helicase domain is indicated. In between the GFP cDNA and the CSB open reading frame an HA tag is present. B. Immunoblot analysis of GFP-CSB expression. Equal amounts of whole cell extracts (WCE) from CS1AN-Sv, HeLa and GFP-CSB transfected CS1AN-Sv fibroblasts (two independent clones, 1 and 2 respectively) were probed with affinity-purified polyclonal anti-CSB antibodies. C. UV-survival of GFP-CSB expressing fibroblasts. The percentage of surviving cells is plotted against the applied UV dose. Survival of clones 1 and 2 and control cell lines after UV-treatment was determined by pulse labelling with  $^3H$ -thymidine: CS1AN-Sv, CS-B (open circles); VH10-Sv, wt (open triangles), clone 1 (triangles), clone 2 (circles). Both clones show a complete restoration of the CS-specific UV-sensitivity, indicating that the GFP-tagged CSB protein is fully functional. D-E. Subnuclear localization of GFP-CSB in living stably transfected CS1AN-Sv human fibroblasts. Images of clone 1 cells are shown in D (epifluorescence) and E (transmission). All cells show a strict nuclear distribution and dispersed focal accumulations of GFP-CSB in the nucleoplasm. F-G. Epifluorescent images of MRC5-Sv human fibroblasts (F) and HeLa cells (G) immuno-stained with affinity-purified anti-CSB antibodies. Scale bars are 10  $\mu m$ .



### *Transcription and DNA damage dependent localization of GFP-CSB*

There is increasing evidence indicating that CSB is involved in transcription [15-17,22,23]. To investigate whether the observed GFP-CSB foci are related to transcriptional activity, transcription in GFP-CSB expressing cells was arrested using different drugs that inhibit RNAP II transcription through different mechanisms: DRB, H8,  $\alpha$ -amanitin and actinomycin D. Inhibition of transcription elongation by DRB resulted in a dramatic decrease in the number of cells containing GFP-CSB foci (compare Fig. 2A with 2B) and a concomitant exclusion of nucleolar fluorescence was observed. Removal of DRB resulted in a complete reversal of the spatial organization (Fig. 2C). Elongation interference by H8 leads to a similar loss of nuclear GFP-CSB foci and of nucleolar accumulation (Fig. 2E). General transcription inhibition by  $\alpha$ -amanitin, which binds to RNAP II, or by the DNA-intercalating agent actinomycin-D showed a comparable change in CSB distribution (Fig. 2E). In contrast, the replication-blocking agent aphidicolin did not interfere with GFP-CSB distribution, emphasizing that the redistribution of GFP-CSB is transcription dependent.

To investigate the potential function of the GFP-CSB foci in DNA repair, we challenged GFP-CSB cells with UV-light. UV-irradiation induced a rapid relocation of GFP-CSB in which the foci and nucleolar accumulation were converted to a uniform distribution of GFP-CSB similar to transcription inhibition (Fig. 2). The percentage of cells presenting GFP-CSB foci significantly decreased within 15 minutes post-UV, in a UV-dose dependent fashion with a more dramatic effect at a high dose of 16 J/m<sup>2</sup> as compared to 4 J/m<sup>2</sup>. The subsequent reappearance of GFP-CSB foci was also UV-dose, and time-dependent (Fig. 2F) and its kinetics strikingly paralleled the recovery of RNA synthesis (RRS) after UV [24]. The fraction of cells that showed restoration of the typical GFP-CSB focal pattern 16 hours after UV is comparable to the fraction that survived the UV treatment (Fig. 2F).

**Figure 2. Distribution of GFP-CSB in time and space after transcriptional interference and DNA damage induction.** A-C. GFP-CSB expressing cells were incubated with the RNAP II-specific transcription inhibitor DRB. Confocal and transmission images of representative cells of the untreated and DRB-treated population are shown in A and B respectively. Cells were subsequently washed and cultured with DRB-free medium (C). D. Confocal and transmission images of representative CS1AN-Sv + GFP-CSB cells after irradiation with UV-light (2 hrs, 16 J/m<sup>2</sup>). E. The percentage of cells presenting GFP-CSB foci were quantified in untreated cells and cells treated with various transcription and replication blocking agents. GFP-CSB cells were incubated with inhibitors of RNA synthesis, DRB, H8,  $\alpha$ -amanitin ( $\alpha$ -aman) and Actinomycin D (Act-D), or with the DNA synthesis inhibitor aphidicolin (Aph), and the proportion of foci-presenting cells was determined. A minimum of 250 cells was analysed for each treatment. F. Cells were irradiated with UV-C (4 J/m<sup>2</sup> or 16J/m<sup>2</sup>) and the proportion of cells presenting GFP-CSB fluorescent foci was determined at the indicated time intervals after treatment. GFP-CSB relocation was i) dependent on the UV dose (compare 16 J/m<sup>2</sup> (open squares) with 4 J/m<sup>2</sup> (filled dots), and ii) was reversible after completion of transcription-coupled repair at 16 hours post-UV. G. Cells were incubated with NA-AAF or MMS and analysed for the presence of foci. Whereas NA-AAF induces a fast reduction of cell containing foci, MMS treatment does not induce loss of foci. H. Cells were irradiated with 5 Gy or 10 Gy  $\gamma$ -ray and the percentage of foci-containing cells was calculated. Ionising radiation induces a fast disappearance of foci, which reappear within two hours after treatment. I. Application of fluorescence recovery after photo bleaching (FRAP) to living GFP-CSB expressing cells. A defined part of the nucleus was bleached and subsequently monitored in time. After 30 seconds the GFP-CSB foci have reappeared as indicated by the white arrows. Scale bars are 5  $\mu$ m.

To investigate whether GFP-CSB distribution is sensitive to NER-type of DNA damage, cells were exposed to: NA-AAF that induces bulky adducts, processed by NER, and the alkylating agent MMS, inducing lesions that are repaired by base excision repair. Only NA-AAF caused loss of the focal GFP-CSB distribution (Fig. 2G). These results show that loss of GFP-CSB foci is specifically caused by NER-type of lesions that inhibit transcription [38].

CSB-deficient cells exhibit, in addition to UV, a sensitivity to ionising radiation (IR), likely due to a defect in TCR of IR-induced oxidative damages, such as thymine glycols (Tg) and 8-oxoguanine (8-oxoG) [7,25]. The rapid effect of UV on the CSB localization prompted us to investigate the effect of gamma irradiation on the sub nuclear distribution of CSB. A rapid and dose-dependent disappearance of GFP-CSB foci was observed (Fig. 2H). Interestingly, when exposed to an equi-toxic dose, the kinetics of reappearance of foci is much quicker than after UV-damage (Fig. 2, compare panels F and H). These findings provide *in vivo* support for a role of CSB in TCR of oxidative lesions and suggest that the processes responsible for CSB relocation after  $\gamma$ -irradiation are completed more quickly than after UV. This is consistent with the notion that transcription-blocking UV-lesions (CPDs) persist longer than those induced by  $\gamma$ -irradiation.

#### *Dynamics of GFP-CSB foci in living cells*

The transcription-dependent redistribution of the CSB foci suggests that these nuclear structures are dynamic assemblies. In order to provide more insight into the dynamic aspects of CSB localization we applied fluorescence recovery after photobleaching (FRAP) to the cells [26]. GFP-CSB fluorescence, including foci, was bleached by a relatively high intensity laser pulse in a defined area of the nucleus (Fig. 2I). Subsequently, the distribution of fluorescent and bleached molecules was monitored in time. A surprisingly quick recovery of fluorescence in the foci was observed almost simultaneously with fluorescence recovery in the nucleoplasm (see white arrows). We conclude that GFP-CSB foci are dynamic structures with a rapid exchange of bound and free molecules at the sites of accumulation.

#### *Nuclear mobility of GFP-CSB in living cells*

To further investigate the GFP-CSB nuclear mobility and the dynamic properties of GFP-CSB molecules outside the foci, we applied FRAP (see Materials and Methods). Analysis of the FRAP data revealed that the majority of GFP-CSB molecules were freely mobile in the nucleoplasm (Fig. 3A). The effective diffusion coefficient ( $D_{eff}$ ) of GFP-CSB was determined by fitting the FRAP data to computer simulated curves from a 3-D computer model (see Materials and Methods). With this procedure the  $D_{eff}$  for GFP-CSB was determined to be  $7 \mu\text{m}^2/\text{s}$  (Fig. 3B), which suggests that the apparent protein size significantly exceeds the predicted size of a single GFP-CSB polypeptide chain (MW ~ 195 kDa) and confirm our previous gel filtration studies, that CSB resides in a high MW complex [15].

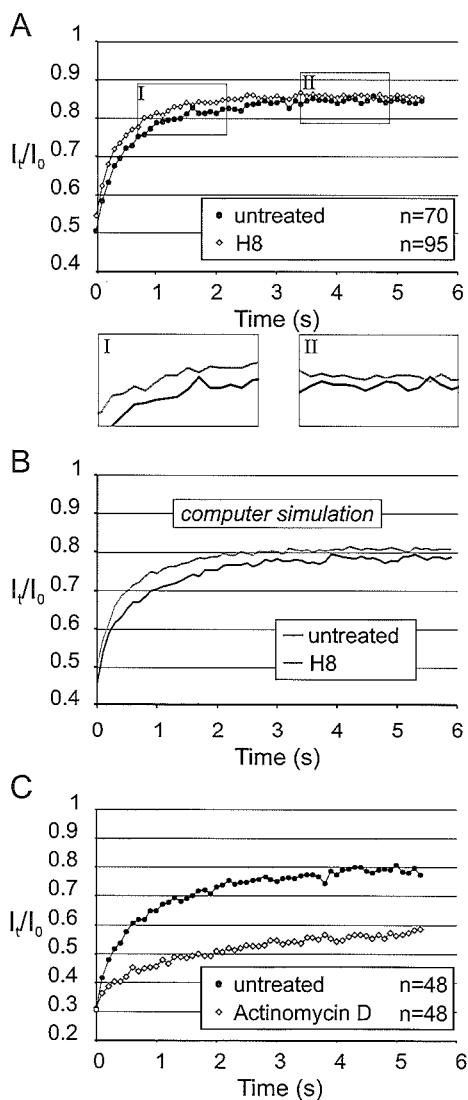
### GFP-CSB dynamics in transcription

The picture emerging from these *in vivo* and previous *in vitro* experiments is that a fraction of CSB resides in a high MW complex that most likely interacts with RNAP II. To study the dynamic behaviour of CSB in transcription *in vivo*, FRAP was applied to GFP-CSB cells treated with transcription inhibitors H8 (Fig. 3A) and DRB (data not shown). Both H8 and DRB treatment resulted in a quicker redistribution. This suggests that either the mobility of the GFP-CSB complex has increased or that in transcriptionally active (untreated) cells a fraction of GFP-CSB molecules is transiently immobilized.

Fitting the FRAP data to computer simulations (Fig. 3B) revealed a biphasic nature of the experimental FRAP curve: an initial fast fluorescence recovery (over the first ~2 s, inset I in Fig. 3A) followed by a slower resumption of fluorescence (inset II in Fig. 3A). The computer simulations fitted best when in the simulation experiment a fraction of 15 to 20% of the CSB molecules were transiently immobilized for two to five seconds.

In striking contrast, inhibiting transcription with Actinomycin D induced a strong reduction (~45%) of the influx of GFP-CSB molecules in the strip, indicative for a large immobile fraction of GFP-CSB (Fig. 3C). Similarly, treatment of GFP-tagged for a large immobile fraction of GFP-CSB (Fig. 3C). Similarly, treatment of GFP-tagged RNA

**Figure 3. FRAP analysis of GFP-CSB nuclear mobility.** A. FRAP analysis of untreated cells (circles;  $n=70$ ) compared to H8-treated cells (open diamonds;  $n=95$ ). H8 treated cells show a faster mobility as compared to untreated cells. Insets I and II show the secondary slower recovery of fluorescence in untreated cells (black line) compared to H8 treated cells (gray line). B. Computer simulations of untreated cells (black line) and H8 treated cells (gray line). The best fitting curve for untreated cells had the following parameters:  $D_{eff} = 7\mu m^2/s$ , bound fraction = 17.5%, binding time = 2 s, and for H8 treated cells:  $D_{eff} = 7\mu m^2/s$ , bound fraction = 0%. C. FRAP analysis of untreated cells (circles;  $n=48$ ) compared to Actinomycin D treated cells (open diamonds;  $n=48$ ). Actinomycin D treatment induces a large immobile fraction of CSB molecules.



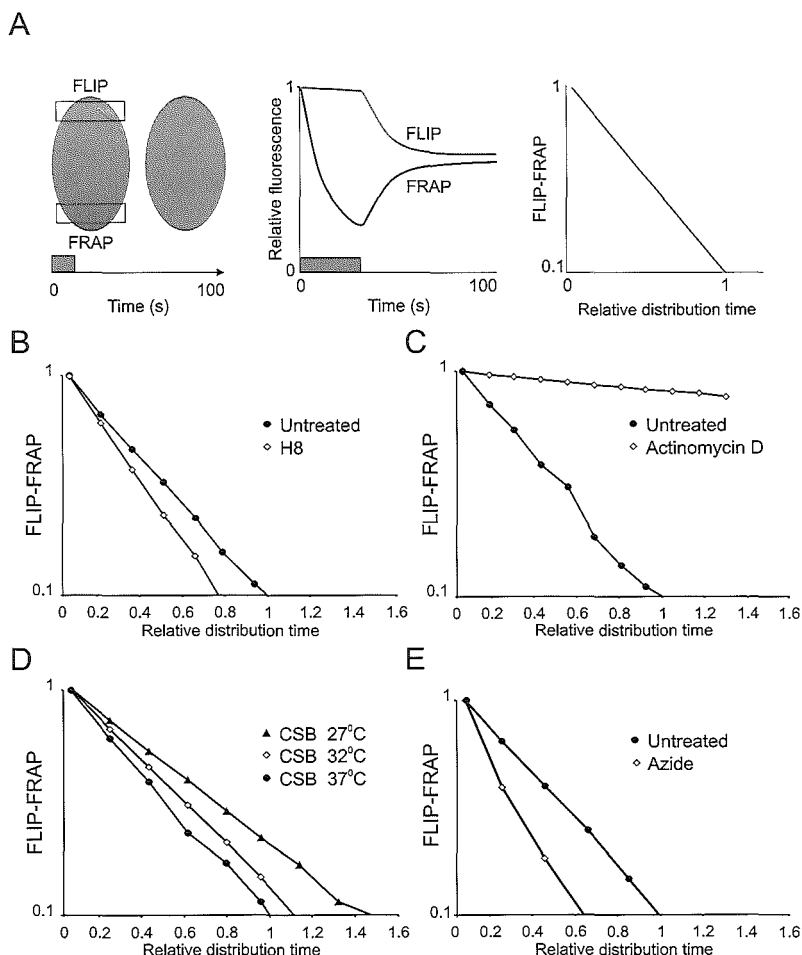


**Figure 4. Dynamic measurements of the GFP-CSB nuclear mobility by combined FLIP/FRAP analysis.** A. Combined FLIP/FRAP analysis was performed by bleaching at one pole of the nucleus and simultaneously monitoring the fluorescent recovery at the bleached (FRAP) and opposite (FLIP) poles of the cell. After bleaching the FRAP curve shows a drop in fluorescent intensity followed by a recovery of fluorescence and the FLIP curve shows a slow decrease of fluorescent intensity due to redistribution of the bleached molecules. The relative intensities of FLIP and FRAP were subtracted and plotted (Y-axis) against the relative redistribution time of untreated cells (X-axis). B. Combined FLIP/FRAP experiment of untreated cells (circles; n=10) and H8-treated cells (open diamonds; n=10). H8 treated cells display a decreased relative redistribution time as compared to untreated cells. C. Combined FLIP/FRAP experiment of untreated cells (circles; n=10) and Actinomycin D-treated cells (open diamonds; n=10). Actinomycin D treatment results in an increased relative redistribution time as compared to untreated cells. D. Combined FLIP/FRAP experiments at different temperatures (27°C (triangles), 32°C (open diamonds) and 37°C (circles). At low temperatures the relative redistribution time is increased. E. Combined FLIP/FRAP experiment of untreated cells (circles; n=10) and azide-treated cells (open diamonds; n=10). Azide treated cells display a decreased relative redistribution time as compared to untreated cells.

polymerase II expressing cells with DRB and Actinomycin D resulted in respectively loss and enhancement of the immobile fraction of RNAP II [27]. This remarkable resemblance in dynamic behaviour suggests a close relationship between elongating RNAP II and CSB in living cells.

#### *Temperature-dependent transient immobilization of GFP-CSB in transcription*

To study the dynamic behaviour of GFP-CSB at a higher resolution we applied another FRAP variant: combined FLIP/FRAP (Fig. 4A) [28]. Briefly, a region at one pole of the nucleus is bleached and the influx of fluorescence in the bleached area is monitored (FRAP) as well as the fluorescence loss in photobleaching (FLIP) at the opposite pole of the nucleus. This provides a measure of the time a GFP-CSB molecule takes to travel from one pole of the nucleus to the other. The difference in relative fluorescent intensity between the FLIP and FRAP region in time is plotted on a logarithmic scale. The time to reach 90% redistribution of GFP-CSB fluorescence was  $59 \pm 8$  seconds. For comparison this value was set to 1 in the subsequent experiments. Treatment of the cells with the transcription inhibitor H8 clearly induced a reduction in redistribution time (20 %) as compared to transcriptionally active cells (Fig. 4B), suggesting a faster overall mobility of GFP-CSB molecules when transcription is inhibited. Again, in sharp contrast with the response to H8, treatment with the DNA intercalating agent Actinomycin D resulted in a severe loss of the ability for GFP-CSB molecules to redistribute, indicative of a long-term immobilization of CSB proteins (Fig. 4C).

Next, we applied the combined FLIP-FRAP procedure to cells cultured at different temperatures. The rationale behind this is that a relatively small difference in (absolute) temperature (Kelvin) has a negligible effect on diffusion rate, but strongly affects the duration of energy-dependent enzymatic processes such as transcription and active transport [28,29]. Combined FLIP-FRAP of GFP-CSB expressing cells cultured at respectively 37, 32 and 27 °C revealed a significant decrease of mobility when the temperature was reduced (Fig. 4D). These observations favour the idea that GFP-CSB molecules are slowed down in transcriptionally active cells due to transient temperature-dependent interactions. To further investigate the observed energy-dependency of CSB mobility, we treated cells with azide to deplete ATP. Combined FRAP -FLIP measurements clearly show an increase of mobility in these cells (Fig. 4E), most likely caused by a loss of transient interactions.

#### *Nuclear mobility of GFP-CSB in UV-irradiated cells*

The localization studies of GFP-CSB revealed that the distribution of CSB molecules respond both to the transcriptional activity and to the presence of DNA damage. To investigate the kinetics of the involvement of GFP-CSB in TCR we determined the overall nuclear mobility in UV-irradiated cells by FRAP analysis. Fluorescence recovery plots of UV-damaged cells ( $16 \text{ J/m}^2$ , a repair-saturating UV dose) (red diamonds, Fig. 5A) revealed a small but consistent reduction of fluorescence recovery when compared to non-UV-damaged cells (blue circles), indicating that a fraction of GFP-CSB molecules is immobilized for a longer period. In addition, the

diffusion rate of the mobile GFP-CSB fraction in untreated and UV-irradiated cells is unaltered (data not shown).

The amount of UV-induced immobilized molecules was proportional to the UV-dose: from ~ 5% at 4 J/m<sup>2</sup> to a plateau of ~ 15 % at 16 J/m<sup>2</sup> (Fig. 5B). A similar UV-dose dependent immobilization was observed with core NER factors, such as ERCC1-GFP/XPF [26], GFP-XPA [30], and TFIIH-GFP [28], although the maximum fraction of GFP-CSB immobilization (~15%) is significantly lower than found with the other NER factors (35–40%). No UV-induced immobilization was found with non-NER factors tagged with GFP [26] supporting the notion that the immobilization is related to NER. An explanation for the observed UV-dependent immobilization is that freely mobile GFP-CSB binds more stably to stalled RNAP II than to elongating RNAP II. When prolonged immobilization is dependent on stalled polymerases, and implicitly on TCR, we predict

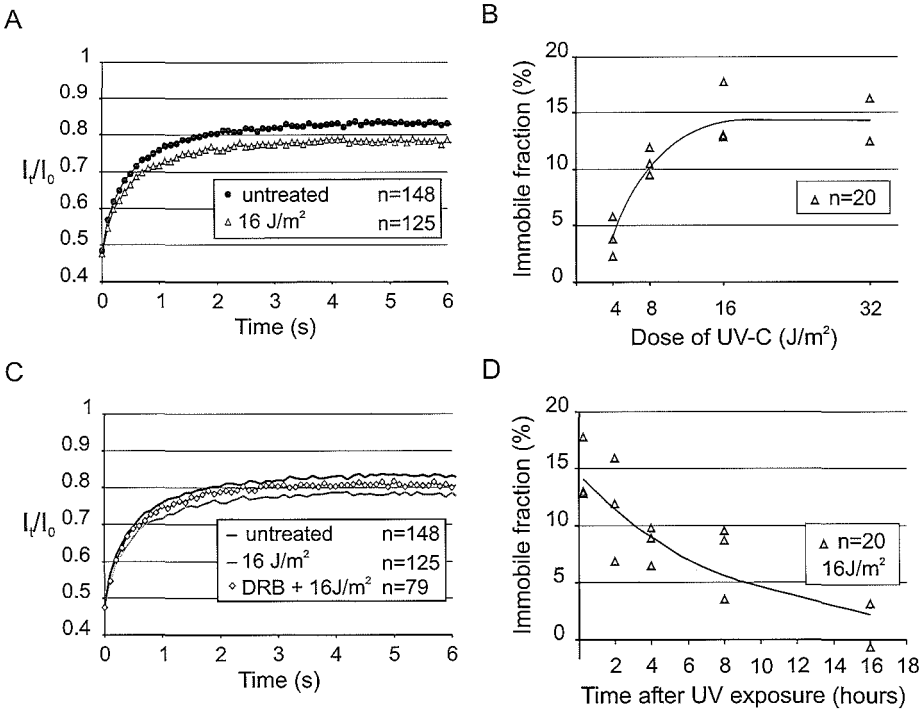


**Figure 5. FRAP analysis of GFP-CSB after UV-irradiation.** A. FRAP analysis of untreated cells (circles; n=148) and UV-irradiated cells (16J/m<sup>2</sup>; open triangles; n=125). UV-treated cells show an immobilization of GFP-CSB. B. Dose-dependency of GFP-CSB immobilization based on three independent experiments. C. FRAP analysis of untreated cells (black line; n=148), cells treated with DRB prior to UV-irradiation (16J/m<sup>2</sup>; open diamonds; n=79) and cells treated with UV solely (16J/m<sup>2</sup>; gray line; n=125). D. Dynamics of the immobile fraction of GFP-CSB in time after UV (16J/m<sup>2</sup>) based on three independent experiments.



that the UV-induced immobilization requires active transcription. Therefore we treated the cells with the transcription inhibitor DRB prior to UV-irradiation. As shown in the mobility plot of figure 5C a significant decrease of the immobile fraction upon transcriptional inhibition was apparent when compared to transcriptional active UV-irradiated cells (DRB did not completely prevent UV-induced immobilization, likely due to incomplete transcription inhibition). This indicates that the observed immobilization of GFP-CSB is most likely due to its engagement in TCR.  $\gamma$ -Irradiated cells did not reveal a clear immobilization using FRAP analysis (data not shown), probably due to the fact that CSB dependent TCR pathway repairs only a small fraction of the oxidative lesions.

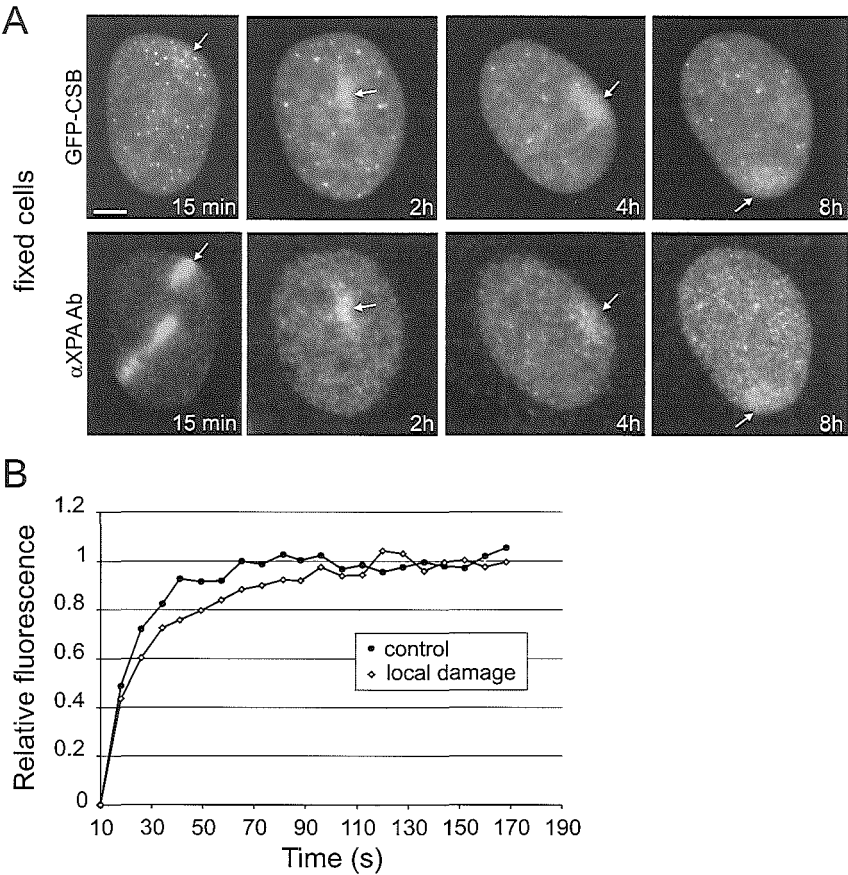


**Figure 6. GFP-CSB accumulates at locally UV-irradiated areas in the cell.** A. Epifluorescent images of fixed GFP-CSB expressing cells at various time points (15 min, 2h, 4h, 8h) after local irradiation. Immunofluorescent analysis with anti-XPA antibody shows accumulation of XPA at sites of damage. GFP-CSB shows accumulation in the same areas. Upper panel: GFP signal, lower panel: Cy3 signal. B. Fluorescence recovery plot of a local damage (open diamonds) and an undamaged control region (circles). The calculated average residence time is  $135 \pm 20$  seconds. Scale bar is 5  $\mu$ m.

When the immobilization of CSB reflects actual participation in TCR we expect that the immobilized fraction will decrease in time depending on progression of repair. Therefore, we measured the UV-dependent immobilization of GFP-CSB molecules at various time points after irradiation ( $16\text{J/m}^2$ ) (Fig. 5D). These experiments revealed that the bound fraction gradually decreased to background levels within 16 hours after UV. This indicates that the UV-dependent immobilization of GFP-CSB is a reversible process with kinetics consistent with the reappearance of GFP-CSB foci approximately 16 hours after UV. Interestingly, the kinetics of this process is much slower than anticipated on the basis of the efficient damage repair by TCR measured in selected genes [6].

#### *GFP-CSB accumulates at sites of local damage*

The DNA damage-dependent immobilization of GFP-CSB argues for a model in which CSB complexes that transiently interact with the transcription machinery remain longer bound to lesion-blocked polymerases than to elongating complexes. To obtain further evidence for this hypothesis we locally inflicted UV-lesions in nuclei of GFP-CSB [31,32]. Shortly after UV-irradiation, we detected local accumulations of GFP-CSB that co-localize with XPA (Fig. 6A), which is a NER factor involved in both GGR and TCR. This indicates that GFP-CSB accumulations represent sites of locally induced TCR. Clearly, GFP-CSB accumulation is less prominent than the accumulation of XPA (Fig. 6A) and other GG-NER factors (data not shown). After irradiation the majority of XPA is located at the damaged spot, contrary to only a small portion of GFP-CSB. In contrast to the expectation for a relatively fast process as TCR (at least faster than GGR of CPDs) [6,33], even eight hours after UV-irradiation local GFP-CSB accumulations were as bright as shortly after UV (Fig. 6A). An explanation for this observation is that CPD lesions are poorly recognized by GGR. These results are in line with our findings that upon overall UV irradiation, immobilization of GFP-CSB is measured until 16 hours after UV and matches with observed reappearance of nuclear foci after UV.

In order to investigate the dynamic engagement of GFP-CSB molecules at locally damaged areas, we measured the residence time of GFP-CSB molecules by measuring FRAP on damaged and non-damaged areas in the nucleus. Clearly, fluorescent recovery in the damaged area is slower than recovery in a control region (Fig. 6B). We calculated an average residence time of GFP-CSB molecules in the local damage of  $135 \pm 20$  seconds, which is short relative to other core NER factors like XPA, TFIIH and ERCC1, which are bound in a locally damaged area for three to five minutes. [26,28,30].

## **Discussion**

Here we present a study on the dynamic behaviour and the differential functioning of the transcription-coupled repair protein CSB in living cells, using a cell-line that stably expresses functional GFP-tagged CSB protein expressed at physiological levels. Confocal microscopy and quantitative digital image analysis of different photobleaching (FRAP) procedures revealed a highly dynamic subnuclear localization

and (transient) interactions of CSB with the transcription machinery and the process of transcription-coupled repair.

#### *Dynamic subnuclear distribution pattern of GFP-CSB*

A striking focal pattern of concentrated GFP-CSB fluorescence and nucleolar accumulation on top of a homogeneous distribution was observed in the majority of cells. Both transcription inhibition and specific types of DNA damage induced a swift but reversible GFP-CSB redistribution. The focal pattern rapidly transformed into a homogeneous distribution, which gradually reverted to the focal pattern again within 8-16 hrs after UV irradiation. The kinetics of the reappearance of these foci strikingly resembles the recovery of RNA synthesis after DNA repair when taken into account the fraction of cells surviving the UV dose [24]. Together, these observations further argue that the presence of nuclear CSB foci is related to transcriptional activity. The dynamic nature of these structures is further highlighted by the high exchange rate of GFP-CSB molecules in the foci with molecules from the nucleoplasm as revealed by the FRAP studies. Interestingly, the recovery of GFP-CSB foci after  $\gamma$ -irradiation shows a different kinetic pattern compared to UV-irradiation, possibly reflecting the differential kinetics of subsequent repair steps in both NER and BER.

Despite the clear relationship with transcriptional status, the nature of these foci remains elusive. Remarkably, they do not represent sites of active transcription, since nascent RNA labelling by Br-UTP incorporation (data not shown) revealed that transcription foci do not co-localize with GFP-CSB foci.

#### *CSB is part of a high molecular weight complex*

Despite the highly dynamic nature of the CSB subnuclear structures, FRAP analysis indicated that the overall CSB mobility is remarkably slow compared to its calculated molecular size and the observed effective diffusion rate ( $D_{\text{eff}}$ ) of other NER-factors tested in a similar fashion. XPA, ERCC1/XPF and TFIIH have a  $D_{\text{eff}}$  that is in concordance with their molecular sizes, arguing against a stable pre-assembled NER 'holo' complex [26,28,30]. The relatively slow mobility of GFP-CSB confirms *in vivo* our previous (biochemical) observation that CSB resides in a complex with an estimated hydrodynamic velocity of particles larger than 700 kDa [15].

Furthermore, it was shown that a fraction of CSB molecules interacts with a minor portion of RNAP II. Interactions between CSB and RNAP II elongation complexes were also found by others [16] and recombinant CSB was claimed to stimulate RNAP II elongation *in vitro* [17]. In addition, RNAP II dependent transcription was reported to be slightly impaired in Cockayne syndrome B cells [23,34]. Furthermore, a specific role in transcription elongation for the Rad26 protein (the yeast homologue of CSB) was deduced from genetic interactions between Rad26 and Spt4 [18], which is implicated in regulation of RNAP II processivity [19,20]. Together these studies support a role for CSB in transcription elongation.

### *Dynamic interactions of CSB with the transcription machinery*

A significant fraction (~25%) of RNAP II in mammalian cells is bound to DNA and that a single polymerase typically is bound for ~ 20 minutes during transcription elongation [27]. The presumed role of CSB in transcription elongation predicts that CSB-containing complexes would show similar dynamics. However, dynamic studies using FRAP analysis and subsequent computer simulation suggest that only a small fraction of CSB-containing complexes (~17%) are immobilized (Fig 3B) for approximately ~2 to 5 seconds in a transcription-dependent fashion. The increased binding time at 27 °C as compared to cells at 37 °C, suggests that this immobilization involves a temperature-dependent step (such as transcription). Interestingly, upon treatment with Actinomycin D an unexpectedly large fraction of CSB appeared to be immobilized. A similar strong immobilization, induced by Actinomycin D treatment, was reported for GFP-tagged RNAP II. The authors explain this observation by a permanent translocation block of the elongating complex caused by the DNA intercalating agent [27]. Apparently, these 'frozen' complexes are a better substrate for CSB than elongating ones, as they trap CSB molecules. In conclusion, our findings suggest a model in which there is a dynamic equilibrium between CSB complexes that are free and that are shortly bound to elongating RNAP II. This transient immobilization involves an energy-dependent step and is dependent on transcription.

Dynamic interactions of transcription factors with active transcription sites have been noticed before using similar procedures. Hager and colleagues [35], described a rapid exchange between chromatin bound and free-diffusing GFP-tagged glucocorticoid receptor. Moreover, our dynamic studies on GFP-tagged TFIIF [28], revealed a corresponding short transcription-dependent interaction. However, both factors stimulate transcription initiation rather than elongation. Obviously, elongating complexes, by virtue of their scanning nature, are longer associated to DNA than we observe here for CSB. The transient interactions of elongation stimulating factors, such as CSB, may provide a flexible response towards different chromosomal conformations or changing conditions during elongation allowing different factors to bind on demand. This is the first *in vivo* example of a transcription elongation-stimulating factor that is not a stably associated component of the RNAP II elongation-holo-complex. The findings with CSB provide a glimpse into the *in vivo* organization of the process of transcription elongation.

Next to a function in RNAP II-driven transcription a more general role for CSB in RNA polymerase I and III mediated transcription was suggested [22,36]. The nucleolar localization of GFP-CSB *in vivo* presented here supports a role of CSB in processivity of other RNA polymerases. This distribution of CSB and its dynamic relocation after transcription inhibition resemble that of RNAP I into the so-called 'nucleolar necklaces' after DRB treatment [37]. Furthermore, the absence of the CSB protein in human fibroblasts derived from CS group B patients caused fragility of metaphase chromosomes at specific loci, these include the U1 and U2 snRNA genes (RNAP II) and the 5S RNA genes (transcribed by RNAP III). It was suggested that this fragility is provoked by the absence of a (general) stimulating function of CSB in elongation during transcription of these highly structured RNAs.

### *Distinct kinetic pools of CSB*

Here we have shown that the equilibrium between different kinetic pools of freely diffusing CSB complexes and a “transcription bound” fraction can shift under different transcriptional conditions. The temperature-dependent enzymatic step involved in the transient interactions might be the ATPase function of CSB during association in transcription. Since CSB is essential for TCR, we investigated the consequences of DNA damage on the distribution of CSB over the distinct kinetic pools. Shortly after UV exposure we observed a change in the duration of the transcription-related immobilization of CSB. The maximal immobilization of ~15% in TCR is significantly smaller than the GGR-induced maximal immobilization of ~40% for other (core) NER factors [26,28,30]. This implies that the molecular equilibrium, which is formed between DNA damage bound and freely diffusing molecules, is different for GGR and TCR. Probably, the bound fraction of GGR proteins is directly dependent on the DNA damage load, whereas the number of stalled RNAP II elongation complexes in a cell determines the immobile fraction of TCR proteins.

The fraction of immobilized molecules after UV-irradiation slowly decreased to background levels (approximately 16 hrs.). In contrast, the immobilization of core NER factors appeared to decrease to background levels in 4 to 6 hrs. after UV [26,28,30]. Assuming that the CSB immobilization reflects TCR, these slow kinetics contrast to the general idea that TCR is faster and more efficient than GGR. In addition, similar to FRAP analysis, the local accumulation of CSB is observed at least until 8 hours after UV-irradiation. Since TCR is particularly targeted to CPDs, our findings suggest that the overall removal of CPDs in active genes by TCR is slower than 6-4PPs repair by GGR, as previously observed by van Hoffen and coworkers [39].

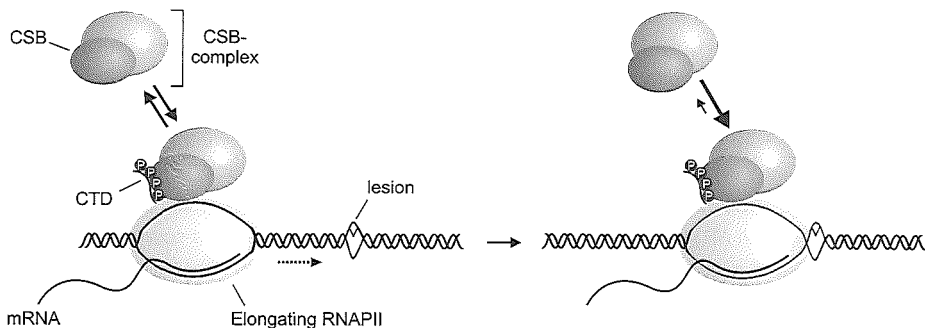


**Figure 7. Model for the function of CSB in transcription and transcription coupled repair.** In transcriptionally active cells a fraction (15-20%) of CSB transiently interacts (approximately two to five seconds) with elongating RNAP II. CSB resides in a high molecular weight complex of unknown identity. Upon transcription blockage on a DNA lesion CSB is immobilized much longer ( $135 \pm 20$  seconds).

A possible explanation for this apparent contradiction is that the relatively fast removal of CPDs by TCR [6,33] is measured on frequently transcribed genes. Since TCR is likely initiated by the blockage of transcription elongation on lesions, the efficiency of TCR-dependent lesion removal (such as CPDs) is likely determined both by the rate of transcription and the size of the transcriptional unit. In summary, we propose a model (Fig.7) in which CSB complex interacts very transiently with the transcription machinery during elongation. This suggests that CSB is constantly monitoring the elongation status of the transcribing polymerases. When a complex is stalled on a DNA lesion the transient interactions of the CSB protein are stabilized, to allow CSB to exert its function in damage removal.

## Materials and methods

### *Generation and characterization of GFP-CSB fusion protein.*

To generate the GFP-CSB fusion gene, the N-terminal HA-tagged CSB cDNA [15] was cloned downstream of the GFP cDNA in the SacI-Sall sites of the pEGFP-C3 expression vector (Clontech). GFP-CSB was stably expressed in CS-B-deficient human fibroblasts (CS1AN-Sv) using SuperFect transfection reagent (Qiagen). After selection with G418 (300 µg/ml), stable transfectants were isolated and selected for UV-resistance by exposing cells three times to a UV dose of 4 J/m<sup>2</sup> UV-C (254 nm) with daily intervals. Stably expressing clones were characterised for protein expression by immunoblot analysis using an affinity-purified rabbit polyclonal anti-CSB and by UV-survival together with VH10-Sv (wt) and untransfected CS1AN-Sv fibroblasts as described [15];

### *Cell culture and specific treatments*

CS1AN-Sv (CS-B) human fibroblasts and wild-type VH10-Sv human fibroblasts were grown in a 1:1 mixture of Ham's F10 and DMEM (Gibco) supplemented with antibiotics and 10% fetal calf serum at 37° C, 5% CO<sub>2</sub>. Transcription inhibitors were used according to the following conditions: 5,6-dichloro-1β-D-ribofuranosyl benzimidazole (DRB, 100 µM, 2 hours), α-amanitin (50 µg/ml, 8 hours), *N*-(2[methylamino]ethyl)-5-isoquinolinesulfonamide (H8, 100 µM, 2 hours), actinomycin D (10 µg /ml, 2 hours). For DRB recovery, cells were washed twice and incubated in fresh culture medium for 3 hours. Replication was blocked by aphidicolin treatment (40 µg/ml, 18 hours). Treatment with ultraviolet (UV) light was at 254 nm (UV-C) using a germicidal lamp at the indicated doses. DNA damage in localized areas of the nucleus was performed as described [31]. For ionising radiation (IR) treatment, cells were exposed to γ-rays from a <sup>137</sup>Cs source at a dose of 5 and 10 Gy. After N-acetoxy-2-acetylaminofluorene (NA-AAF, 100 µM, 30 min) treatment cells were washed twice with PBS, fresh medium was added and cells were analysed after 30 minutes. For methyl methanesulfonate (MMS), cells were incubated for 50 minutes in medium containing 0.01% or 0.02% MMS, washed twice with PBS, fresh medium was added and cells were cultured for 2 hours before analysis. For azide treatment cells were cultured for 15 minutes in glucose-free medium (Gibco) supplemented with 60mM deoxyglucose and 0.2% Na-azide.

### *Light microscopy and image analysis*

Cells were cultured on sterile glass cover slips. For indirect immunofluorescence (IF), fixation was in 2% paraformaldehyde in PBS for 10 minutes at room temperature. After fixation, cells were permeabilised with 0.1% TritonX-100 in PBS. Endogenous CSB in wild type VH10-Sv cells was detected with affinity-purified, rabbit polyclonal anti-CSB. Secondary antibody staining was performed with anti-rabbit Alexa 594-conjugated antibodies (Molecular Probes). For fixed cells, fluorescent microscopy images were obtained with a Leitz Aristoplan microscope equipped with epifluorescence optics and a PLANAPO 63x/1.40 oil immersion lens. Confocal laser scanning microscopy images of live cells were recorded with a Zeiss LSM 410. GFP images were obtained after excitation with 455-490 and long pass emission filter (>510 nm). Alexa-595 images were obtained after excitation with 515-560 and long pass emission filter (580 nm).

### *Fluorescence recovery after photobleaching (FRAP)*

A Zeiss LSM410 was used for the FRAP experiments. Recovery curves for evaluation of protein mobility were obtained as described before [28]. For FRAP analysis, a 2µm wide strip, spanning the entire nucleus, was bleached for 200 ms at highest intensity of the 488 nm line of a 15 mW Ar-laser focused by a 40X 1.3 n.a. oil immersion lens. Subsequently the recovery of fluorescence in the strip was monitored at intervals of 100 ms with the same laser at 5% of the intensity applied for bleaching, using a dichroic beamsplitter (488/543nm) and an additional 515-540 nm band pass filter for emission detection. Similarly, combined FLIP and FRAP analysis was performed by giving a 6 second bleach pulse to a strip at the bottom side of the cell. Next, the fluorescent images were made with low laser intensity every 6 seconds for a total of 3 minutes.

### *Computer Simulation*

For optimal interpretation of the FRAP data we developed a computer modelling environment to simulate FRAP applied to fluorescent molecules inside a finite volume. The FRAP procedures were simulated using experimentally obtained parameters describing lens (beam shape and 3-D intensity distribution, during monitoring and during bleach pulse), GFP (quantum yield, susceptibility to bleaching) and nuclear properties (size and shape). Three protein mobility parameters, diffusion coefficient, bound fraction and duration of binding of individual molecules were varied and the best fit with experimental data was obtained using least square fitting.

### **Acknowledgements**

We thank Drs. L.H.F. Mullenders, A.A. van Zeeland, R. van Driel and G. Mari-Giglia for helpful suggestions and discussion. This work was supported by the Centre for Biomedical Genetics (CBG), the Dutch Scientific Organization (NWO-ALW, NWO-ZonMW and Spinoza award), the EC contract (Dnage), and the Dutch Cancer Society (KWF).

## References

1. Yamaizumi, M. and Sugano, T. (1994) U.v.-induced nuclear accumulation of p53 is evoked through DNA damage of actively transcribed genes independent of the cell cycle. *Oncogene*, 9, 2775-84.
2. Ljungman, M. and Zhang, F. (1996) Blockage of RNA polymerase as a possible trigger for u.v. light-induced apoptosis. *Oncogene*, 13, 823-831.
3. de Boer, J., Andressoo, J.O., de Wit, J., Huijmans, J., Beems, R.B., van Steeg, H., Weeda, G., van der Horst, G.T., van Leeuwen, W., Themmen, A.P., Meradji, M. and Hoeijmakers, J.H. (2002) Premature aging in mice deficient in DNA repair and transcription. *Science*, 296, 1276-9.
4. Friedberg, E.C., Walker, G.C. and Siede, W. (1995) *DNA repair and mutagenesis*. ASM Press, Washington D.C.
5. Hoeijmakers, J.H. (2001) Genome maintenance mechanisms for preventing cancer. *Nature*, 411, 366-74.
6. Mellon, I., Spivak, G. and Hanawalt, P.C. (1987) Selective removal of transcription-blocking DNA damage from the transcribed strand of the mammalian *DHFR* gene. *Cell*, 51, 241-249.
7. Le Page, F., Kwoh, E.E., Avrutsкая, A., Gentil, A., Leadon, S.A., Sarasin, A. and Cooper, P.K. (2000) Transcription-coupled repair of 8-oxoguanine: requirement for XPG, TFIIH, and CSB and implications for Cockayne syndrome. *Cell*, 101, 159-171.
8. Nance, M.A. and Berry, S.A. (1992) Cockayne syndrome: Review of 140 cases. *Am. J. of Med. Genet.*, 42, 68-84.
9. Henning, K.A., Li, L., Iyer, N., McDaniel, L., Reagan, M.S., Legerski, R., Schultz, R.A., Stefanini, M., Lehmann, A.R., Mayne, L.V. and Friedberg, E.C. (1995) The Cockayne syndrome group A gene encodes a WD repeat protein that interacts with CSB protein and a subunit of RNA polymerase II TFIIH. *Cell*, 82, 555-564.
10. Troelstra, C., Van Gool, A., De Wit, J., Vermeulen, W., Bootsma, D. and Hoeijmakers, J.H.J. (1992) ERCC6, a member of a subfamily of putative helicases, is involved in Cockayne's syndrome and preferential repair of active genes. *Cell*, 71, 939-953.
11. Neer, E.J., Schmidt, C.J., Nambudripad, R. and Smith, T.F. (1994) The ancient regulatory-protein family of WD-repeat proteins. *Nature*, 371, 297-300.
12. Pazin, M.J. and Kadonaga, J.T. (1997) SWI2/SNF2 and related proteins: ATP-driven motors that disrupt protein-DNA interactions? *Cell*, 88, 737-740.
13. Citterio, E., Rademakers, S., van der Horst, G.T., van Gool, A.J., Hoeijmakers, J.H. and Vermeulen, W. (1998) Biochemical and biological characterization of wild-type and ATPase- deficient Cockayne syndrome B repair protein. *J. Biol. Chem.*, 273, 11844-11851.
14. Citterio, E., Van Den Boom, V., Schnitzler, G., Kanaar, R., Bonte, E., Kingston, R.E., Hoeijmakers, J.H. and Vermeulen, W. (2000) ATP-dependent chromatin remodeling by the Cockayne syndrome B DNA repair-transcription-coupling factor. *Mol Cell Biol*, 20, 7643-53.
15. van Gool, A.J., Citterio, E., Rademakers, S., van Os, R., Vermeulen, W., Constantinou, A., Egly, J.M., Bootsma, D. and Hoeijmakers, J.H.J. (1997) The Cockayne syndrome B protein, involved in transcription-coupled DNA repair, resides in a RNA polymerase II containing complex. *EMBO J.*, 16, 5955-5965.
16. Tantin, D., Kansal, A. and Carey, M. (1997) Recruitment of the putative transcription-repair coupling factor CSB/ERCC6 to RNA polymerase II elongation complexes. *Mol. Cell. Biol.*, 17, 6803-6814.
17. Selby, C.P. and Sancar, A. (1997) Cockayne syndrome group B protein enhances elongation by RNA polymerase II. *Proc. Natl. Acad. Sci. USA*, 94, 11205-11209.
18. Jansen, L.E.T., den Dulk, H., Brouns, R.M., de Ruijter, M., Brandsma, J.A. and Brouwer, J. (2000) Spt4 modulates Rad26 requirement in transcription-coupled nucleotide excision repair. *EMBO J.*, 19, 6498-6507.
19. Hartzog, G.A., Wada, T., Handa, H. and Winston, F. (1998) Evidence that Spt4, Spt5, and Spt6 control transcription elongation by RNA polymerase II in *Saccharomyces cerevisiae*. *Genes Dev*, 12, 357-69.



20. Wada, T., Takagi, T., Yamaguchi, Y., Ferdous, A., Imai, T., Hirose, S., Sugimoto, S., Yano, K., Hartzog, G.A., Winston, F., Buratowski, S. and Handa, H. (1998) DSIF, a novel transcription elongation factor that regulates RNA polymerase II processivity, is composed of human Spt4 and Spt5 homologs. *Genes Dev.*, 12, 343-356.
21. Donahue, B.A., Yin, S., Taylor, J.-S., Reines, D. and Hanawalt, P.C. (1994) Transcript cleavage by RNA polymerase II arrested by a cyclobutane pyrimidine dimer in the DNA template. *Proc. Natl. Acad. Sci. USA*, 91, 8502-8506.
22. Yu, A., Fan, H.-Y., Liao, D., Bailey, A.D. and Weiner, A.M. (2000) Activation of p53 or Loss of the Cockayne Syndrome Group B Repair Protein Causes Metaphase Fragility of Human U1, U2, and 5S Genes. *Molecular Cell*, 5, 801-810.
23. Balajee, A.S., May, A., Dianov, G.L., Friedberg, E.C. and Bohr, V.A. (1997) Reduced RNA polymerase II transcription in intact and permeabilized Cockayne syndrome group B cells. *Proc. Natl. Acad. Sci. USA*, 94, 4306-4311.
24. Van Hoffen, A., Natarajan, A.T., Mayne, L.V., Van Zeeland, A.A., Mullenders, L.H.F. and Venema, J. (1993) Deficient repair of the transcribed strand of active genes in Cockayne's syndrome cells. *Nucl. Acids Res.*, 21, 5890-5895.
25. Cooper, P.K., Nousepikel, T., Clarkson, S.G. and Leadon, S.A. (1997) Defective transcription-coupled repair of oxidative base damage in Cockayne syndrome patients from XP group G. *Science*, 275, 990-993.
26. Houtsmuller, A.B., Rademakers, S., Nigg, A.L., Hoogstraten, D., Hoeijmakers, J.H.J. and Vermeulen, W. (1999) Action of DNA repair endonuclease ERCC1/XPF in living cells. *Science*, 284, 958-961.
27. Kimura, H., Sugaya, K. and Cook, P.R. (2002) The transcription cycle of RNA polymerase II in living cells. *J Cell Biol*, 159, 777-82.
28. Hoogstraten, D., Nigg, A.L., Heath, H., Mullenders, L.H., van Driel, R., Hoeijmakers, J.H., Vermeulen, W. and Houtsmuller, A.B. (2002) Rapid switching of TFIIH between RNA polymerase I and II transcription and DNA repair in vivo. *Mol Cell*, 10, 1163-74.
29. Phair, R.D. and Misteli, T. (2000) High mobility of proteins in the mammalian cell nucleus. *Nature*, 404, 604-609.
30. Rademakers, S., Volker, M., Hoogstraten, D., Nigg, A.L., Mone, M.J., Van Zeeland, A.A., Hoeijmakers, J.H., Houtsmuller, A.B. and Vermeulen, W. (2003) Xeroderma Pigmentosum Group A Protein Loads as a Separate Factor onto DNA Lesions. *Mol Cell Biol*, 23, 5755-5767.
31. Volker, M., Mone, M.J., Karmakar, P., van Hoffen, A., Schul, W., Vermeulen, W., Hoeijmakers, J.H., van Driel, R., van Zeeland, A.A. and Mullenders, L.H. (2001) Sequential assembly of the nucleotide excision repair factors in vivo. *Mol Cell*, 8, 213-24.
32. Mone, M.J., Volker, M., Nikaido, O., Mullenders, L.H., van Zeeland, A.A., Verschure, P.J., Manders, E.M. and van Driel, R. (2001) Local UV-induced DNA damage in cell nuclei results in local transcription inhibition. *EMBO Rep*, 2, 1013-7.
33. Bohr, V.A., Smith, C.A., Okumoto, D.S. and Hanawalt, P.C. (1985) DNA repair in an active gene: removal of pyrimidine dimers from the *DHFR* gene of CHO cells is much more efficient than in the genome overall. *Cell*, 40, 359-369.
34. Dianov, G.L., Houle, J.F., Iyer, N., Bohr, V.A. and Friedberg, E.C. (1997) Reduced RNA polymerase II transcription in extracts of cockayne syndrome and xeroderma pigmentosum/Cockayne syndrome cells. *Nucleic Acids Res*, 25, 3636-42.
35. McNally, J.G., Müller, W.G., Walker, D., Welford, R. and Hager, G.L. (2000) The glucocorticoid receptor: rapid exchange with regulatory sites in living cells. *Science*, 287, 1262-1265.
36. Bradsher, J., Auriol, J., Proietti de Santis, L., Iben, S., Vonesch, J.L., Grummt, I. and Egly, J.M. (2002) CSB is a component of RNA pol I transcription. *Mol Cell*, 10, 819-29.
37. Haaf, T. and Ward, D.C. (1996) Inhibition of RNA polymerase II transcription causes chromatin decondensation, loss of nucleolar structure, and dispersion of chromosomal domains. *Exp Cell Res*, 224, 163-73.
38. Van Oosterwijk, M.F., Filon, R., de Groot, A.J.L., van Zeeland, A.A. and Mullenders, L.H.F. (1998) Lack of transcription-coupled repair of acetylaminofluorene DNA adducts in human fibroblasts contrasts their efficient inhibition of transcription. *J. Biol. Chem.*, 273, 13599-13604.

39. **Van Hoffen, A., Venema, J., Meschini, R., van Zeeland, A.A. and Mullenders, L.H.F.** (1995) Transcription-coupled repair removes both cyclobutane pyrimidine dimers and 6-4 photoproducts with equal efficiency and in a sequential way from transcribed DNA in xeroderma pigmentosum group C fibroblasts. *EMBO J.*, 14, 360-367.

# Chapter 8

The Cockayne Syndrome B protein is  
connected to mRNA processing

*Manuscript in preparation*

# The Cockayne Syndrome B protein is connected to mRNA processing

Vincent van den Boom<sup>1</sup>, Elisabetta Citterio<sup>2</sup>, Frederic Coin<sup>3</sup>, Jean-Marc Egly<sup>3</sup>, Jan H.J. Hoeijmakers<sup>1</sup> and Wim Vermeulen<sup>1</sup>

1) *Department of Cell Biology and Genetics, Medical Genetic Center, Erasmus MC Rotterdam, P.O. Box 1738, 3000 DR Rotterdam, The Netherlands.* 2) *Present address: IFOM-FIRC Institute of Molecular Oncology, via Adamello 16, 20139 Milano, Italy.* 3) *Institut de Génétique et de Biologie Moléculaire et Cellulaire, CNRS/INSERM/Université Louis Pasteur, Strasbourg, France.*

## Abstract

The Cockayne Syndrome B (CSB) protein is essential for transcription-coupled repair (TCR) of highly cytotoxic transcription-blocking lesions and plays a role in transcription elongation. Mutations in the *CSB* gene lead to the severe hereditary disorder Cockayne Syndrome. Here we describe the cellular localization of CSB with respect to RNA polymerase II-dependent transcription and mRNA processing factors. CSB appeared to co-localize with proteins involved in mRNA modification and splicing but not with nascent transcripts. Immunoprecipitation experiments show that CSB interacts with these mRNA processing factors but also with *in vitro* active RNA polymerase II. We suggest that CSB dynamically interacts with both transcription elongation complexes and the mRNA processing machinery. The focal accumulations may represent storage- or complex assembly sites for CSB.

## Introduction

The integrity of our DNA is continuously challenged by DNA-damaging agents. DNA damages directly interfere with fundamental cellular processes, such as DNA replication, transcription and cell cycle progression. DNA lesions can induce mutations, which eventually can lead to cancerous growth of cells. Damage-induced blockage of transcription triggers the apoptotic pathway, ultimately leading to segmental aging [1-3]. As a cellular defense mechanism multiple DNA repair pathways collectively remove most DNA lesions from the genome. For removal of the highly cytotoxic transcription-blocking lesions a specific transcription-coupled repair (TCR) mechanism is responsible. Transcription blockage is mainly caused by helix-distorting lesions such as UV-light

induced pyrimidine dimers and the oxidative injuries like thymine glycols and 8-oxo-guanines caused by oxygen radicals, which are repaired by the nucleotide excision repair (NER) and base excision repair (BER) pathway respectively.

In humans, a defect in TCR leads to the severe hereditary and progeroid disorder Cockayne Syndrome (CS). This disease is characterized by photosensitivity, growth failure and severe neuro-developmental problems [4]. Within classical CS patients two genes were implicated, the CSA and CSB genes. CSA is a 44 KDa protein, which contains 5 WD-40 repeats and is a member of the WD-repeat family of proteins [5,6]. The 168kDa CSB protein is a member of the SWI/SNF family of putative helicases [7,8]. CSB was shown to be a dsDNA-dependent ATPase, which can remodel chromatin at the expense of ATP [9,10].

Multiple reports have strengthened the idea that next to its role in TCR, CSB may function as an elongation stimulatory factor *in vivo*. CSB was found to co-immunoprecipitate with RNA polymerase II (RNAPII) and was found to interact with ternary complexes containing RNAPII, DNA and nascent RNA [11,12]. Furthermore, addition of CSB to a *in vitro* transcription reaction containing stalled RNAPII on a CPD lesion induced lengthening of the transcript with one nucleotide [13]. Recently, analysis of a cell line expressing GFP-tagged CSB showed that CSB transiently interacts with elongating RNAPII complexes [14]. Upon damage-induced stalling of RNAPII elongation the binding time of CSB to the polymerase is prolonged.

Additionally, a more general function for CSB in the total transcriptional program was suggested. First, a role RNA polymerase III transcription was suggested by the finding that in CSB mutated cells loci transcribed by RNA polymerase III appeared to give rise to fragile sites in metaphase chromosomes [15]. This is most likely due to a role for CSB in transcription elongation through these highly structured genes. Secondly, the immunofluorescence studies by Bradsher and colleagues show on top of an overall nuclear distribution also nucleolar accumulation of CSB [16]. A potential role for CSB in RNA polymerase I-dependent transcription was further corroborated with biochemical evidence showing that CSB functions in ribosomal RNA transcription. Upon closer inspection using high resolution microscopy on living cells expressing at physiological levels fully functional GFP-tagged CSB, a more detailed view of the nuclear distribution was obtained [14]. Besides a diffuse nuclear distribution and nucleolar accumulations also small foci of high local concentrations of CSB were observed. These nuclear structures, both foci and nucleolar accumulations, appeared to be highly dynamic structures. Photobleaching studies [17,18] revealed that GFP-CSB molecules within the foci and nucleoli quickly exchange with freely mobile molecules from the nucleoplasm. Although the exact nature of these foci was not resolved, these structures appeared to critically depend on the environmental and or experimental conditions. Both DNA-damage induction and transcription inhibition causes the foci to disperse through the nucleoplasm.

In this report we further investigate the composition of these CSB-containing foci and the relation with transcription and mRNA processing. For this purpose we combine localization studies using immunofluorescence experiments and transcription assays using purified CSB complexes *in vitro* [11].

## Results

To analyze the distribution of CSB in time and space we previously used a cell line expressing the green fluorescent protein (GFP) tagged to the amino-terminus of CSB, resulting in a GFP-CSB fusion [14]. This GFP-CSB fusion protein was stably expressed in a CSB-deficient background (CS1AN-Sv) at levels comparable to endogenous expression in HeLa cells. In living cells CSB is homogeneously distributed throughout the nucleus in addition to focal accumulation and appeared also accumulated in nucleoli [14].

### *GFP-CSB distribution relative to mRNA transcription*

Previously, a portion of CSB was found to co-immunoprecipitate with a fraction of RNA polymerase II (RNAP II) [11]. Surprisingly no interaction with the other TCR protein CSA and core NER factors XPC, HHR23B, XPG, TFIIH and transcription factor TFIIIF was found. This suggests that CSB is part of a complex linked to RNAPII transcription. In living cells, the focal accumulations of GFP-CSB were found to depend on the transcriptional activity in the cell [14]. In addition, photobleaching studies show that GFP-CSB transiently interacts with RNAPII in living cells. These observations resulted in the hypothesis that the CSB foci may actually represent sites of active transcription. To verify this hypothesis we labeled nascent RNA with BrUTP and subsequently performed immuno-detection using an anti-BrUTP antibody. Initial studies using this type of RNA visualization showed that in HeLa cells ~300-500 focal accumulation of RNA can be detected [19], which were designated as transcription 'factories'. Surprisingly, the GFP-CSB foci do not co-localize to sites of nascent transcription but rather seem to be excluded from each other, so in CSB foci no active transcription seemed to occur (Fig. 1).

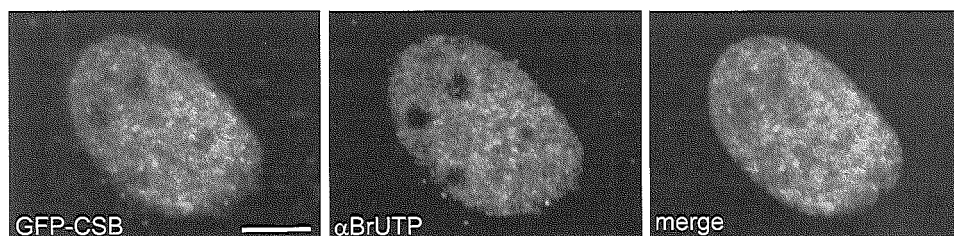


**Figure 1. Labeling of nascent RNA transcripts in GFP-CSB expressing cells.** Nascent RNA was visualized by incorporation of BrUTP. Scale bars are 10  $\mu$ m.

However, an interaction of CSB with nascent RNA outside of the foci can not be excluded. These findings do suggest that the observed interaction of CSB with RNAPII, using immunoprecipitation analysis and photobleaching studies, most likely occurs outside the foci, although these foci depend on the transcriptional status of the cell.

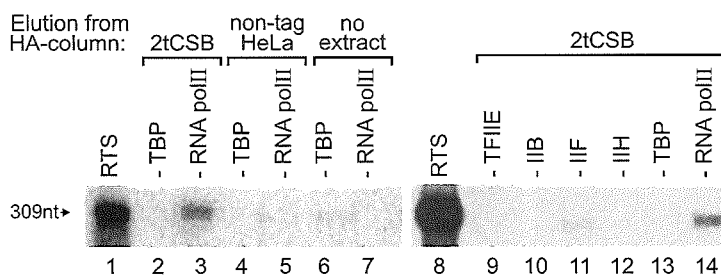


**Figure 2. *In vitro* transcriptional activity of CSB-associated RNA polymerase II.** RNAP II transcriptional activity is present in the 2tCSB HA-eluate. *In vitro* transcription was performed in a reconstituted transcription system (RTS) containing human recombinant TBP, TFIIB, TFIIE, and highly purified HeLa TFIIA, TFIIF and RNAP II and the adenovirus major late promoter (AdMLP) as a template (309 nt). Lanes 1 and 8 show complete reactions. To determine the presence of transcription components in the tagged-CSB fraction, individual transcription factors (indicated on top of each lane) were omitted from reactions containing HA-eluate from 2tCSB WCE (lanes 2 and 3, and 9 to 14). As a control, HA-eluate from HeLa WCE (lanes 4 and 5), or no protein (lanes 6 and 7) were added to reactions lacking TBP or RNAP II.

#### *Transcriptional activity of RNA polymerase II co-immunoprecipitated with CSB*

The observed absence of co-localization of CSB with transcription foci gave rise to the question if CSB indeed interacts with the transcriptionally active form of RNAP II. In order to answer this question we isolated the CSB-RNAP II complex as described before using our previously generated human cell line expressing CSB tagged with a HA epitope (HA-CSB-[His]<sub>6</sub>; referred as dtCSB) [11] and immuno-affinity purified CSB by binding to an anti-HA antibody resin followed by elution with excess of HA-peptide. Immuno-purified CSB was tested in an *in vitro* reconstituted transcription system (RTS) using an adenovirus major late promoter template (AdMLP) [20,21]. The HA-eluate from dtCSB WCE was able to support the synthesis of the 309 nt transcript when RNAP II was omitted from the RTS (Fig. 2, compare lanes 3 and 14 with lanes 1 and 8, respectively), indicating that the CSB-associated RNAP II is transcriptionally active. In contrast, no signal was detected by addition of HA-eluate from normal HeLa WCE expressing wild type CSB without a HA-tag (lane 5) or in the absence of any extract (lane 7), supporting the specificity of the CSB-RNAP II interaction. To determine the presence of additional basal transcription factors in the dtCSB HA-eluate, transcription was performed in the absence of TBP (lanes 2, 4, 6 and 13), TFIIE, TFIIB, TFIIF or TFIIH (lanes 9 to 12, respectively). In neither of these cases complementation for the lack of any of these factors was detected (compare lane 2 with lane 1 and lanes 9 to 12 with lane 8), indicating that none of the transcription initiation factors were present in the 2tCSB (HA-elution) fraction in detectable amounts. Taken together, this experiment clearly shows that although CSB does not localize to transcription foci, at least a fraction of it does interact with *in vitro* active RNAPII, supporting our previous finding that the dynamic behavior of CSB in living cells is dependent on transcriptional activity [14].

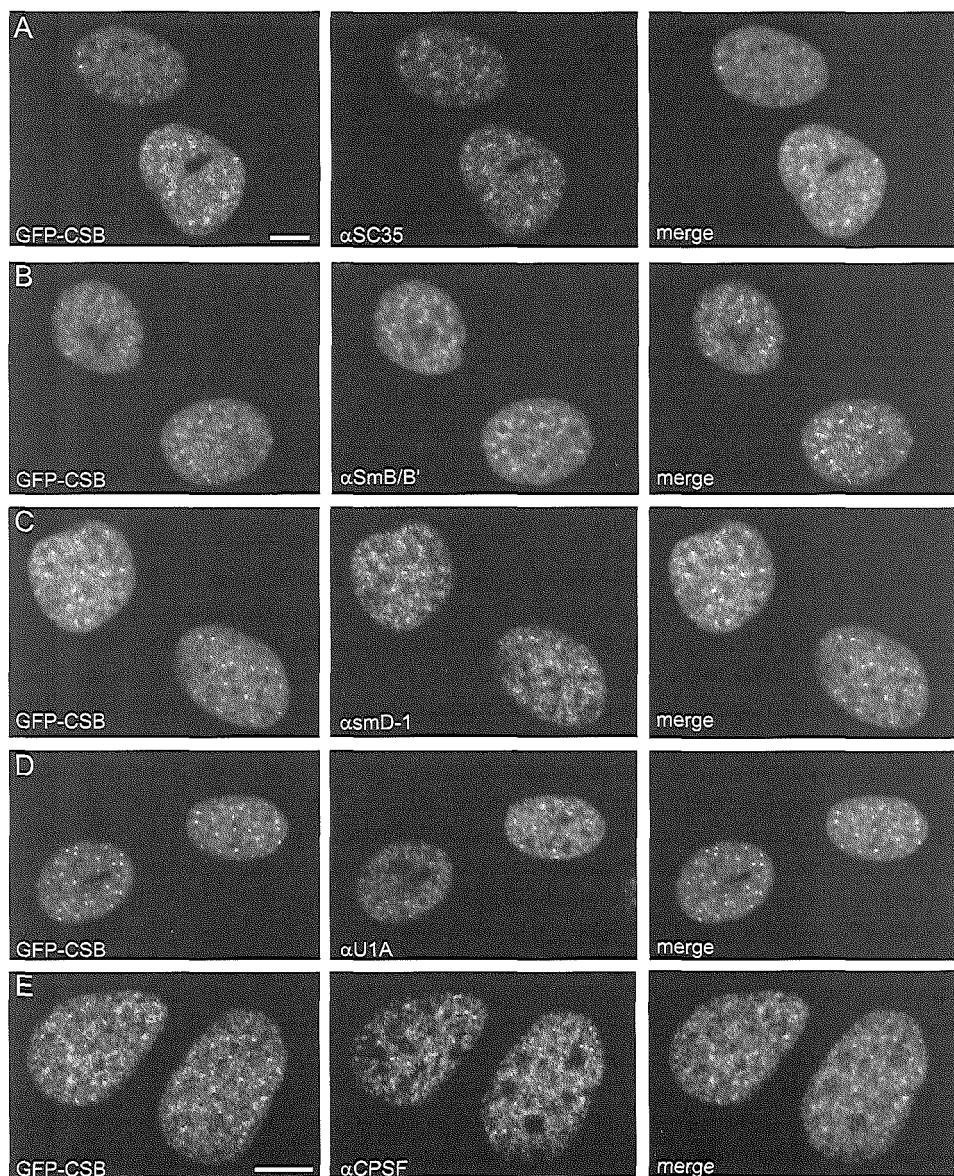


**Figure 3. Immunofluorescence analysis of localization of mRNA processing factors compared to GFP-CSB.** A-E. Immunofluorescent staining using an anti-SC35 antibody (A), a marker of speckles, an antibody directed against SmB/B' (B), an antibody directed against smD-1 (C), an antibody directed against U1A (D) and an antibody directed against the p100 subunit of CPSF (E). Scale bars are 10 μm.



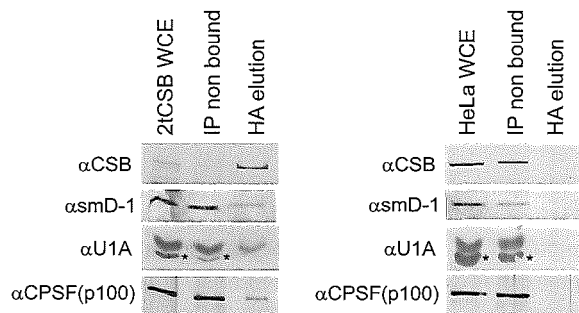
### *CSB distribution relative to the mRNA processing factors*

Since the number of CSB foci resembles the number of speckles, structures in which mRNA splicing factors accumulate, we investigated whether CSB foci also contained splicing factors. For this purpose we used an antibody directed against the non-small nucleolar ribonucleoprotein (snRNP) splicing factor SC-35, which specifically localizes to these subnuclear structures. Clearly, GFP-CSB foci partially co-localize with the speckled structures, indicating that CSB may be linked to the process of mRNA splicing (Fig. 3A). To further study the localization of GFP-CSB with respect to splicing factors we performed immunofluorescent analysis on GFP-CSB cells with antibodies directed against the core snRNP proteins smB/B' (Fig. 3B) and smD-1 (Fig. 3C) and the U1 snRNP specific protein U1A (Fig. 3D). Interestingly, all of these factors show a partial co-localization with the focal accumulation of GFP-CSB. In addition, we performed an immuno staining with an antibody directed against the cleavage and polyadenylation specificity factor CPSF (Fig. 3E). The distribution pattern of this protein also showed overlap with the GFP-CSB localization in the foci. Taken together, the localization of CSB shows overlap with the subcellular organization of the mRNA processing machinery.

### *Interactions of CSB with splicing factors*

Co-localization of proteins does not imply that the proteins also effectively interact. To further study the possible interaction between CSB and the mRNA processing machinery we performed co-immunoprecipitation experiments using the HA-CSB-(His)<sub>6</sub> expressing cell line. Incubation of CS1AN-dtCSB whole cell extract (WCE) with an antibody directed against the HA-tag of CSB resulted in complete depletion of the CSB protein (Fig. 4). Interestingly, the immunoprecipitated fraction contains portions of the splicing factors smD-1 and U1A and the CPSF (p100). To investigate if the immunoprecipitation of proteins was not due to a-specific binding of the antibody, antibody incubation and immunoprecipitation was also performed from HeLa WCE (Fig. 4). The immunoprecipitated fractions in this experiment did not show the presence of

**Figure 4. Immuno-detection of mRNA processing factors co-immunoprecipitating with CSB.** A. Immunoprecipitations of CSB from WCEs from CS1AN + 2tCSB cells directed against the HA-tag of CSB. Immunoprecipitations were done in buffer A. The asterisk indicates a nonspecific band. The WCE, non-bound (n.b.) and bound (b.) proteins were tested on immunoblot using the indicated antisera. B. Binding of smD-1, U1A and CPSF to HA affinity resin is specific for tagged CSB. A similar immunoprecipitation as in (A) was done using HeLa WCE containing non-tagged CSB protein.



CSB or one of the other proteins, indicating that the immunoprecipitation from dtCSB WCE is not due to non-specific binding of the antibody to either one of the precipitated proteins.

## Discussion

In this study we characterize the spatial distribution of CSB in comparison with the nuclear processes of mRNA transcription and processing. Immunofluorescence experiments and immunoprecipitation analysis show that the CSB protein localizes to and to interacts with several mRNA processing factors. In addition, CSB interacts with *in vitro* active RNAPII.

### *Spatial and molecular relation between CSB and RNAPII transcription*

Labeling of nascent RNA in GFP-CSB expressing cells using BrUTP incorporation clearly showed that the focal GFP-CSB accumulations did not localize to regions of active transcription. The number of transcription foci (~300-500) however largely exceeds the number of GFP-CSB accumulations and their size seems much smaller [19]. Although CSB foci do not seem to co-localize to the transcription foci, an interaction between RNAPII elongation complexes and CSB outside the foci may occur but can not be visualized due to resolution problems. Similar to CSB, the nuclear distribution of other factors implicated in transcription (e.g. glucocorticoid receptor, Oct-1 and E2F-1) was found to be distinct from RNAPII and transcription foci [22,23]. Other transcription factors like TFIIH and Brg1 showed a partial overlap with transcription sites. The absence of a vivid overlap of these established transcription factors with active transcription sites is likely due to their short interaction with transcription initiation sites [18,24,25]. Similarly, also CSB appeared to only transiently interact (~ 2-5 seconds) with elongating RNA polymerase II, explaining its apparent absence in transcription foci. In addition, it should also be noted that not all GFP-CSB expressing cell contain foci, most likely due to resolution problems [14].

Analysis of immunoprecipitated CSB revealed that a fraction of the CSB molecules interacts with a minor portion of RNAP II [11]. Here we demonstrate that the RNAP II within this immuno-purified complex is transcriptionally competent, as shown in a reconstituted transcription assay, lacking RNAP II, underscoring the clear involvement of CSB in transcription elongation of RNAPII *in vivo*.

### *Relation between CSB and mRNA processing*

Subsequent to polymerization of a new mRNA or even during elongation, it is modified by the mRNA processing machinery. Capping, splicing and polyadenylation of mRNAs is directly performed after synthesis before the transcripts move to the cytoplasm, where they serve as a template for polymerization of new proteins. Factors essential for splicing of transcripts were found to be present in discrete speckled pattern within the nucleoplasm [26,27]. Immunofluorescence analysis of these speckles in GFP-CSB cells showed a partial co-localization although the size of the structures did not correlate. In

addition, we also find other mRNA processing factors involved in either splicing or cleavage or polyadenylation of mRNA, like smB/B', smD-1, U1A and CPSF to partially co-localize to GFP-CSB accumulations. Furthermore, co-immunoprecipitation studies confirm that these co-localizations are bona fide interactions between CSB and smD-1, U1A and CPSF.

Despite the function of CSB in transcription elongation [12-14], it does not clearly colocalize with transcription foci. Interestingly, evidence was provided that although mRNA processing factors are highly concentrated in speckles, these locations do not represent their site of action. Speckles were found to contain stable polyadenylated RNAs rather than pre-mRNA [28,29]. High concentrations of pre-mRNAs were found in the vicinity of transcription foci [30]. Careful analysis of the localization of splicing factors, using low concentration of antibodies specific for snRNPs, showed several hundreds of accumulations of these factors consistent with the distribution of transcription units [31].

The C-terminal domain (CTD) of the largest subunit of RNAP II, consisting of 52 heptad repeats (consensus, YSPTSPS) has a function in regulating the processivity of transcription elongation but is also required for efficient mRNA processing [32,33]. Furthermore, the CTD is required for accumulation of splicing factors and snRNPs at transcription sites [34]. This suggests that speckles, although containing high concentrations of splicing factors, may serve as assembly, modification or storage sites for mRNA processing-competent complexes, from where they continuously move to their site of action [35]. Similarly, CSB in speckles may be assembled into a mRNA processing factor-containing complex or stored. Characterization of the high molecular weight complex in which CSB resides may give more information about the relation between the spatial distribution of CSB and its functional implication in transcription elongation and transcription-coupled repair.

Taken together, we provide evidence for a distribution of CSB, which reflects the spatial distribution of mRNA processing factors in speckles and transcription. The functional relevance of this distribution has yet to be determined.

## **Materials and Methods**

### *Cell culture*

In this study the following cell lines were used: CS1AN-Sv (CS-B) human fibroblasts expressing GFP-CSB, CS1AN-Sv cells expressing HA-CSB-(His)<sub>6</sub> (dtCSB) and HeLa cells, which were cultured in a 1:1 mixture of Ham's F10 and DMEM (Gibco) supplemented with antibiotics and 10% fetal calf serum at 37° C, 5% CO<sub>2</sub>.

### *Light microscopy and image analysis*

Cells were cultured on glass coverslips and fixation was performed by incubation with 2% paraformaldehyde in PBS for 10 minutes at room temperature. Subsequently, cells were permeabilized with 0.1% TritonX-100 in PBS. First antibody staining was performed using

monoclonal antibodies directed against SC-35 (Sigma), smB'/B (Y12), smD-1 (7.13), U1A (9A9) and the polyclonal antibody recognizing CPSF(p100). Secondary antibody staining was performed with anti-mouse or anti-rabbit Alexa 594-conjugated antibodies (Molecular Probes). Images were obtained by confocal laser scanning microscopy using a Zeiss LSM 410. GFP imaging was performed by excitation with 455-490 and long pass emission filter (>510 nm). Alexa-595 images were obtained after excitation with 515-560 and long pass emission filter (580 nm).

### *BrUTP labeling*

Cells were grown to 50-70% confluency on sterile glass coverslips. BrUTP (end concentration 1mM) was transfected into the cells using FuGENE 6 (Roche). Coverslips were placed on a droplet of the transfection mix for 15' at 4°C. Subsequently, coverslips were put in medium and BrUTP incorporation was allowed for 15' at 37°C. Next, cells were washed twice with cold PBS and fixed in 2% paraformaldehyde in PBS. Immunofluorescent analysis using a monoclonal rat anti-BrdUTP antibody (Harlan Sera-Lab) as a first antibody and goat anti-rat Alexa 594-conjugated antibodies (Molecular Probes) as a second antibody was performed as described above.

### *In vitro transcription assay*

Transcription was measured in a reconstituted *in vitro* run-off transcription assay containing human recombinant TBP, TFIIB and TFIIE and purified HeLa TFIIA, TFIIF, TFIIH and RNAP II as described earlier [20]. Briefly, HA-elution fractions containing CSB were pre-incubated with the indicated transcription factors and with 100 ng of the adenovirus 2 major late promoter (Ad2MLP)-containing template for 15 minutes at 25°C. After the addition of nucleotides, transcription was allowed to proceed for 45 minutes at 25°C. The 309 nt [ $\alpha^{32}$ P]-CTP run off transcripts were resolved by electrophoresis through a 5% acrylamide/50% urea gel and analyzed by autoradiography.

### *Immunoprecipitation*

Immunoprecipitation of HA-CSB-(His)<sub>6</sub> was done by incubating a monoclonal anti-HA antibody (12CA5) overnight at 4°C with WCE from CS1AN-dtCSB cells. Subsequently, protein G beads were added and the mixture was incubated for an additional 5 hours at 4°C. Immunoblotting was performed on the depleted extract and the bound proteins after boiling the beads. Control immunoprecipitations from HeLa WCE were performed identically.

## **Acknowledgements**

We thank Walter van Venrooy for supplying us with antibodies against smD-1, SmB/B' and U1A and Lazlo Tora for giving us the CPSF(p100) antibody. This work was supported by the Center for Biomedical Genetics (CBG), the Dutch Scientific Organization (NWO-ALW, NWO-ZonMW and Spinoza award), the EC contract (Dnage), and the Dutch Cancer Society (KWF).

## References

1. Ljungman, M. and Zhang, F. (1996) Blockage of RNA polymerase as a possible trigger for u.v. light-induced apoptosis. *Oncogene*, 13, 823-831.
2. Yamaizumi, M. and Sugano, T. (1994) U.v.-induced nuclear accumulation of p53 is evoked through DNA damage of actively transcribed genes independent of the cell cycle. *Oncogene*, 9, 2775-84.
3. de Boer, J., Andressoo, J.O., de Wit, J., Huijman, J., Beems, R.B., van Steeg, H., Weeda, G., van der Horst, G.T., van Leeuwen, W., Themmen, A.P., Meradji, M. and Hoeijmakers, J.H. (2002) Premature aging in mice deficient in DNA repair and transcription. *Science*, 296, 1276-9.
4. Nance, M.A. and Berry, S.A. (1992) Cockayne syndrome: Review of 140 cases. *Am. J. of Med. Genet.*, 42, 68-84.
5. Henning, K.A., Li, L., Iyer, N., McDaniel, L., Reagan, M.S., Legerski, R., Schultz, R.A., Stefanini, M., Lehmann, A.R., Mayne, L.V. and Friedberg, E.C. (1995) The Cockayne syndrome group A gene encodes a WD repeat protein that interacts with CSB protein and a subunit of RNA polymerase II TFIIH. *Cell*, 82, 555-564.
6. Neer, E.J., Schmidt, C.J., Nambudripad, R. and Smith, T.F. (1994) The ancient regulatory-protein family of WD-repeat proteins. *Nature*, 371, 297-300.
7. Troelstra, C., Odijk, H., de Wit, J., Westerveld, A., Thompson, L.H., Bootsma, D. and Hoeijmakers, J.H.J. (1990) Molecular cloning of the human DNA excision repair gene ERCC-6. *Mol. Cell Biol.*, 10, 5806-5813.
8. Pazin, M.J. and Kadonaga, J.T. (1997) SWI2/SNF2 and related proteins: ATP-driven motors that disrupt protein-DNA interactions? *Cell*, 88, 737-740.
9. Citterio, E., Rademakers, S., van der Horst, G.T., van Gool, A.J., Hoeijmakers, J.H. and Vermeulen, W. (1998) Biochemical and biological characterization of wild-type and ATPase- deficient Cockayne syndrome B repair protein. *J. Biol. Chem.*, 273, 11844-11851.
10. Citterio, E., Van Den Boom, V., Schnitzler, G., Kanaar, R., Bonte, E., Kingston, R.E., Hoeijmakers, J.H. and Vermeulen, W. (2000) ATP-dependent chromatin remodeling by the Cockayne syndrome B DNA repair-transcription-coupling factor. *Mol Cell Biol*, 20, 7643-53.
11. van Gool, A.J., Citterio, E., Rademakers, S., van Os, R., Vermeulen, W., Constantinou, A., Egly, J.M., Bootsma, D. and Hoeijmakers, J.H.J. (1997) The Cockayne syndrome B protein, involved in transcription-coupled DNA repair, resides in a RNA polymerase II containing complex. *EMBO J.*, 16, 5955-5965.
12. Tantin, D., Kansal, A. and Carey, M. (1997) Recruitment of the putative transcription-repair coupling factor CSB/ERCC6 to RNA polymerase II elongation complexes. *Mol. Cell Biol.*, 17, 6803-6814.
13. Selby, C.P. and Sancar, A. (1997) Cockayne syndrome group B protein enhances elongation by RNA polymerase II. *Proc. Natl. Acad. Sci. USA*, 94, 11205-11209.
14. van den Boom, V., Citterio, E., Hoogstraten, D., Van Cappellen, W.A., Coin, F., Egly, J.M., Hoeijmakers, J.H., Houtsmuller, A.B. and Vermeulen, W. Transient interactions of CSB with transcription elongation complexes are stabilized by DNA damage-induced stalling. *submitted*.
15. Yu, A., Fan, H.-Y., Liao, D., Bailey, A.D. and Weiner, A.M. (2000) Activation of p53 or Loss of the Cockayne Syndrome Group B Repair Protein Causes Metaphase Fragility of Human U1, U2, and 5S Genes. *Molecular Cell*, 5, 801-810.
16. Bradsher, J., Auriol, J., Proietti de Santis, L., Iben, S., Vonesch, J.L., Grummt, I. and Egly, J.M. (2002) CSB is a component of RNA pol I transcription. *Mol Cell*, 10, 819-29.
17. Houtsmuller, A.B., Rademakers, S., Nigg, A.L., Hoogstraten, D., Hoeijmakers, J.H.J. and Vermeulen, W. (1999) Action of DNA repair endonuclease ERCC1/XPF in living cells. *Science*, 284, 958-961.
18. Hoogstraten, D., Nigg, A.L., Heath, H., Mullenders, L.H., van Driel, R., Hoeijmakers, J.H., Vermeulen, W. and Houtsmuller, A.B. (2002) Rapid switching of TFIIH between RNA polymerase I and II transcription and DNA repair in vivo. *Mol Cell*, 10, 1163-74.
19. Jackson, D.A., Hassan, A.B., Errington, R.J. and Cook, P.R. (1993) Visualization of focal sites of transcription within human nuclei. *Embo J.*, 12, 1059-1065.

20. **Gerard, M., Fischer, L., Moncollin, V., Chipoulet, J.-M., Chambon, P. and Egly, J.-M.** (1991) Purification and interaction properties of the human RNA polymerase B(II) general transcription factor BTF2. *J. Biol. Chem.*, 266, 20940-20945.
21. **Coin, F., Bergmann, E., Tremeau-Bravard, A. and Egly, J.M.** (1999) Mutations in XPB and XPD helicases found in xeroderma pigmentosum patients impair the transcription function of TFIIH. *EMBO J.*, 18, 1357-1366.
22. **van Steensel, B., Brink, M., van der Meulen, K., van Binnendijk, E.P., Wansink, D.G., de Jong, L., de Kloet, E.R. and van Driel, R.** (1995) Localization of the glucocorticoid receptor in discrete clusters in the cell nucleus. *J Cell Sci*, 108 ( Pt 9), 3003-11.
23. **Grande, M.A., van der Kraan, I., de Jong, L. and van Driel, R.** (1997) Nuclear distribution of transcription factors in relation to sites of transcription and RNA polymerase II. *J. Cell. Sci.*, 110, 1781-1791.
24. **McNally, J.G., Müller, W.G., Walker, D., Wolford, R. and Hager, G.L.** (2000) The glucocorticoid receptor: rapid exchange with regulatory sites in living cells. *Science*, 287, 1262-1265.
25. **Becker, M., Baumann, C., John, S., Walker, D.A., Vigneron, M., McNally, J.G. and Hager, G.L.** (2002) Dynamic behavior of transcription factors on a natural promoter in living cells. *EMBO Rep*, 3, 1188-94.
26. **Fu, X.D. and Maniatis, T.** (1990) Factor required for mammalian spliceosome assembly is localized to discrete regions in the nucleus. *Nature*, 343, 437-441.
27. **Spector, D.L.** (1990) Higher order nuclear organization: three-dimensional distribution of small nuclear ribonucleoprotein particles. *Proc Natl Acad Sci U S A*, 87, 147-51.
28. **Fakan, S., Leser, G. and Martin, T.E.** (1984) Ultrastructural distribution of nuclear ribonucleoproteins as visualized by immunocytochemistry on thin sections. *J Cell Biol*, 98, 358-63.
29. **Mattaj, I.W.** (1994) RNA processing. Splicing in space. *Nature*, 372, 727-8.
30. **Zhang, G., Taneja, K.L., Singer, R.H. and Green, M.R.** (1994) Localization of pre-mRNA splicing in mammalian nuclei. *Nature*, 372, 809-12.
31. **Neugebauer, K.M. and Roth, M.B.** (1997) Distribution of pre-mRNA splicing factors at sites of RNA polymerase II transcription. *Genes Dev*, 11, 1148-59.
32. **McCracken, S., Fong, N., Yankulov, K., Ballantyne, S., Pan, G., Greenblatt, J., Patterson, S.D., Wickens, M. and Bentley, D.L.** (1997) The C-terminal domain of RNA polymerase II couples mRNA processing to transcription. *Nature*, 385, 357-61.
33. **Kobor, M.S. and Greenblatt, J.** (2002) Regulation of transcription elongation by phosphorylation. *Biochim Biophys Acta*, 1577, 261-275.
34. **Misteli, T. and Spector, D.L.** (1999) RNA polymerase II targets pre-mRNA splicing factors to transcription sites in vivo. *Mol Cell*, 3, 697-705.
35. **Lamond, A.I. and Spector, D.L.** (2003) Nuclear speckles: a model for nuclear organelles. *Nat Rev Mol Cell Biol*, 4, 605-12.

# Chapter 9

Differential cellular localization and  
dynamics of CSA and CSB in relation  
to transcription and TCR

*Manuscript in preparation*

# Differential cellular localization and dynamics of CSA and CSB in relation to transcription and TCR

Vincent van den Boom<sup>1</sup>, Francesca Martinato<sup>4</sup>, Arjan Theil<sup>1</sup>, Wiggert A. van Cappellen<sup>2</sup>, Adriaan B. Houtsmuller<sup>3</sup>, Jan H.J. Hoeijmakers<sup>1</sup>, Wim Vermeulen<sup>1</sup> and Giuseppina Mari-Giglia<sup>1</sup>.

1) Department of Cell Biology and Genetics, Medical Genetic Center, 2) Department of Endocrinology and Reproduction, Medical Genetic Center, 3) Department of Pathology, Josephine Nefkens Institute, Erasmus MC Rotterdam, P.O. Box 1738, 3000 DR Rotterdam, The Netherlands. 4) Present address: Department of Experimental Oncology, European Institute of Oncology (IEO), Via Ripamonti 435, 20141 Milan, Italy.

## Abstract

Transcription-coupled repair (TCR) is a DNA repair pathway specialized in removal of transcription-blocking lesions. The Cockayne Syndrome A (CSA) and B (CSB) proteins are essential for TCR. Mutations either in CSA or CSB give rise to identical phenotype: the severe hereditary disorder Cockayne Syndrome. Whereas CSB is known to be involved in the TCR reaction itself and was reported to enhance transcription elongation by RNA polymerase II the function of CSA in TCR is still unknown. Here we describe the kinetic behavior of CSA as measured using a cell line expressing GFP-tagged CSA. CSA was found to be mobile although no change in subnuclear localization was observed upon UV exposure, as found with most NER/TCR factors. The mobility of CSA is not affected by the presence of TCR lesions and an inhibition of the transcriptional activity as found for CSB. In addition, we find an aberrant chromatographic behavior of CSB in the absence of CSA. We suggest a role for CSA in modification of CSB, making the protein active in TCR.

## Introduction

DNA is continuously attacked by a wide variety of DNA damaging agents like the short-wave component of sunlight, ionizing radiation, reactive oxygen species and carcinogenic compounds giving rise to distortions of the DNA structure. As a consequence, essential cellular processes like DNA replication, transcription and cell cycle are affected. During replication, lesions can induce mutations in the genome, which on the long run can lead to cancerous growth of cells. In contrast, damage-induced



blockage of transcription induces short-term effects by triggering cellular apoptosis [1,2], contributing to accelerated aging of tissues [3]. Therefore it is very important that DNA lesions in the genome are quickly removed. Fortunately, an intricate network of DNA damage removing pathways has evolved in the cell [4,5]. To eliminate the highly cytotoxic transcription-blocking lesions, a specialized transcription-coupled repair (TCR) pathway is exploited by the cell [6,7]. This repair pathway is activated upon damage-dependent transcription arrest and accomplishes strand-specific removal of helix-distorting DNA injuries (such as UV-induced photoproducts and oxidative DNA lesions from transcribed genes). These lesions are normally genome-wide removed by the nucleotide excision repair (NER) pathway and the base excision repair (BER) pathway respectively.

Defective TCR gives rise to the severe autosomal recessive disorder Cockayne Syndrome (CS), which is characterized by cutaneous photosensitivity, neurodevelopmental problems, growth retardation and progeroid symptoms but does not show increased occurrence of cancer [8]. At the cellular level the TCR defect leads to failure to recover RNA synthesis after UV-irradiation. Genetic analysis showed the presence of two complementation groups: CS-A and CS-B. The CSA gene encodes a 44 kDa protein containing five WD-40 repeats, a structural motif which is thought to be implicated in mediating protein-protein interactions [9,10]. The 168 kDa CSB gene product is a member of the SWI/SNF family of putative helicases [11]. This dsDNA-dependent ATPase was observed to interact with histones and remodel the nucleosome structure [12,13]. Furthermore, phosphorylation of CSB *in vitro* was found to diminish the ATPase activity of CSB, suggesting phosphorylation to be a regulating mechanism for the activity of CSB [14].

Mechanistically, the process of TCR remains elusive. TCR is initiated by stalling of an RNA polymerase II (RNAP II) molecule on a DNA lesion. Since the arrested RNAP II enzyme covers ~35 nucleotides around the lesion, repair can not initiate until the stalled complex is removed [15,16]. CSB is thought to be required for displacement of the stalled RNAP II molecule, possibly by remodeling the RNAP II-DNA interface. Furthermore, CSB resides in a high molecular weight complex (>700 kDa), co-immunoprecipitates with RNAP II and was able to interact with the ternary RNAP II-DNA-RNA complex *in vitro* [17-19]. Recently, analysis of a cell line expressing green fluorescent protein (GFP) tagged to CSB showed that the protein transiently interacts with transcription elongation complexes and displays a prolonged binding time upon DNA damage-induced arrest of the polymerase [20].

In contrast to CSB the role of CSA in TCR is mysterious. Gelfiltration experiments showed CSA to reside in a high molecular weight complex of ~420kDa [17] and *in vitro* interacts with CSB, TFIIH and XAB2 [9,21]. Furthermore, CSA was reported to translocate to the nuclear matrix in a CSB-dependent manner [22]. Recently, epitope-tagging of CSA resulted in the purification of a CSA-containing complex [23]. This complex consists of a core unit containing CSA, DDB1, Cul4A (cullin 4A) and Roc1 and exhibits ubiquitin ligating activity, which is stimulated by conjugation of NEDD8 to Cul4A (neddylation). Upon UV exposure an increased fraction of CSA core complexes displayed association of CSN (COP9 signalosome), resulting in deneddylation of Cul4A and inhibition of the ubiquitin ligating activity of the complex. The *in vivo* target for this

modifying activity is as yet not understood. Interestingly, upon UV-irradiation, no increased association of the CSA complex with the chromatin fraction was observed [23]. In contrast, analysis of GFP-CSB kinetics in living cells using photobleaching experiments showed a clear UV-dependent immobilization of the protein [20].

Since mutations both in the CSA and CSB gene cause a very similar phenotype it is most likely that the same cellular process is disturbed in both types of CS patients. The phenotype of CS is suggested to be the consequence of a transcription elongation machinery to be very sensitive to transcription blocking lesions [24]. This idea is supported by reports suggesting a role for CSB in monitoring transcription elongation [20,25]. However, it remains unknown if also CSA is directly involved in the process of monitoring transcription elongation. To investigate the role of CSA in TCR we generated a cell line expressing green fluorescent protein (GFP) tagged to the amino-terminus of CSA. This allowed us to study the localization of the protein and measure protein mobility in the presence or absence of DNA damage using fluorescence recovery after photobleaching (FRAP) techniques. Using a GFP-CSB expressing cell line we compared the *in vivo* kinetic behavior of CSA and CSB in living cells.

## Results

### *Expression and functionality of GFP-CSA in CS3BE human fibroblasts*

In order to gain insight into the function of CSA in TCR in the most relevant context (i.e. the living cell) we tagged the protein to the N-terminus with GFP, creating a GFP-CSA fusion protein (Fig. 1A). The cDNA encoding the chimeric protein was expressed in CSA-deficient SV40-transformed (CS3BE) human fibroblasts and stably expressing clones were isolated. To study the localization of the fusion protein it is important that it is functional and expressed at physiological levels. Immunoblot analysis using an anti-CSA (Fig. 1B) and anti-GFP antibodies (data not shown) showed that the full-length fusion protein was correctly expressed at levels close to endogenous CSA expression in HeLa cells. Functionality of the GFP-CSA protein was tested by survival analysis. UV-irradiation of a GFP-CSA expressing clone resulted in a survival similar to wild type cells, whereas CSA-deficient CS3BE cells show a strong hypersensitivity to UV (Fig. 1C). This indicates that GFP-CSA is functional and able to restore the UV-sensitivity of CS3BE cells up to wild type levels. Subsequently, we measured RNA synthesis recovery (RRS) after UV, which is used to specifically measure the activity of TCR (Fig. 1D). The clone expressing GFP-CSA protein did show substantial (albeit incomplete) recovery of RNA synthesis when measured 24 hours after UV compared to wild type cells, indicating that the fusion protein is largely functional in TCR.

### *Cellular localization of GFP-CSA*

High-resolution confocal imaging of the GFP-CSA expressing cells shows a homogeneous distribution of GFP-CSA throughout the nucleoplasm but no apparent accumulation in subnuclear structures (Fig. 1E). Importantly, the GFP-CSA cells stably expressed the fusion protein and were very homogenous with respect to the localization

of the polypeptide. Epifluorescent imaging of anti-CSA stained cells reveals a similar distribution of CSA in HeLa cells and MRC5 human fibroblasts (Fig. 1F), indicating that addition of the GFP-tag does not alter the nuclear distribution of the CSA protein. Upon UV-irradiation CSA localization is not altered (data not shown). Interestingly, this CSA localization pattern contrasts to the previously reported localization of CSB, which is dispersed throughout the nucleus in addition to bright focal and nucleolar accumulations

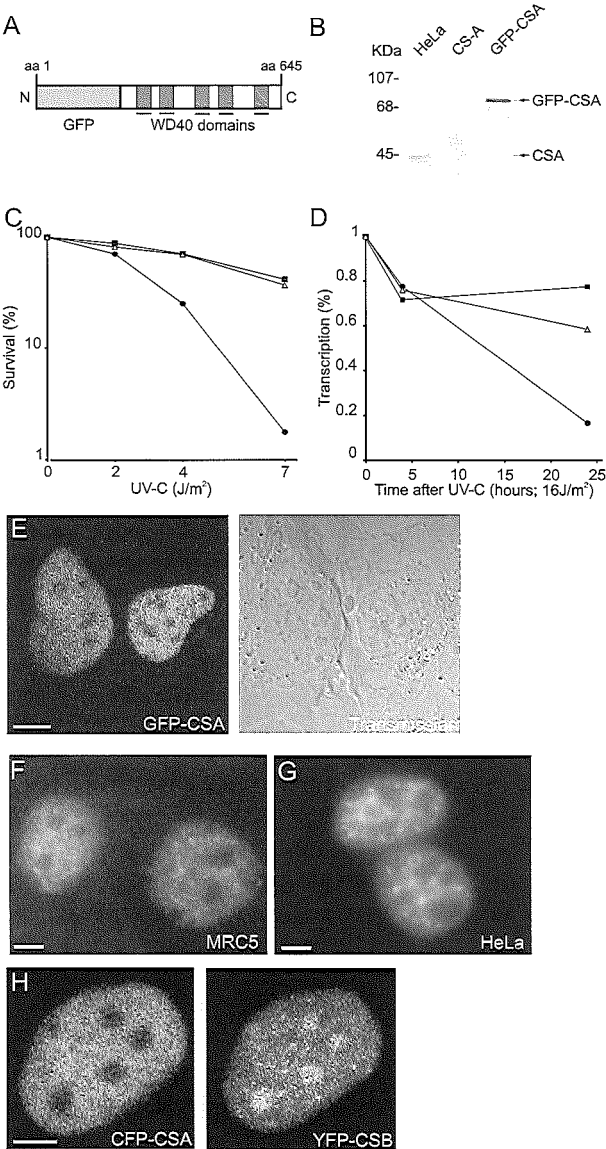


**Figure 1. Characterization of GFP-CSA expressing cell line.** A. Schematic representation of the GFP-CSA fusion gene. The five WD-40 domains in CSA are indicated. B. Immunoblot analysis of CSA expression in wild-type HeLa cells, CSA-deficient CS3BE cells and CS3BE cells expressing GFP-CSA cells using a polyclonal anti-CSA antibody. C. UV-survival assay using wild-type VH-10 cells (open triangles), CS3BE cells (circles) and GFP-CSA cells (squares). D. RNA synthesis recovery (RRS) assay using wild-type MRC5 cells (squares), CS3BE cells (circles) and GFP-CSA cells (open triangles). E. Confocal and transmission image of GFP-CSA cells. Note the homogenous distribution over the nucleus and the lower GFP-CSA signal in the nucleoli. F. Immunofluorescence analysis of wild type CSA in MRC5 cells using a monoclonal CSA antibody. G. Immunofluorescence analysis of wild type CSA in HeLa cells using a monoclonal CSA antibody. H. Confocal images of a cell stably expressing CFP-CSA and transiently transfected with YFP-CSB in a CSB-deficient (CS1AN) background. Note that CFP-CSA does not accumulate in the nucleoli and nuclear foci like YFP-CSB.

[20]. The difference in localization of CSA and CSB in living cells was further investigated by creating a cell line stably expressing CFP-CSA in CSB-deficient human fibroblasts (CS1AN) that were transiently transfected with YFP-CSB (Fig. 1G). Clearly, CFP-CSA does not localize to the YFP-CSB foci and, unlike YFP-CSB, is excluded from the nucleoli. This surprising finding shows that although CSA and CSB are both involved in TCR they do not have a similar distribution in living cells. A possible explanation for this different localization may be that in living cells, unlike CSB, CSA is immobilized to nuclear structures [20].

#### *Mobility of GFP-CSA under conditions of TCR*

To learn more about the connection between CSA and CSB in living cells and find out whether or not CSA is mobile we applied FRAP analysis to cells expressing GFP-tagged versions of these proteins. The YFP-CSB/CFP-CSA expressing cell line was not used for this purpose because the YFP-CSB protein is not stably expressed and these cells also contain endogenously expressed CSA protein, which may be preferentially used in TCR resulting in distorted mobility measurements of GFP-CSA. Briefly, FRAP analysis is performed by monitoring the fluorescence intensity in a defined strip in the middle of the nucleus. Fluorescent molecules in a marked strip are bleached by applying a high

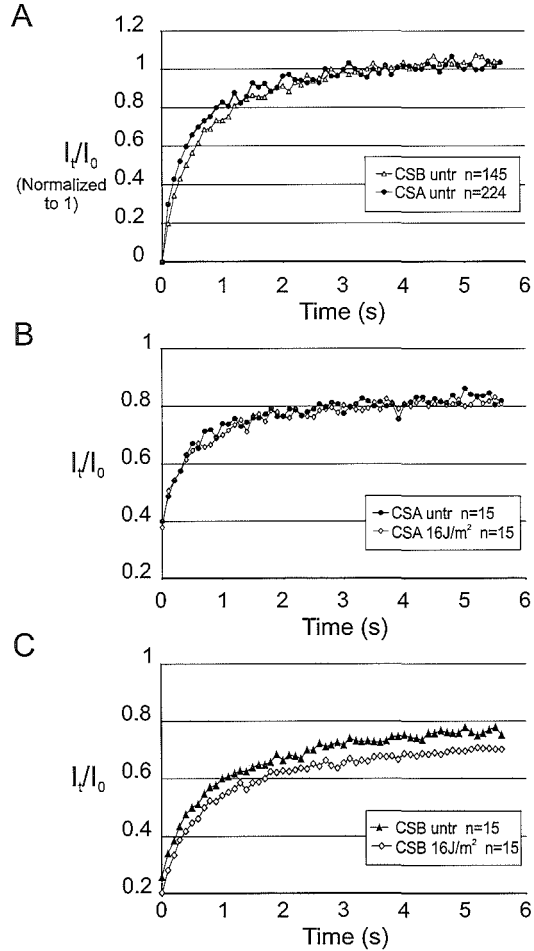


**Figure 2. FRAP analysis of GFP-CSA mobility in TCR.** A. FRAP recovery curves of GFP-CSA (circles) and GFP-CSB (open triangles) normalized to 1. B. GFP-CSA fluorescent recovery in untreated (circles) and UV-irradiated (open diamonds) cells ( $16\text{J}/\text{m}^2$ ). C. GFP-CSB fluorescent recovery in untreated (triangles) and UV-irradiated (open diamonds) cells ( $16\text{J}/\text{m}^2$ ). D. Application local damage to GFP-CSA cells. Locally UV-irradiated ( $48\text{J}/\text{m}^2$ ) GFP-CSA cells are stained with a polyclonal XPA antibody.

intensity laser pulse. The initial recovery of fluorescence in the strip is a measure for the effective diffusion rate ( $D_{\text{eff}}$ ) of the GFP-tagged protein. To directly compare the dynamic behavior of the CSA and CSB proteins we performed experiments to concomitantly on cells expressing GFP-CSA and cells expressing GFP-CSB. The initial influx of GFP-CSA molecules in the strip indicates that GFP-CSA does not diffuse as a single polypeptide but likely resides in a high molecular weight complex (Fig. 2A). Interestingly, GFP-CSA shows a slow fluorescent recovery in the strip, indicating that CSA does not roam the nucleus as a single polypeptide. Furthermore, the influx of GFP-CSA is slightly faster compared to GFP-CSB, suggesting that both proteins do not reside in the same complex, at least for the major part of the molecules. The mobility of GFP-CSB was the same as detected previously [20]. This is in concordance with our previous biochemical gel filtration studies and is also suggested by the recent affinity purification of a CSA-containing complex that does not harbor CSB [17,23]. Subsequently, we measured the response of the GFP-CSA protein to the induction of UV DNA photoproducts, which are lesions typically repaired by GGR and TCR. Surprisingly, GFP-CSA did not show an altered dynamic behavior upon UV, whereas GFP-CSB does show a clear immobilization within the same experiment as observed before [20] (Fig. 2B,C). To further investigate these findings we applied local damage to GFP-CSA expressing cells. As reported previously other NER factors like TFIIH, XPA and CSB accumulate at locally UV-irradiated areas in the cell [20,26,27]. Locally irradiated GFP-CSA expressing cells were stained with an anti-XPA antibody to demonstrate the accumulation of NER factors at the site of damage. Interestingly, GFP-CSA did not detectably accumulate at sites of local damage (Fig. 2D). This makes CSA the first NER protein, which does not exhibit a significant UV-induced immobilization in repair and localization at DNA lesions, suggesting that CSA is not specifically present at the sites of DNA damage.

#### *Kinetics of GFP-CSA upon transcription inhibition*

To further study the role of CSA in TCR we investigated whether the dynamic behavior of CSA is dependent on transcriptional activity, as was previously found for CSB and TFIIH, which transiently interacts with elongation complexes for 2-5 seconds [20] or transcription initiation sites for 2-10 seconds respectively [26]. When GFP-CSA expressing cells were treated with Actinomycin D we detected no changes in the mobility of GFP-CSA, whereas GFP-CSB was largely immobilized as observed previously (Fig. 3A, B) [20]. This suggests that CSA, unlike CSB, has not a transient interaction with the RNAPII elongation complexes of a similar duration as CSB. In addition, as described above, CSA and CSB do not react similarly to DNA damage induction suggesting quite different roles for both proteins in TCR.

#### *Protein characteristics of CSB in the absence of CSA*

Above findings suggest that the relationship between both TCR factors does not involve stable interactions of significant fractions of both proteins with each other. To search for indirect effects of CSA on CSB we investigated the stability and post-translational modification of CSB (as detected by mobility shift in SDS-PAGE) in the absence of CSA in either untreated or UV-irradiated cells. Therefore, we loaded equal

amounts of HeLa and CS3BE extracts and detected CSB using a polyclonal CSB antibody [17]. However, no apparent change in the stability of CSB in a CSA-background was observed (Fig. 4A). In addition, in time after UV-irradiation the protein level and gel mobility of CSB do not change in HeLa and CS3BE cell extracts, suggesting that CSA is not required for the stability or large post-translational modifications of CSB either in the absence or presence of DNA damage.

To study whether CSB is modified in the presence of CSA in other manners, we examined the chromatographic behavior of CSB on a heparin sepharose column in extracts from wild type (HeLa) cells and CSA-deficient (CS3BE) cells, prepared as described previously (Fig. 4B) [28]. First, detection of CSA, using an affinity-purified polyclonal antibody, showed that protein mainly elutes in the 0.22M KCl wash (lane 3; Fig. 4B) and the 0.4M KCl elution fraction (lane 6 and 7). Subsequently, all elution fractions were analysed for the presence of CSB. Fractionation of HeLa WCEs showed that CSB is present in the 0.4 M KCl elution fraction (lane 6-9; Fig. 4C) and the 1M KCl elution step (lane 12-14). This resembles the behavior of recombinant CSB protein on a heparin

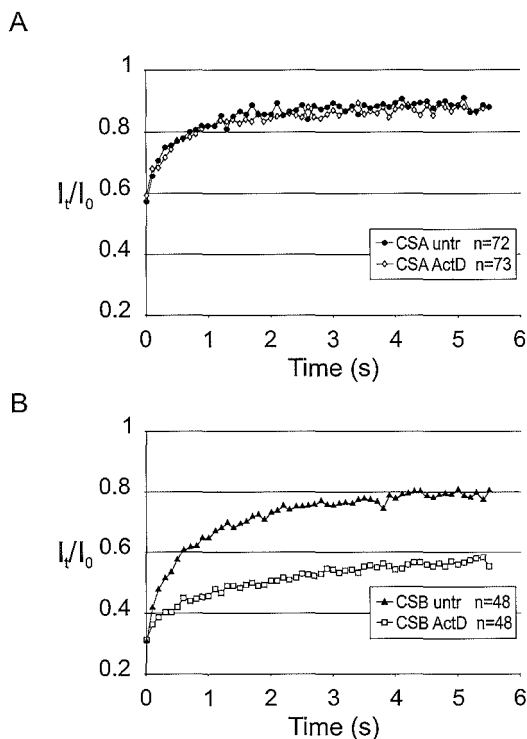
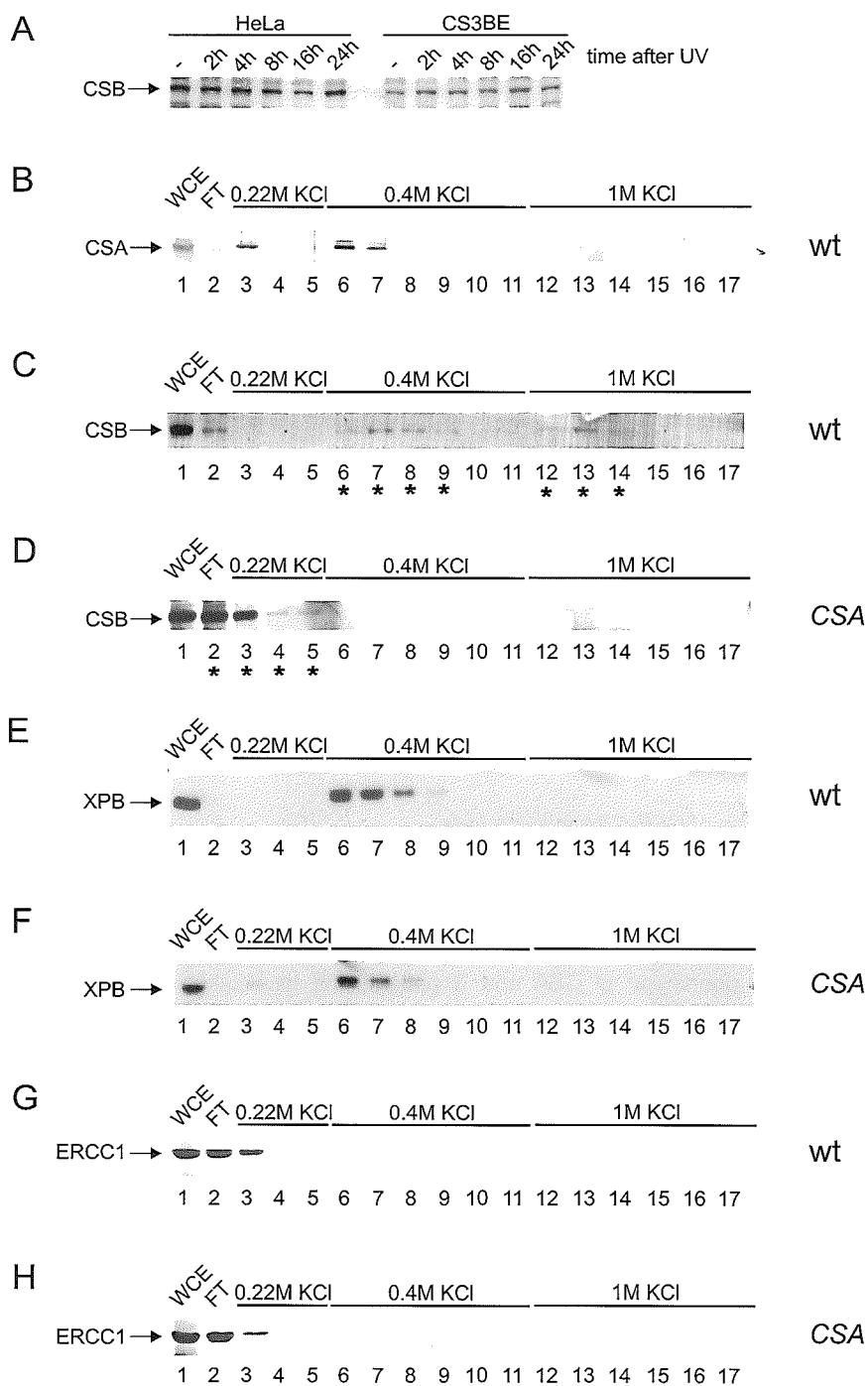


**Figure 3. FRAP analysis of GFP-CSA mobility in transcription.** A. Fluorescent recovery of untreated (circles) and actinomycin D-treated (open diamonds) GFP-CSA cells. B. Fluorescent recovery of untreated (triangles) and actinomycin D-treated (open squares) GFP-CSB cells.

**Figure 4. Quantification of CSB stability and chromatographic behavior in the presence and absence of CSA.** A. CSB expression levels in untreated (-) or UV-irradiated HeLa and CS3BE cells. Extract preparation was performed at times after UV as indicated. B. Chromatographic behavior of CSA in wildtype HeLa extracts on a heparin sepharose column. Lane 1: WCE, lane 2: flow-through, lane 3-5: 0.22M elution fraction, lane 6-11 0.4M KCl elution fractions, lane 12-17: 1M KCl elution fractions. C. Chromatographic behavior of CSB in wildtype HeLa extracts on a heparin sepharose column. Asterisks indicate the elution fractions of CSB. D. Chromatographic behavior of CSB in CSA-deficient CS3BE extracts on a heparin sepharose column. Asterisks indicate the elution fractions of CSB. E. Chromatographic behavior of XPB in wildtype HeLa extracts on a heparin sepharose column. F. Chromatographic behavior of CSB in CSA-deficient CS3BE extracts on a heparin sepharose column. G. Chromatographic behavior of ERCC1 in wildtype HeLa extracts on a heparin sepharose column. H. Chromatographic behavior of ERCC1 in CSA-deficient CS3BE extracts on a heparin sepharose column.



sepharose column, which does not elute with a buffer containing 0.3M KCl [12]. Surprisingly, CSB detection on a fractionation of a CS3BE extract showed that the protein is mainly present in the flow-through (lane 2; Fig. 4D) and the 0.22M KCl wash (lane 3-5), showing that CSB has a different chromatographic behavior in the absence of CSA. To investigate if the observed changes in CSB were due to erroneous elution of proteins in the extract we studied the elution pattern of TFIIH and ERCC1. Immunoblot analysis using antibodies recognizing the XPB subunit of TFIIH (Fig. 4E, F) and ERCC1 (Fig. 4G, H) showed that both in the presence or absence of CSA their elution pattern is identical, stressing that the observed shift in the chromatographic behavior of CSB is not due to an artifact of the experiment. Taken together, this unexpected finding suggested that in the presence of CSA, CSB is differently charged. Currently we are investigating the nature of this modification.

## Discussion

Here we describe the behavior of the transcription-coupled repair protein CSA, using a cell line expression GFP-tagged CSA. Careful analysis shows the fusion protein to be functional in TCR. We measured the dynamic behavior of GFP-CSA by confocal photobleaching studies. We find that CSA is not located to the site of damage, like was found for other TCR/NER protein (complexes) such as CSB, TFIIH, XPA, XPG, PCNA, RPA and ERCC1/XPF [20,26,27,29,30]. Moreover, we find CSA to be required for a normal chromatographic behavior of CSB, suggesting that CSA may induce modification of the CSB protein.

### *Nuclear localization of GFP-CSA in living cells*

GFP-CSA is homogeneously distributed throughout the nucleus and is (partially) excluded from the nucleolus. This nuclear localization is in contrast to the distribution of CSB, which is also dispersed through the nucleus but in addition resides at higher concentration in focal structures and nucleoli [20]. This shows that, despite the indistinguishable phenotype of CSA and B patients the localization of the expressed proteins has a distinct character.

### *CSA resides in a high molecular weight complex*

The inert behavior of CSA upon DNA-damage induction suggested that the protein might be immobilized to nuclear structures. However, FRAP studies of the GFP-CSA fusion protein show that it roams the nucleus with a diffusion rate, which correlates to the diffusion of a high molecular weight complex. This is in line with our earlier gelfiltration studies, which indicated that CSA resides in a complex of approximately 420 kDa, and the purification of a CSA-containing complex by Groisman and coworkers [17,23]. The diffusion rate of GFP-CSA is slightly faster compared to GFP-CSB, indicating that both proteins are different diffusing species and reside in different complexes. In addition, also the affinity-purified CSA complex did not contain the CSB polypeptide and co-immunoprecipitation studies of CSA with CSB did never show a detectable, stable



interaction between the two proteins [17,23]. On the other hand, *in vitro* experiments showed an interaction between CSA and CSB, indicating that the two proteins are able to interact [9]. Taken together, these findings suggest that CSA and CSB are for most of the time in distinct protein complexes, but may transiently interact during the TCR reaction for a very short period of time. Alternatively, only a very small fraction of the CSA and CSB molecules interact at any time or under very specific conditions *in vivo*.

#### *Dynamic behavior of CSA in TCR and transcription*

FRAP analysis of GFP-CSA expressing cells after UV-damage induction does not show a change in the kinetics of fluorescent recovery of the protein, which is distinct from the partial immobilization observed for CSB. Furthermore, local irradiation of GFP-CSA cells does not result in detectable accumulation of GFP-CSA at the site of damage as was found for CSB and other NER proteins, like XPA, TFIIH and ERCC1 [20,26,27,29]. One option to explain these findings is that the immobilized fraction of GFP-CSA is below our detection levels. Another explanation may be that CSA is not required at the site of damage to execute its function in TCR. In this case no CSA will be immobilized upon UV damage induction.

FRAP analysis of the dynamic behavior of the CS proteins in transcription shows a distinct behavior for both polypeptides. CSB was found to interact with the RNAPII elongation machinery in a transient manner [20]. This is reflected by the large immobilization of GFP-CSB upon treatment with actinomycin D, most likely because of stable binding of CSB to stalled RNAPII complexes. Interestingly, the fluorescent recovery of GFP-CSA in the strip is not altered upon transcription inhibition. This may imply that CSA does not interact with elongating RNAPII molecules. Taken together, CSA and CSB do not share their localization pattern in the cell and do not have the same dynamics in TCR and transcription.

#### *Is CSA required for proper functioning of CSB in TCR?*

Despite the differences in the dynamic behavior of CSA and CSB, mutations in both proteins result in the same clinical phenotype: Cockayne Syndrome. This raises the question how CSA interferes with TCR without having a detectable direct involvement in the repair reaction itself that is visible as change in mobility or localization. Our biochemical experiments show that the stability of CSB is not affected in the absence of CSA, both in the presence or absence of DNA damage. However, the chromatographic behavior of CSB on a heparin sepharose column is severely changed. The elution pattern of CSB in extracts derived from a CSA-deficient background suggest that the protein is more negatively charged under these conditions. This change in protein charge results in elution of CSB under less stringent conditions from the negatively charged heparin sepharose resins. An explanation for these differences is a modification of CSB in the absence of CSA (e.g. phosphorylation). Recently it was shown that CSB can be phosphorylated *in vitro* and *in vivo* [14]. In addition, CSB was found to be dephosphorylated 4 hours after UV and partially regained its phosphorylated state 24 hours after UV. Furthermore, the dephosphorylated state of CSB showed to have an approximately 40% increased ATPase activity *in vitro*. Although this is only a marginal

increase in the enzymatic activity, the effect of the ATPase activity of CSB may be stronger in the presence of its natural kinase *in vivo*. Our data suggest that, in the presence of CSA, CSB may be dephosphorylated rendering the protein more active in TCR.

Taken together, we suggest that CSA is not needed for the actual repair reaction but is required to induce a modification of the CSA protein, inducing the CSB protein to be active in TCR. This study sheds new light on the functional implications of the CSA protein in TCR. The next challenge is to further characterize what is the exact reason for the change in the chromatographic behavior of CSB. Various proteomics-based approaches should provide an answer to this question.

## Materials and Methods

### *Generation and characterization GFP-CSA.*

To create the GFP-CSA fusion gene, the CSA cDNA was cloned in-frame to the EGFP cDNA in the EcoRI site of the pEGFP-C3 expression vector (Clontech), resulting in the pEGFP-CSA plasmid (hereafter, GFP-CSA). GFP-CSA was stably expressed in CS-A-deficient (UV-sensitive) human fibroblasts (CS3BE-Sv) using FuGENE 6 transfection reagent (Roche). Stable clones were isolated after selection with G418 (200 µg/ml). Expression level and functionality of the GFP-CSA expressing clones was further analysed by western blot analysis and UV-survival respectively. The expression level of the tagged protein was determined by immunoblot analysis by affinity-purified, rabbit polyclonal anti-CSB as previously described [17]. For UV-survival GFP-CSA expressing clones were compared to VH10-Sv (wt) human fibroblasts and untransfected CS3BE-Sv fibroblasts as described [17,31] RNA synthesis recovery (RRS) was measured by comparing the RRS of GFP-CSA expressing clones with MRC5-Sv (wt) human fibroblasts and CS3BE-Sv cells as described [32].

### *Cell culture and specific treatments*

The cell lines used in this study were CS3BE-Sv (CS-A) human fibroblasts, wild-type VH10-Sv human fibroblasts, wild type MRC5-Sv human fibroblasts and HeLa cells. Cells were grown at 37° C in 5% CO<sub>2</sub> atmosphere in a 1:1 mixture of Ham's F10 and DMEM (Gibco) supplemented with antibiotics and 10% fetal calf serum. Transcription inhibition was performed by treatment of cells with actinomycin D (10 µg /ml, 2 hours). Treatment with ultraviolet (UV) light at 254 nm (UV-C) was performed using a germicidal lamp at the indicated doses. DNA damage in localized areas of the nucleus was done by applying an UV-resistant polycarbonate filter with 5 mm pores (Millipore) on the cells during UV irradiation [30].

### *Light microscopy and image analysis*

For indirect immunofluorescence (IF), fixation was performed in 2% paraformaldehyde in PBS for 10 minutes at room temperature. After fixation, cells were permeabilized with 0.1% TritonX-100 in PBS. Endogenous CSA in wild type MRC5-Sv and HeLa cells was detected with a monoclonal CSA antibody. Secondary antibody staining was performed with anti-rabbit Alexa 594-conjugated antibodies (Molecular Probes). For fixed cells, fluorescent microscopy images were

obtained with a Leitz Aristoplan microscope equipped with epi-fluorescence optics and a PLANAPO 63x/1.40 oil immersion lens. Confocal laser scanning microscopy images of live cells were recorded with a Zeiss LSM 510. GFP images were obtained after excitation with 455-490 and long pass emission filter (>510 nm). Alexa-595 images were obtained after excitation with 515-560 and long pass emission filter (580 nm).

#### *Fluorescence recovery after photobleaching (FRAP)*

A Zeiss LSM410 was used for the FRAP experiments [29]. Recovery curves for evaluation of protein mobility were obtained as described before [26,29,33]. For FRAP analysis, a 2  $\mu$ m wide strip, spanning the entire nucleus, was bleached for 200 ms at highest intensity of the 488 nm line of a 15 mW Ar-laser focused by a 40X 1.3 n.a. oil immersion lens. Subsequently the recovery of fluorescence in the strip was monitored at intervals of 100 ms with the same laser at 5% of the intensity applied for bleaching, using a dichroic beamsplitter (488/543nm) and an additional 515-540 nm band pass filter for emission detection.

#### *Extract preparation and chromatography*

Protein extract preparation and chromatography were performed as described previously [28]. Extract from HeLa and CS3BE cells were loaded on a Heparin Sepharose CL-6B (Amersham Biosciences). Step-wise elution was done using a 0.22M, 0.4M and 1M KCl buffer D.

#### **Acknowledgements**

We thank members of the lab for helpful suggestions and discussions. This work was supported by the Center for Biomedical Genetics (CBG), the Dutch Scientific Organization (NWO-ALW, NWO-ZonMW and Spinoza award), the EC contract (Dnage), and the Dutch Cancer Society (KWF).

#### **References**

1. **Yamaizumi, M. and Sugano, T.** (1994) U.v.-induced nuclear accumulation of p53 is evoked through DNA damage of actively transcribed genes independent of the cell cycle. *Oncogene*, 9, 2775-84.
2. **Ljungman, M. and Zhang, F.** (1996) Blockage of RNA polymerase as a possible trigger for u.v. light-induced apoptosis. *Oncogene*, 13, 823-831.
3. **de Boer, J., Andressoo, J.O., de Wit, J., Huijman, J., Beems, R.B., van Steeg, H., Weeda, G., van der Horst, G.T., van Leeuwen, W., Themmen, A.P., Meradji, M. and Hoeijmakers, J.H.** (2002) Premature aging in mice deficient in DNA repair and transcription. *Science*, 296, 1276-9.
4. **Friedberg, E.C., Walker, G.C. and Siede, W.** (1995) *DNA repair and mutagenesis*. ASM Press, Washington D.C.
5. **Hoeijmakers, J.H.** (2001) Genome maintenance mechanisms for preventing cancer. *Nature*, 411, 366-74.
6. **Bohr, V.A., Smith, C.A., Okumoto, D.S. and Hanawalt, P.C.** (1985) DNA repair in an active gene: removal of pyrimidine dimers from the *DHFR* gene of CHO cells is much more efficient than in the genome overall. *Cell*, 40, 359-369.

7. Mellon, I., Spivak, G. and Hanawalt, P.C. (1987) Selective removal of transcription-blocking DNA damage from the transcribed strand of the mammalian *DHFR* gene. *Cell*, 51, 241-249.
8. Nance, M.A. and Berry, S.A. (1992) Cockayne syndrome: Review of 140 cases. *Am. J. of Med. Genet.*, 42, 68-84.
9. Henning, K.A., Li, L., Iyer, N., McDaniel, L., Reagan, M.S., Legerski, R., Schultz, R.A., Stefanini, M., Lehmann, A.R., Mayne, L.V. and Friedberg, E.C. (1995) The Cockayne syndrome group A gene encodes a WD repeat protein that interacts with CSB protein and a subunit of RNA polymerase II TFIIH. *Cell*, 82, 555-564.
10. Neer, E.J., Schmidt, C.J., Nambudripad, R. and Smith, T.F. (1994) The ancient regulatory-protein family of WD-repeat proteins. *Nature*, 371, 297-300.
11. Troelstra, C., Van Gool, A., De Wit, J., Vermeulen, W., Bootsma, D. and Hoeijmakers, J.H.J. (1992) ERCC6, a member of a subfamily of putative helicases, is involved in Cockayne syndrome and preferential repair of active genes. *Cell*, 71, 939-953.
12. Citterio, E., Rademakers, S., van der Horst, G.T., van Gool, A.J., Hoeijmakers, J.H. and Vermeulen, W. (1998) Biochemical and biological characterization of wild-type and ATPase- deficient Cockayne syndrome B repair protein. *J. Biol. Chem.*, 273, 11844-11851.
13. Citterio, E., Van Den Boom, V., Schnitzler, G., Kanaar, R., Bonte, E., Kingston, R.E., Hoeijmakers, J.H. and Vermeulen, W. (2000) ATP-dependent chromatin remodeling by the Cockayne syndrome B DNA repair-transcription-coupling factor. *Mol Cell Biol*, 20, 7643-53.
14. Christiansen, M., Stevnsner, T., Modin, C., Martensen, P.M., Brosh, R.M., Jr. and Bohr, V.A. (2003) Functional consequences of mutations in the conserved SF2 motifs and post-translational phosphorylation of the CSB protein. *Nucleic Acids Res*, 31, 963-73.
15. Selby, C.P., Drapkin, R., Reinberg, D. and Sancar, A. (1997) RNA polymerase II stalled at a thymine dimer: footprint and effect on excision repair. *Nucleic Acids Res*, 25, 787-93.
16. Tornaletti, S., Reines, D. and Hanawalt, P.C. (1999) Structural characterization of RNA polymerase II complexes arrested by a cyclobutane pyrimidine dimer in the transcribed strand of template DNA. *J. Biol. Chem.*, 274, 24124-24130.
17. van Gool, A.J., Citterio, E., Rademakers, S., van Os, R., Vermeulen, W., Constantinou, A., Egly, J.M., Bootsma, D. and Hoeijmakers, J.H.J. (1997) The Cockayne syndrome B protein, involved in transcription-coupled DNA repair, resides in a RNA polymerase II containing complex. *EMBO J.*, 16, 5955-5965.
18. Tantin, D., Kansal, A. and Carey, M. (1997) Recruitment of the putative transcription-repair coupling factor CSB/ERCC6 to RNA polymerase II elongation complexes. *Mol. Cell. Biol.*, 17, 6803-6814.
19. Tantin, D. (1998) RNA polymerase II elongation complexes containing the Cockayne syndrome group B protein interact with a molecular complex containing the transcription factor IIH components xeroderma pigmentosum B and p62. *J. Biol. Chem.*, 273, 27794-27799.
20. van den Boom, V., Citterio, E., Hoogstraten, D., Van Cappellen, W.A., Coin, F., Egly, J.M., Hoeijmakers, J.H., Houtsmuller, A.B. and Vermeulen, W. Transient interactions of CSB with transcription elongation complexes are stabilized by DNA damage-induced stalling. *submitted*.
21. Nakatsu, Y., Asahina, H., Citterio, E., Rademakers, S., Vermeulen, W., Kamiuchi, S., Yeo, J.P., Khaw, M.C., Saijo, M., Kodo, N., Matsuda, T., Hoeijmakers, J.H. and Tanaka, K. (2000) XAB2, a novel tetratricopeptide repeat protein involved in transcription-coupled DNA repair and transcription. *J. Biol. Chem.*, 275, 34931-34937.
22. Kamiuchi, S., Saijo, M., Citterio, E., de Jager, M., Hoeijmakers, J.H. and Tanaka, K. (2002) Translocation of Cockayne syndrome group A protein to the nuclear matrix: possible relevance to transcription-coupled DNA repair. *Proc Natl Acad Sci U S A*, 99, 201-6.
23. Groisman, R., Polanowska, J., Kuraoka, I., Sawada, J., Saijo, M., Drapkin, R., Kisselev, A.F., Tanaka, K. and Nakatani, Y. (2003) The Ubiquitin Ligase Activity in the DDB2 and CSA Complexes Is Differentially Regulated by the COP9 Signalingosome in Response to DNA Damage. *Cell*, 113, 357-67.

24. **Bootsma, D. and Hoeijmakers, J.H.J.** (1993) Engagement with transcription. *Nature*, 363, 114-115.
25. **Selby, C.P. and Sancar, A.** (1997) Cockayne syndrome group B protein enhances elongation by RNA polymerase II. *Proc. Natl. Acad. Sci. USA*, 94, 11205-11209.
26. **Hoogstraten, D., Nigg, A.L., Heath, H., Mullenders, L.H., van Driel, R., Hoeijmakers, J.H., Vermeulen, W. and Houtsmuller, A.B.** (2002) Rapid switching of TFIIH between RNA polymerase I and II transcription and DNA repair in vivo. *Mol Cell*, 10, 1163-74.
27. **Rademakers, S., Volker, M., Hoogstraten, D., Nigg, A.L., Mone, M.J., Van Zeeland, A.A., Hoeijmakers, J.H., Houtsmuller, A.B. and Vermeulen, W.** (2003) Xeroderma Pigmentosum Group A Protein Loads as a Separate Factor onto DNA Lesions. *Mol Cell Biol*, 23, 5755-5767.
28. **Marinoni, J.C., Rossignol, M. and Egly, J.M.** (1997) Purification of the transcription/repair factor TFIIH and evaluation of its associated activities in vitro. *Methods*, 12, 235-53.
29. **Houtsmuller, A.B., Rademakers, S., Nigg, A.L., Hoogstraten, D., Hoeijmakers, J.H.J. and Vermeulen, W.** (1999) Action of DNA repair endonuclease ERCC1/XPF in living cells. *Science*, 284, 958-961.
30. **Volker, M., Mone, M.J., Karmakar, P., van Hoffen, A., Schul, W., Vermeulen, W., Hoeijmakers, J.H., van Driel, R., van Zeeland, A.A. and Mullenders, L.H.** (2001) Sequential assembly of the nucleotide excision repair factors in vivo. *Mol Cell*, 8, 213-24.
31. **Sijbers, A.M., Van der Spek, P.J., Odijk, H., Van den Berg, J., Van Duin, M., Westerveld, A., Jaspers, N.G.J., Bootsma, D. and Hoeijmakers, J.H.J.** (1996) Mutational analysis of the human nucleotide excision repair gene ERCC1. *Nucleic Acids Res.*, 24, 3370-3380.
32. **Troelstra, C., Odijk, H., de Wit, J., Westerveld, A., Thompson, L.H., Bootsma, D. and Hoeijmakers, J.H.J.** (1990) Molecular cloning of the human DNA excision repair gene ERCC-6. *Mol. Cell Biol.*, 10, 5806-5813.
33. **Ellenberg, J., Siggia, E.D., Moreira, J.E., Smith, C.L., Presley, J.F., Worman, H.J. and Lippincott-Schwartz, J.** (1997) Nuclear membrane dynamics and reassembly in living cells: targeting of an inner nuclear membrane protein in interphase and mitosis. *J. Cell. Biol.*, 138, 1193-1206.



# Chapter 10

Concluding remarks and future  
directions

## Concluding remarks and future directions

Research during the past decades underlined the importance of TCR as an essential mechanism to promote cellular survival. In the absence of TCR, highly cytotoxic transcription-blocking lesions cause induction of apoptosis, eventually leading to segmental aging of the organism. Moreover, when TCR is defective, humans develop the severe hereditary disorder Cockayne Syndrome.

Part of the work described in this thesis uses an *in vivo* approach to study the molecular mechanism of TCR. GFP-tagging of both the CSA and CSB proteins allowed to study their function in TCR in its natural context, the living cell. CSB is homogeneously distributed throughout the nucleus in addition to bright fluorescent foci and nucleolar accumulations (chapter 7). Upon inhibition of transcription or DNA damage infliction (NER and BER type of lesions) the protein becomes homogeneously dispersed throughout the nucleus and the nucleoli become empty. In time after UV the localization pattern was restored with kinetics resembling the recovery time of RNA synthesis after UV (~16 hours). Interestingly, ionizing radiation-induced redistribution of CSB was found to restore within 2 hours after DNA damage induction, suggesting that TC-BER is much faster than TC-NER. This may be explained by the fact that GG-NER is very inefficient in removal of CPDs, which provokes an increased need for TCR of CPD lesions. In contrast, GG-BER is very efficient, decreasing the chance for transcription stalling on oxidative lesions.

Fluorescence recovery after photobleaching (FRAP) experiments revealed that CSB transiently interacts for 2-5 seconds with elongating RNAPII molecules (chapter 7). It suggests that CSB is constantly monitoring transcribing RNAPII complexes for their processivity. The momentary character of these interactions may also imply that interactions of other elongation factors with RNAPII molecules are also dynamic. This is in contrast to the idea that both elongation factors and RNAPII form a stable holo complex. An interesting question is whether CSB also plays an active role in transcription resumption after non-damage-induced transcription stalling (e.g. transcriptional pausing). Despite the observed transcriptional involvement of CSB, deduced from our live cell photobleaching studies, the precise molecular actions of CSB in transcription elongation can be studied in more detail using an *in vitro* reconstituted transcription elongation reaction. Interestingly, Mfd, the bacterial homologue of CSB was found to translocate backtracked RNA polymerase in a forward direction, returning the 3'-end of the mRNA back in the catalytic site of the polymerase [1]. Similarly, CSB may promote forward translocation of stalled RNAPII molecules. This type of activity has as yet not been found for other known elongation factors and seems to provide an additional mechanism to release stalled RNAPII molecules (see chapter 3). This may add a new pathway to regulate the activity of RNAPII, which may be required in specific types stalling. This idea is strengthened by the fact that deleting *Dst1* (yeast homologue of TFIIIS) in a *Rad26* (yeast homologue of CSB) background leads to a synergistic increase of the phenotype (i.e. impaired growth) [2], indicating that both proteins stimulate transcription elongation, although by different means.



Another enigma is the question what happens when an RNAPII elongation complex stalls on a DNA lesion. Our live cell studies show that the binding time of CSB to RNAPII is prolonged to 115-155 seconds upon infliction of DNA damage, most likely reflecting CSB, which is actively engaged in TCR (chapter 7). *In vitro* systems can be a powerful tool to study complex cellular processes like transcription, replication and repair. However, all attempts to set up an experimental system for TCR thus far have proven unsuccessful though. This suggests that TCR is not such a clear-cut mechanism as for example GGR, which can be reconstituted *in vitro*. Most likely, TCR is dependent on structural elements in the cell (e.g. chromatin environment and the nuclear matrix) and the integration of nuclear events (e.g. transcription and chromatin assembly). To bridge the gap between low resolution *in vivo* analysis and lack of a functional *in vitro* assay the fate and structural consequences of a stalled polymerase, both in the presence and absence of the CS factors can be investigated using novel approaches like (1) CHIP (*in vivo* protein contacts), (2) scanning force microscopy (SFM; structure) and (3) mass spectrometry (protein complex composition; CSB-RNAPII, RNAPII-DNA, CSB-NER). Our live cell studies and earlier biochemical analysis showed that CSB resides in high molecular weight complex (chapter 7) [3]. One of the direct challenges for this moment is to purify this complex and identify the possible complex partners of CSB. Mass spectrometry of a purified complex will be a useful tool to characterize this complex.

Several models have been postulated for a function of CSB in TCR. Generally, CSB is thought to either (1) displace, (2) translocate or (3) induce ubiquitination and subsequent proteosomal degradation of the stalled polymerase (chapter 2). Evidence is available for all of these models, suggesting that in a living cell these scenarios can coexist. Indications for integration of these models was found studying TCR in yeast [4,5]. Purification of the Rad26 protein from yeast revealed a co-purifying polypeptide: Def1 (RNAPII degradation factor 1). This protein was found to stimulate damage-dependent polyubiquitination and proteosomal degradation of yeast RNAPII. The authors postulate a model in which Rad26 stimulates repair of the lesion without degrading RNAPII. If Rad26 fails to displace the polymerase Def1 can act as an escape by targeting the stalled polymerase for degradation. This finding leaves the question whether such a Def1 homologue exists in humans. Purification and characterization of the CSB complex from human cells may shed light on the presence of a Def1 homologue in humans. However, in contrast to *Rad26* cells, human fibroblasts from CS-B patients show an absence of UV-dependent polyubiquitination of RNAPII, indicating that CSB itself also has a direct or indirect role in this modification of the polymerase in humans.

In addition, apart from the question how CSB makes a DNA lesion accessible for the repair machinery, it is important to know what intrinsic activity of the protein causes this action. In chapter 6 the identification of an ATP-dependent chromatin remodeling activity of CSB is described. The functional implications of this activity are as yet unknown. Remodeling the chromatin structure around the stalled polymerase could be a prerequisite for TCR to initiate repair. In addition, this activity may be implicated in resumption of transcription after non-damage-induced stalling of RNAPII. Otherwise, the remodeling activity of CSB may extend to remodeling the RNAPII-DNA interaction surface, thereby increasing the accessibility of the DNA lesion. An *in vitro* reconstituted

system for TCR in its natural chromatin context is likely to provide an answer to these questions. As a first step, scanning force microscopy can be used to investigate the physical interaction of CSB and stalled RNAP II and the influence of CSB on the geometry of chromatin.

Next to CSB, CSA also is required for TCR. Characterization of a GFP-CSA expressing cell line showed that both CSA and CSB have distinct nuclear distributions (Chapter 8). CSA does not accumulate in foci or in the nucleolus. FRAP experiments showed that CSA has a different effective diffusion rate compared to CSB, indicating that both proteins do not reside in the same complex, like was found in gel filtration experiments [3]. In addition, CSA is not immobilized upon UV-induced DNA damage. This was confirmed by the absence of an apparent accumulation of CSA at locally damaged sites. Furthermore, the mobility of CSA is not affected by changes in transcriptional activity like was seen for CSB. These surprising findings led to the hypothesis that CSA is not directly involved in the TCR process itself but may be required to activate or modulate CSB prior to action in TCR. This would directly explain the phenotypical overlap between both CSA and CSB. In this case not the absence of CSA, but rather the presence of non-functional CSB in CSA-A cells causes the CS phenotype. The changed chromatographic behavior of CSB in WCEs from CSA-deficient cells suggests that CSB is more negatively charged in the absence of CSA. A possible candidate modification for CSB is phosphorylation on the potential casein kinase sites in the absence of CSA. *In vitro*, dephosphorylation of CSB enhances the ATPase activity, suggesting a role for phosphorylation in regulating the activity of the CSB protein in repair [6]. In wild type cells this CSB-modifying activity may be sequestered by CSA. 2D-gel analysis and/or mass-spectrometry of CSB from wildtype and CSA-extracts may provide more information on the details of this modification. In addition, FRAP-based mobility studies of GFP-CSB in a CSA-deficient background will be very interesting. Does CSB still display the characteristics in repair and transcription in the absence of CSA? To obtain this cell line different approaches can be used like expression of short interfering RNAs (siRNA) directed against CSA mRNA in GFP-CSB expressing cells or creating a stable GFP-CSB expressing cell line in CSA<sup>-/-</sup>/CSB<sup>-/-</sup> DKO MEFs.

Very recent advances in our lab made it possible to create knock-in mice expressing GFP-tagged proteins from their endogenous promoter. This allows to study the protein behavior in its most natural context and avoid overexpression of the fusion-protein, a phenomenon, which is common when proteins are expressed from an exogenous promoter (e.g. CMV promoter). GFP-tagged protein knock-in mice make it possible to measure protein dynamics in living tissues. Tissue-specific localization and mobility of proteins can be studied. Most importantly, these mice can be crossed with every relevant mouse model that directly or indirectly affect DNA repair. However, biochemical *in vitro* techniques will remain inevitable to mechanistically study the process of TCR. Integration of data harvested from different fields of research like proteomics, microarray analysis and life cell studies hopefully will induce a new step in our understanding of DNA repair.

## References

1. **Park, J.S., Marr, M.T. and Roberts, J.W.** (2002) E. coli Transcription Repair Coupling Factor (Mfd Protein) Rescues Arrested Complexes by Promoting Forward Translocation. *Cell*, 109, 757-67.
2. **Lee, S.K., Yu, S.L., Prakash, L. and Prakash, S.** (2001) Requirement for yeast RAD26, a homolog of the human CSB gene, in elongation by RNA polymerase II. *Mol Cell Biol*, 21, 8651-6.
3. **van Gool, A.J., Citterio, E., Rademakers, S., van Os, R., Vermeulen, W., Constantinou, A., Egly, J.M., Bootsma, D. and Hoeijmakers, J.H.J.** (1997) The Cockayne syndrome B protein, involved in transcription-coupled DNA repair, resides in a RNA polymerase II containing complex. *EMBO J.*, 16, 5955-5965.
4. **Woudstra, E.C., Gilbert, C., Fellows, J., Jansen, L., Brouwer, J., Erdjument-Bromage, H., Tempst, P. and Svejstrup, J.Q.** (2002) A Rad26-Def1 complex coordinates repair and RNA pol II proteolysis in response to DNA damage. *Nature*, 415, 929-33.
5. **van den Boom, V., Jaspers, N.G. and Vermeulen, W.** (2002) When machines get stuck—obstructed RNA polymerase II: displacement, degradation or suicide. *Bioessays*, 24, 780-4.
6. **Christiansen, M., Stevnsner, T., Modin, C., Martensen, P.M., Brosh, R.M., Jr. and Bohr, V.A.** (2003) Functional consequences of mutations in the conserved SF2 motifs and post-translational phosphorylation of the CSB protein. *Nucleic Acids Res*, 31, 963-73.

## Summary

The integrity of DNA, the carrier of our genetic information is continuously challenged by errors during replication, intrinsic instabilities of the polymer and oxygen species reacting with its chemical structure. Furthermore, environmental factors like ionizing radiation, the UV-component of sunlight and various carcinogenic compounds interfere with the correct organization of DNA.

**Chapter 1** describes the direct consequences of DNA damages like inhibition of DNA replication, transcription and cell cycle progression. Different DNA repair mechanisms, each specialized to a particular group of lesions, collectively remove most injuries from the genome. Nucleotide excision repair (NER) is specifically responsible for the repair of helix-distorting lesions, such as UV-induced damage. The first step in each repair mechanism is the detection of the lesion. Within NER two different modes of DNA damage recognition coexist. First, global genome repair (GGR) is capable of recognizing lesions all over the genome and damage sensing is performed by the XPC/hHR23B heterodimer. Secondly, NER is initiated via transcription-coupled repair (TCR), which specifically removes DNA injuries from the transcribed strand of active genes. TCR is activated upon stalling of an RNA polymerase II molecule on a DNA lesion. Subsequent to lesion detection by either GGR or TCR, the damages are processed similarly by core NER factors. The coordinated action of ~30 proteins results in lesion demarcation, unwinding of the DNA helix around the injury, excision a DNA fragment containing the damage, polymerization of a new piece of DNA and ligation.

A more detailed description of the TCR pathway is presented in **chapter 2**. TCR has been identified in multiple organisms ranging from bacteria to mammals. In humans, defects in TCR give rise to the severe hereditary disorder Cockayne Syndrome (CS). Genetic analysis showed that CS is caused by mutations in either the *CSA* or *CSB* gene, which encode for respectively a 44kDa WD40 repeat-containing protein (*CSA*) and a 169 kDa member of the SWI/SNF family of putative helicases (*CSB*). *CSA* has no apparent enzymatic function, although its WD40 domains may be important for mediating protein-protein interaction as has been found for other WD40 repeat family members. The mechanistic role for *CSA* in TCR remains illusive. The SWI/SNF protein family member *CSB* is a dsDNA-dependent ATPase. Members of this group of proteins are often implicated in DNA transacting processes. Several models have been postulated for a molecular model for *CSB* in TCR, like displacement, translocation and degradation of stalled RNAP II molecules.

A potential role for *CSB* in transcription elongation is reviewed in **chapter 3**. The presence of *CSB* in a ternary complex of RNAPII, DNA and RNA and an interaction of the protein with RNAPII together with the observation that the absence of *CSB* results in lower levels of transcription *in vitro* and *in vivo* led to the suggestion that *CSB* may stimulate elongation. In addition, when *CSB* is incubated with RNAPII molecules stalled on a DNA lesion lengthening of the transcript with one nucleotide was reported.

**Chapter 4 and 5** describe the recently developed tools to study protein behavior in its natural context: the living cell. Tagging of proteins with the green fluorescent protein

(GFP) opened the possibility to visualize tagged proteins in live cells and to determine its dynamic behavior using photobleaching. This new field of research has shed new light on the dynamic aspects of various nuclear processes like transcription and DNA repair. In short, a probabilistic model is postulated in which multidisciplinary proteins do not reside in stable holocomplexes but rather transiently interact with its complex partners. This allows rapid adaptation to changing intra- and extracellular conditions.

**Chapter 6** describes enzymatic properties of the CSB protein. Using topological assays, CSB was found to induce negative super coils in a relaxed plasmid upon binding. In addition, like other SWI/SNF family members, CSB is able to remodel chromatin at the expense of ATP. *In vitro* analysis showed that CSB can alter the structure of reconstituted chromatin templates as envisaged by a change of the DNase I accessibility to mononucleosomes and redistribution of regularly spaced nucleosomes on plasmid DNA. This activity is dependent on the presence of the N-terminal tails of the histones. In addition, the interaction of CSB with the histones was examined. Both immunoprecipitation and Far Western analysis revealed an interaction of CSB with histones.

The localization and dynamic properties of GFP-tagged CSB proteins in living cells are presented in **chapter 7**. High-resolution microscopy reveals that CSB is homogeneously distributed throughout the nucleus in addition to highly dynamic accumulations of the protein in focal structures and in nucleoli. Induction of both UV and ionizing radiation-induced DNA damage and transcription inhibition results in a reversible redistribution of the CSB molecules from and back to these foci. Analysis of the mobility of the homogeneously distributed fraction of CSB molecules shows that these polypeptides move through the nucleus with a diffusion rate according to the size of a high molecular weight complex. In addition, a transient interaction of CSB molecules with the transcription elongation machinery is observed, most likely representing CSB polypeptides that monitor the processivity of elongating RNAPII molecules. Upon DNA-damage infliction, CSB molecules were reversibly immobilized in a dose-dependent manner suggesting engagement in TCR. The calculated binding time of single molecules to DNA damage of approximately 2-2.5 minutes most likely reflects the average association time of CSB molecules to a repair reaction.

In **chapter 8** the nature of the focal CSB accumulations with respect to other nuclear processes is investigated. Labeling of nascent mRNA shows that the foci do not colocalize to active sites of transcription. However, detailed analysis of the immunoprecipitated fraction of CSB shows that CSB-associated RNAPII is active in an *in vitro* reconstituted transcription system, suggesting that CSB interacts with elongating RNAPII molecules. Immune-fluorescent analysis using antibodies against mRNA processing factors shows that CSB foci partially colocalize with speckles; i.e. structures with high concentrations of mRNA splicing factors. In addition, the immunoprecipitated fraction of CSB further confirms the presence of several mRNA processing factors. In analogy to the model postulated for splicing factors, the focal accumulations of CSB in speckles may represent complex assembly or storage sites whereas its enzymatic function is performed co-transcriptionally in different areas in the nucleoplasm.

**Chapter 9** describes the analysis of the *in vivo* dynamics of the CSA protein using GFP-tagging. Unlike CSB, CSA does not accumulate in focal structures and not within nucleoli. Photobleaching experiments show that also CSA moves through the nucleoplasm as part of a high molecular weight complex, however of a different species than the CSB containing complex. In contrast to CSB, CSA does not show any changes in its mobility upon induction of DNA damage or transcription inhibition. These findings suggested that CSA might not be implicated directly in the actual repair reaction. To investigate a possible indirect role for CSA modulating the activity of CSB we assayed the (DNA damage-dependent) stability and the gel mobility of the CSB protein in the presence or absence of CSA. Both parameters of the CSB protein were unaffected by absence of the CSA protein. Importantly however, the chromatographic behavior of CSB on a DNA-resembling affinity column was severely affected by a deficiency of CSA, suggesting that CSB is differently charged in the absence of CSA. An explanation for this aberrant behavior may be the absence or presence of a CSA-induced modification of CSB in these extracts. Currently we are investigating the nature of this phenomenon.

Taken together, the work described in this thesis sheds new light on the process of TCR in living cells and how the CSA and CSB proteins are implicated in this repair pathway. The results, as obtained using advanced photobleaching techniques, raise new questions and create new approaches for both *in vitro* and *in vivo* experiments. This effort eventually will contribute to our understanding of the molecular mechanism of TCR and how TCR is integrated in the complex orchestration of various nuclear processes *in vivo*.

# Samenvatting

Het menselijk lichaam bestaat uit miljarden cellen die elk een volledige kopie van de totale erfelijke informatie, opgeslagen in het DNA, bevatten. Dit DNA is de drager van alle genetische informatie nodig voor de normale ontwikkeling van een individu. Goede conservering van deze informatie is daarom van levensbelang. De structuur van DNA wordt echter voortdurend bedreigd door fouten tijdens replicatie, intrinsieke instabiliteit van het DNA en reactieve zuurstofmoleculen die reageren met de chemische structuur. Daarnaast wordt de correcte organisatie van het DNA aangetast door omgevingsfactoren zoals ioniserende straling, de UV-component van het zonlicht en verschillende kankerverwekkende stoffen.

**Hoofdstuk 1** beschrijft de directe consequenties van DNA schade zoals remming van DNA verdubbeling (replicatie), overschrijven van het DNA (transcriptie) en celdeling. Verwijdering van laesies wordt verzorgd door verschillende DNA reparatie mechanismen, elk gespecialiseerd in eliminatie van een specifieke groep DNA schades. Het nucleotide excisie reparatie (NER) mechanisme is verantwoordelijk voor het herstel van schades die de structuur van de DNA helix verstoren. Dit soort laesies worden onder andere veroorzaakt door UV-licht. Herkenning van de schade is een eerste voorwaarde voor DNA herstel. Schade herkenning door NER vindt plaats op twee verschillende manieren. Ten eerste worden DNA laesies in het hele genoom herkend door het globaal genoom herstel (GGR) mechanisme met behulp van een specifiek schade bindend eiwitcomplex. Ten tweede worden schades in de getranscribeerde streng van actieve genen herkend door het transcriptie gekoppeld herstel (TCR) mechanisme. TCR wordt actief wanneer een RNA polymerase tijdens het vertalen van de genetische code in het DNA naar mRNA vastloopt op een DNA schade. Uiteindelijke verwijdering van de schade na herkenning door GGR of TCR gebeurt op identieke wijze. Door de gecoördineerde samenwerking van ongeveer 30 verschillende eiwitten die achtereenvolgens de laesie afbakenen, het beschadigde stukje DNA uitknippen en het ontstane gat opvullen (synthese) en dichtplakken (ligatie).

In **hoofdstuk 2** wordt TCR in meer detail beschreven. TCR blijkt in een groot aantal verschillende organismen, variërend van bacteriën tot zoogdieren, voor te komen. Een genetische defect in TCR resulteert in de ernstige erfelijke afwijking Cockayne Syndroom (CS). CS wordt veroorzaakt door een mutatie in het CSA of CSB gen. Het CSA gen codeert voor een 44 kDa WD40 motief bevattend eiwit (CSA). Deze WD40 domeinen vervullen waarschijnlijk een belangrijke rol in het reguleren van eiwit-eiwit interacties zoals eerder gezien voor andere WD40-motief familieleden. De mechanistische rol van CSA in TCR is vooralsnog onduidelijk. Het CSB gen is een eiwit van 169 kDa (CSB) dat op grond van geconserveerde aminozuurdomeinen behoort tot de SWI/SNF familie van DNA helicases. CSB is een dubbelstrengs DNA afhankelijke ATPase. Er zijn verschillende modellen voor de moleculaire rol van CSB in TCR, zoals voorwaartse/achterwaartse verschuiving of afbraak van het geblokeerde RNA polymerase.

**Hoofdstuk 3** beschrijft de potentiële rol van CSB in transcriptie elongatie. De observaties dat CSB aanwezig is in een complex met RNA polymerase II, DNA en RNA, dat het een interactie aan kan gaan met RNA polymerase II en dat in de afwezigheid van CSB transcriptie niveaus zijn verlaagd *in vitro* en *in vivo* heeft geleid tot de suggestie dat CSB transcriptie elongatie kan stimuleren. Incubatie van CSB met polymerases geblokkeerd op een schade resulteert bovendien in een verlenging van een transcript met een nucleotide.

**Hoofdstuk 4 en 5** beschrijven de recentelijk ontwikkelde hulpmiddelen om de mobiliteit van eiwitten in levende cellen te bestuderen. Door cellen eiwitten te laten aanmaken die gefuseerd zijn aan het groen fluorescente eiwit (GFP) is het mogelijk deze te visualiseren en met behulp van fotobleking het dynamisch gedrag te bepalen in levende cellen. Dit jonge onderzoeksveld heeft nieuwe inzichten gegeven in de dynamische aspecten van verschillende nucleaire processen zoals transcriptie en DNA herstel. Dit heeft geleid tot het model dat multidisciplinaire eiwitten zich niet in stabiele holocomplexen bevinden maar kortstondig een interactie aangaan met complex partners. Doordat eiwitten hierdoor snel kunnen switchen tussen verschillende processen, kunnen cellen zeer snel reageren op wisselende intra- en extracellulaire condities.

**Hoofdstuk 6** beschrijft de enzymatische eigenschappen van het CSB eiwit. Topologische experimenten laten zien dat CSB door binding aan plasmide DNA in staat is de 3-dimensionale structuur van het DNA te veranderen waardoor negatieve superhelicaliteit ontstaat. In de celkern is het DNA aanwezig in een zeer gecompriëerde vorm: chromatine. Chromatine bestaat uit histon-eiwitcomplexen met daaromheen DNA gewikkeld, ook wel nucleosomen genoemd. Dit hoofdstuk beschrijft dat CSB, net als andere leden van de SWI/SNF eiwit familie, op een ATP-afhankelijke manier de structuur van het chromatine kan veranderen. Dit werd op de volgende manier gevisualiseerd: CSB induceert een verandering van de DNase I toegankelijkheid tot mononucleosomen en redistribueert regelmatig gepositioneerde nucleosomen op plasmide DNA. Verder werd gevonden dat CSB een interactie kan aangaan met histonen en dat voor de verandering van de chromatine structuur door CSB de amino-termini van de histonen nodig zijn.

De lokalisatie en dynamische eigenschappen van GFP-CSB fusie-eiwitten in levende cellen worden gepresenteerd in **hoofdstuk 7**. Microscopische analyse laat zien dat CSB een gelijkmatige verdeling heeft in de kern en ophoopt in kleine lokale concentraties (foci) en de kernlichaampjes (nucleoli). Blootstelling aan UV- en ioniserende straling en remming van de transcriptie induceert een omkeerbare herverdeling van de CSB moleculen van en naar de foci en nucleoli. Analyse van de mobiliteit van de gelijkmatig verspreide fractie van CSB moleculen laat zien dat deze eiwitten door de kern bewegen met een diffusie snelheid die gelijk is aan de verwachte snelheid van een groot eiwitcomplex. Dit houdt in dat CSB waarschijnlijk onderdeel is van een groot eiwitcomplex. Verder heeft CSB een kortstondige interactie in de orde van seconden met de transcriptie elongatie machine. Waarschijnlijk houdt CSB toezicht op de continuïteit van elongerende RNA polymerase II moleculen. Na inductie van DNA schade gaat een deel van de CSB moleculen langer vast zitten op een dosis afhankelijke manier. Vermoedelijk zijn deze moleculen actief bij DNA reparatie betrokken. De berekende bindingstijd van individuele moleculen aan DNA schade is ongeveer twee tot tweeënhalve



minuut en het is aannemelijk dat dit de tijd is dat CSB moleculen daadwerkelijk betrokken zijn in de reparatie reactie.

In **hoofdstuk 8** wordt de aard van de CSB foci met betrekking tot andere nucleaire processen onderzocht. Labelen van nieuw getranscribeerd RNA laat zien dat de CSB foci niet colocaliseren met plaatsen waar actieve transcriptie plaatsvindt. Analyse van de immuunprecipiteerde CSB fractie toont aan dat CSB-geassocieerd RNA polymerase II actief is in een transcriptie reactie *in vitro*. Localisatie studies met antilichamen gericht tegen mRNA modificatie factoren laat zien dat CSB foci gedeeltelijk overlappen met zogenaamde speckles. Dit zijn kernstructuren met hoge concentraties van mRNA modificatie factoren. Verder bevat de immuunprecipiteerde CSB fractie naast RNA polymerase II ook verschillende mRNA modificatie factoren. In overeenstemming met het model voor splicing factoren in speckles, fungeren de CSB foci waarschijnlijk als locaties voor opbouw van het eiwitcomplex of opslagplaatsen voor CSB. De enzymatische functie van CSB vindt waarschijnlijk co-transcriptioneel plaats in andere delen van de kern.

**Hoofdstuk 9** beschrijft de analyse van de dynamiek van GFP-gefuseerd CSA eiwit in levende cellen. In tegenstelling tot CSB hoopt CSA niet op in foci of de nucleoli. Eiwit-kinetiek metingen met behulp van fotobleking laten zien dat CSA door de kern beweegt als onderdeel van een groot complex, echter van andere grootte dan het CSB complex. Anders dan CSB verandert de mobiliteit van CSA niet na inductie van DNA schade of transcriptie remming. Deze resultaten doen vermoeden dat CSA waarschijnlijk niet direct betrokken is bij de reparatie reactie. Vervolgens werd een mogelijke indirecte rol van CSA in de regulering van de activiteit van CSB onderzocht. Hierbij is gekeken naar de (DNA schade afhankelijke) stabiliteit en de mobiliteit van CSB in een gel (grootte) in de aan- of afwezigheid van CSA. Beide parameters waren onveranderd in de afwezigheid van CSA. Echter, het chromatografisch gedrag van CSB op een DNA-gelijke affiniteitkolom was volledig veranderd in de afwezigheid van CSA. Dit deed vermoeden dat de lading van het CSB eiwit is veranderd in CSA-deficiënte cellen. Een mogelijke verklaring voor deze verandering van chromatografisch gedrag zou de aan- of afwezigheid van een CSA geïnduceerde modificatie van CSB kunnen zijn. Op het moment bestuderen we de verdere aard van het afwijkend gedrag van CSB in CSA-deficiënte cellen.

Het onderzoek beschreven in dit proefschrift geeft nieuwe inzichten in de manier waarop TCR plaatsvindt in levende cellen en hoe het CSA en CSB eiwit hierin betrokken zijn. De resultaten van de eiwit-dynamiek experimenten doen nieuwe vragen opkomen en zijn daarmee een voedingsbodem voor nieuwe *in vitro* en *in vivo* experimenten. Dit zal zeer waarschijnlijk leiden tot meer inzicht in het moleculair mechanisme van TCR en hoe dit DNA reparatie mechanisme is geïntegreerd in het complex netwerk van processen die zich in de celkern afspelen.

## List of abbreviations

BER	base excision repair
CAK	cyclin-activating kinase complex
CDK7	cyclin-dependent kinase 7
CPD	cyclobutane pyrimidine dimer
CS	Cockayne syndrome
CSA/CSB	Cockayne syndrome A/B protein
CTD	C-terminal domain of the large subunit of RNA polymerase 2
DEF1	RNAPII degradation factor 1
ss/dsDNA	single/double stranded DNA
DNA	deoxyribonucleic acid
DRB	5,6-dichloro-1 $\beta$ -D-ribofuranosyl benzimidazole
ERCC1	human excision repair cross complementing gene 1
FLIP	fluorescence loss in photobleaching
FRAP	fluorescence recovery after photobleaching
GFP	green fluorescent protein
GG-NER	global genome NER
HA	hemagglutinin
hHR23B	human homolog of <i>S.cerevisiae</i> repair protein RAD23B
HR	homologous recombination
kDa	kilodalton
MAT1	menage-à-trois 1
MEF	mouse embryonic fibroblast
Mfd	mutation frequency decline
m/rRNA	messenger/ribosomal ribonucleic acid
NER	nucleotide excision repair
NHEJ	non-homologous end-joining
nt	nucleotide
PCNA	proliferating cell nuclear factor
(6-4) PP	(6-4) pyrimidine –pyrimidone photoproduct
RAD	radiation sensitive
RNAPI/II/III	RNA polymerase I/II/III
RPA	replication factor A
SNF	refers to <i>S.cerevisiae</i> sucrose non-fermenting mutants
SWI	refers to <i>S.cerevisiae</i> mutants defective in mating type switching
TBP	TATA-binding protein
TC-NER	transcription-coupled NER
TFIIH	transcription factor IIH
TPR	tetratricopeptide repeat
TTD	trichothiodystrophy
UDS	unscheduled DNA synthesis
UV	ultraviolet light
(UV)DDB	(UV- light) DNA damage binding protein
WCE	whole cell extract
XAB2	XPA binding protein 2
XP	xeroderma pigmentosum
XPA to –G	xeroderma pigmentosum group A to –G protein

## List of publications

**Van Der Knaap J.A., Van Den Boom V., Kuipers J., Van Eijk M.J., Van Der Vliet P.C., Timmers H.T.** (2000) The gene for human TATA-binding-protein-associated factor (TAFII) 170: structure, promoter and chromosomal localization. *Biochem J.*, 3:521-7.

**Citterio E., Van Den Boom V., Schnitzler G., Kanaar R., Bonte E., Kingston R.E., Hoeijmakers J.H.J. and Vermeulen W.** (2000) ATP-dependent chromatin remodeling by the Cockayne syndrome B DNA repair-transcription-coupling factor. *Mol Cell Biol*, 20, 7643-53.

**Pereira L.A., Van der Knaap J.A., Van den Boom V., van den Heuvel F.A., Timmers H.T.** (2001) TAF(II)170 interacts with the concave surface of TATA-binding protein to inhibit its DNA binding activity. *Mol Cell Biol*, 21:7523-34

**Van den Boom V., Jaspers N.G. and Vermeulen W.** (2002) When machines get stuck-obstructed RNA polymerase II: displacement, degradation or suicide. *Bioessays*, 24, 780-4.

**Van den Boom V., Citterio E., Hoogstraten D., van Cappellen W.A., Hoeijmakers J.H.J., Houtsmuller A.B. and Vermeulen W.** (2003) Transient interactions of CSB with transcription elongation complexes are stabilized by DNA damage-induced stalling. *Submitted*.

# Curriculum Vitae

Naam: Vincent van den Boom  
Geboren: 6 maart 1975 te Utrecht

1988-1993 VWO, Koningin Wilhelmina College te Culemborg

1993-1999 Studie Medische biologie, Universiteit Utrecht  
1997 Bijvakstage  
Universiteit Utrecht, Universitair Medisch Centrum, afdeling  
Celbiologie onder begeleiding van Dr. J.A.W. Leusen en Dr. P.J.  
Peters

1997-1998 Hoofdvakstage  
Universiteit Utrecht, Universitair Medisch Centrum, Laboratorium  
voor Fysiologische Chemie onder begeleiding van Dr. J.A. van  
der Knaap en Prof. Dr. H.Th.M. Timmers

1999-2003 Promotie onderzoek  
Erasmus MC Rotterdam, afdeling Celbiologie en Genetica  
Promotor: Prof. Dr. J.H.J. Hoeijmakers  
Co-promotor: Dr. W. Vermeulen

2001 (juni en november) Onderzoek in het laboratorium van Dr. J. Q.  
Svejstrup

# Dankwoord

Eindelijk ben ik dan toch aangeland bij deze pagina. Ik heb in m'n tijd als AIO vaak naar dit moment uitgekeken en moet zeggen dat het erg goed voelt. Dit was echter nooit mogelijk geweest zonder grote en kleine bijdragen van vele mensen op professioneel en sociaal terrein.

Allereerst ben ik veel dank verschuldigd aan mijn promotor Prof. Dr. Jan Hoeijmakers. Beste Jan, jouw enthousiasme heeft mij zeer gestimuleerd de afgelopen jaren. Je scherpzinnigheid en verfrissende inzichten hebben veel bijgedragen aan het GFP werk. Verder ben ik zeer veel dank verschuldigd aan mijn copromotor Dr. Wim Vermeulen. Beste Wim, dit boekje was niet in zijn huidige vorm verschenen zonder jouw enorme inzet de laatste maanden. Ik kijk met ontzettend veel plezier terug op onze samenwerking de afgelopen jaren. Je enthousiasme, in combinatie met een gezonde dosis Hollandse nuchterheid, heeft me veel geleerd over het overleven in de jungle die wetenschap heet. Veel van het GFP werk in dit proefschrift zou niet gelukt zijn zonder de inzet van Adriaan Houtsmuller. Beste Adriaan, onze vele werkbesprekingen en simulatiesessies stonden vaak garant voor de nodige (humoristische) discussies. I'm also very thankful to Dr. Jesper Svejstrup. Dear Jesper, I enjoyed my stay in your lab very much. Thanks for giving me the opportunity to get familiar with the basics of large-scale protein purification.

Dan nu mijn collega's van lab 1053 (inmiddels 1030). Betty, ik heb de eerste twee jaar met zeer veel plezier met jou samengewerkt. Jouw precieze begeleiding heeft ertoe bijgedragen dat ik snel ingewerkt was. Ik hoop snel weer 's in Milaan langs te komen. Deborah, bedankt voor je hulp met de voorbereidingen voor mijn promotie. De directe aanwezigheid van een ervaringsdeskundige als jij kwam zeer goed van pas. Francesca, it was a pleasure to have you as a student on the Cockayne project. I have very good memories about your presence in the lab and all the great italian dishes you introduced to us. Good luck with your own PhD. Ambra, thanks for your efforts on the CSA project the last year. Nils, bedankt voor je hulp met allerlei praktische zaken in het lab en zonder Arjan geen groene cellen en sigaretje met bijbehorende analyse van de korfbalcompetitie. Steven, ik kijk met veel plezier terug op menig 'klein biertje' in Dizzy. Ana, thanks for your daily smiles (soon my pipets will be free to use). Verder natuurlijk ook mijn dank aan alle voormalige en nieuwe labgenoten: Nancy, Angelica, Claire, Chris en Astrid. Jessie, ontzettend leuk dat jij paranimf bent tijdens m'n promotie. Jouw heerlijke (on)zinnige verhalen waren altijd zeer vermakelijk. Succes verder met je werk in Memphis.

Verder bedank ik iedereen van de afdeling celbiologie en genetica die op een of andere manier bijgedragen heeft aan m'n werk. In het bijzonder de dames van de keuken, Jasperina, Rita en Marieke van het secretariaat, Tom en Ruud van fotografie en Sjozef, Ton en Pim voor hun hulp bij computerproblemen. Ook heb ik altijd genoten van de collegiale sfeer en de daaruit voortvloeiende sociale activiteiten.

Natuurlijk zijn ook veel goede vrienden onmisbaar geweest voor het tot stand komen van dit boekje. Joost, Daan en Onno, ik heb altijd met veel plezier de stress van

me afgespeeld tijdens onze wekelijkse oefenavondjes met de band. Joost, ik vind het hartstikke leuk dat jij m'n paranimf wilt zijn. De jaarlijkse zeilavonturen met Theo, Ernst-Jan, Park en Peter zijn ook altijd meer dan welkom geweest om het hoofd even helemaal leeg te maken.

Verder wil ik m'n familie bedanken voor al hun begrip en steun de afgelopen jaren. Beste pa en ma, bedankt dat jullie altijd klaar voor me hebben gestaan, ook als het allemaal niet zo makkelijk was. Nu dan jij Ingrid. Je beseft niet half wat je voor me hebt betekend de afgelopen tijd. Jouw enorme liefde en enthousiasme verwonderen me telkens weer. Ik kijk ernaar uit samen met jou het leven verder te ontdekken.

Vincent



